Air Cooling for AECM Module

Final Project Report

The Sector h team:
Bruno Caulk
Kevin Whipp

Senior Project Advisor:
Sarah Harding

Project Sponsor:
Boeing
Charlie Kusuda P.E.

California Polytechnic State University

San Luis Obispo

12 / 03 / 09

STATEMENT OF DISCLAIMER

Since this project is a result of a class assignment, it has been graded and accepted as fulfillment of the course requirements. Acceptance does not imply technical accuracy or reliability. Any use of information in this report is done at the risk of the user. These risks may include catastrophic failure of the device or infringement of patent or copyright laws. California Polytechnic State University at San Luis Obispo and its staff cannot be held liable for any use or misuse of the project.

ABSTRACT

Advancements in electronics have created the need for improved cooling standards. The AECM standard, created to replace the antiquated ARINC 600 specification, draws inspiration from a cooling specification known as VITA 48.2. The ARINC standard is in early stages of development and this project researches the feasibility of using air as a convective fluid instead of a liquid, the fluid used in the VITA specification.

A performance factor calculated from the ratio of the heat dissipated by convective heat exchanger plates over the power used to cause forced convective flow over said plates helps to quantify the effectiveness of various cooling scenarios.

Design development of the heat exchangers resulted in a plan to manufacture and test six different heat exchanger configurations. Five of these used various assortments of porous foam aluminum; the sixth used a more conventional finned design. To house and test the effectiveness of these configurations a testing platform was created to control and measure appropriate testing values. Before each configuration was tested, the setup was sealed to prevent leaks and insulated to minimize heat transfer sources beyond the effects of the controlled and measured convective air.

Notable results include the 7.0”x9.3”x0.87”, 10ppi, 8% density porous aluminum foam heat exchanger which resulted in both the largest pressure drop, 2.7 inches of water and heat dissipated at 301 watts at a flow rate of 72 CFM. The performance factor of this plate was the lowest at 13 [Watts/Watts]. Conversely, the largest performance factor at similar flow rate was seen in the finned plate design as 58 [Watts/Watts] at 71 CFM. However, its heat transfer for this flow rate was 167 Watts. Appendices H though K display all test results and analysis for each prototype.

A general plot of the results, seen in Section 9.3, provides a valuable selection tool for choosing an appropriate starting design point to develop AECM air cooling.

The heat dissipation seen from the heat exchanger plates is competitive with the liquid-cooled module plates and deserves further investigation. The added benefits of natural convection and the weight savings of air cooling further endorse this conclusion.

TABLE OF CONTENTS

LIST OF FIGURES

LIST OF TABLES

1 INTRODUCTION

Boeing, the sponsor for this senior project, is a world leader in aircraft manufacturing and design. In the continual struggle to improve and build upon past successes, the company has begun to investigate solutions for some of today's engineering problems. In efforts to reduce the volume and power consumption associated with the cooling of electrical equipment Boeing has begun research into a new electronics cabinet standard. Known as the AECM, or Advanced Equipment Cooling Method, this proposed design retains the circuit board sizing and connector standards from the antiquated ARINC 600 standard but introduces a "clam-shell" design casing similar to those in a much newer VITA 48.2 specification standard. The goal of this upgrade is to obtain a reverse-compatible system capable of handling a greater amount of heat while staying lightweight and appropriate for an airplane installation.

An initial computational fluid dynamics (CFD) analysis of a proposed AECM module generated a number of noteworthy features that warranted additional investigation. One of these follow-ups involves analyzing the heat distribution using forced air convection as an alternative to liquid-cooling solutions. The goal of this Senior Project, henceforth referred to as "Air Cooling for AECM Module," is to research various air-cooling techniques and develop a prototype utilizing a chosen design. This prototype will be tested to determine the most effective method of heat dissipation using convective cooling techniques.

The conclusions and results from this senior project report will be valuable resources for Boeing in the process of developing the AECM module standards, or any other entity faced with weighing the pros and cons of different methodologies of air-cooling electronic equipment.

Bruno Caulk and Kevin Whipp are Mechanical Engineering Students at California Polytechnic State University, San Luis Obispo. The capstone senior project program presents students with real-world engineering problems and expectations in a format that allows them to apply experience and knowledge gained during their education. Over the span of three academic quarters students design, build and test a working prototype to fulfill the needs of the project sponsors. During the duration of this project Bruno Caulk and Kevin Whipp will operate under a fictitious business name of Sector h. This name provides a first impression for the team and the logo draws inspiration from the convective heat transfer coefficient h and a simulated finite-element-analysis output plot.

2 BACKGROUND

Figure 2-1: A modern CPU, in extreme cases a single device such as this is capable of heat generation of 130 Watts. (© fr3d.org)

Current cooling standards for avionic electronics boards cannot match present advancements in computer processing technology. Modern computer components generate much more heat than these standards allow. Therefore, new cooling methods must be developed. This section includes background research into relevant analysis and technologies that may be used to make informed decisions in later sections. Works cited can be found in Appendix A.

2.1 Existing Standards

2.1.1 ARINC 600

The ARINC 600 Standard includes requirements relating to module dimensions and air flow distribution. As a standard, these modules must be ~12.5" long, ~7.6" tall, and ~1.1" wide. (Kusuda)

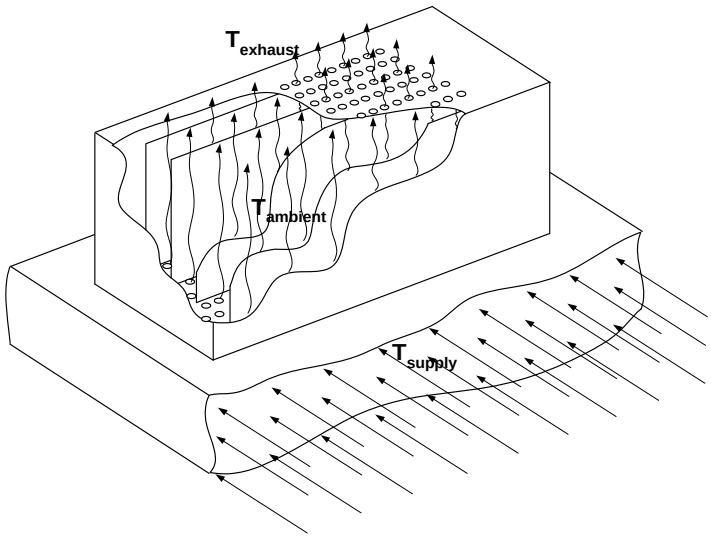

Figure 2-2: An example of a cabinet meeting ARINC 600 Specifications. (© Boeing)

In Figure 2-2 a typical 4 module concept unit is shown; this enclosure has a maximum wattage of 100W with 11.4 CFM of cooling air supplied. The temperatures involved are not provided. Pressure drops through the module package are typically in the range of 0.2 to 1.0 inches of water. The module weight range is 22.1 to 30.7 lbs.

2.1.2 VITA 48.2 Specification

The Vita Specification dictates specific procedures for module dimensions and clamping procedures. It serves as a primary inspiration for the liquid cooled AECM module design. Beyond the primary thermal uses the clamshell design serves to protect the components from damage during transport as well as serve as electronic shielding while in operation.

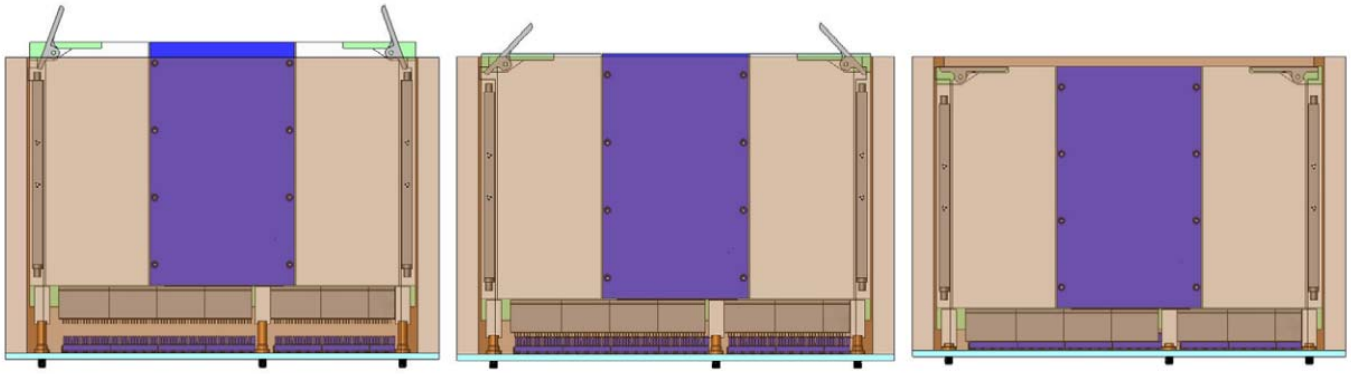

Figure 2-3: Insertion procedure for an example VITA 48.2 module. (© VITA)

2.2 Theoretical Analysis

2.2.1 Calculating Convective Heat Transfer using Newton's Law of Heat Transfer

Newton's Law of Heat Transfer is used to calculate the total heat transfer rate due to convection. This classical equation has limited use in this scenario as it is used to calculate the theoretical heat transfer from a surface undergoing convective heat transfer. It relies on accurate values for h, a term that cannot be determined using closed-form hand calculations. Regardless, the equation is useful to regard as an all-encompassing guideline for convective heat transfer. To maximize the desired variable, q or heat transfer rate, you can only vary three things: h, A or delta T.

$$q = h \cdot A \cdot (T_{surface} - T_{environment})$$

Equation 2-1

From this equation, one can define a few are key variables to always keep in mind when attempting to increase heat transfer with the design.

- **Rate of heat transfer, q**

Measured in Watts, this value is one of the key elements this project revolves around. It should be noted that this is a time dependent variable, it is not overall heat transfer which is often noted using Q but is, as stated, the rate of heat transfer and referred to using the symbol q. Alternative notations make use of the symbol $\dot{Q}$ to reinforce the notation that it is time dependent, but for the sake of clarity, the symbol q, will be utilized henceforth.

- **Heat Convection Constant, h**

The heat convection constant, h, is directly proportional to a specific systems ability to dissipate heat; it has units of $[W/(m^2 \cdot K)]$ This constant, h, is a function of many different parameters, but most notably, the Reynolds Number, Re, of the flow. The Reynolds Number is a dimensionless number used to better characterize fluid flow. A larger Reynolds number can be caused by increased flow velocity, more abrupt changes in geometry, and more turbulent flow. In short, air with more turbulent mixing (higher Re #) will more easily transfer heat within itself and its surroundings than a smoother flow. However, this can require a greater difference between up-stream and down-stream pressures to keep the flow constant. This will increase the power required to pump the air through the system, a sacrifice for greater heat dissipation.

- **Area, A**

Area, A, exposed to air flow is also directly proportional to heat dissipation. Keeping units consistent with the SI system, area here is measured in $[m^2]$. The more area the flow can contact, the more chances the air will have to carry heat away. However, increased area can also increase the backpressure.

- **Delta T**

This delta T refers to the difference in temperature between the convective fluid (in this case, air) and the hotter surface. Larger temperature differences between the incoming air and the surface to be cooled also increase heat transfer. The colder incoming air can more easily wick the heat away and is able to absorb more heat before reaching equilibrium with the surface.

2.2.2 Measuring Heat Transfer into the Air using Energy Balance.

Unlike certain specifications such as temperature or pressure calculating some of the features desirable to measure cannot be accomplished using common measurement devices. One good example of this is heat transfer.

Measuring the heat transfer into the air is an important part of this project and is one of the important values upon which the success of the project will be gauged.

$$q = \dot{m} \cdot c_p \cdot (T_{outlet} - T_{inlet})$$

Equation 2-2

This is a formula that will be appropriate for calculating heat transfer into the air. Given this formula critical testing measurement will include, the air intake and exit temperatures and the mass flow rate of the air. The specific heat capacity will be estimated based on the average air temperature and other system conditions.

- **Rate of heat transfer, q**

  Similar to the earlier q in representing heat transfer and being measured in watts, this value will actually be determined and used in the experimental results. This q represents heat transfer rate into the air flow. This value can be used as one method to determine the heat transfer rates from the system.

- **Mass airflow rate, mdot**

  The value of mdot is measured in *[kg/sec]*. The determination of mdot involves a number of factors including air temperature, density, and volumetric flow rate. The metric units of mdot will ensure that the final value of q is properly represented as watts.

- **Specific Heat Capacity of Air, Cp**

  Specific heat is the measure of the heat energy required to increase the temperature of an object by a certain temperature interval. (Lader) The specific heat of an ideal gas is a function only of temperature and is measured in *[kJ/kg/K]*. Assuming that air acts as an ideal gas is a fairly reasonable assumption; for the case of forced convection the difference in Cp is deemed negligible.

- **Delta T**

  This delta T (measured °C or K) refers to the difference in temperature between the inlet air and the outlet air. Larger temperature differences between these values indicate that the air is drawing greater amounts of heat from the system and causing larger q values.

2.2.3 Heat transfer from extruded surfaces

2.2.3.1 Heat transfer from one rectangular extruded fin

$$q_{Fin} = M \tanh(m \cdot L_C)$$

Equation 2-3

- **M and m**

  M and m are common shortenings for a combination of factors often seen heat transfer equations. P is perimeter around the fin [meters]. k is the thermal conductivity of the fin material [watts/m*K]. A_C is the fin's cross sectional area [m^2]. T_b is the temperature of the base of the fin [K]. T_{inf} is the temperature of the environment [K].

$$M = \sqrt{hPkA_C} \cdot (T_b - T_\infty)$$

$$m = \sqrt{hPkA_C}$$

- **L_C**

  Corrected length of the fins, this factor adds the 1/2 the thickness to the length to account for heat loss through the thickness which would otherwise be neglected. Unit is meters.

2.2.3.2 Infinitely long fin

$$L_\infty \approx 2.646\sqrt{\frac{kA_C}{hP}}$$

Equation 2-4

The value determined with this equation is the length (in meters) of a fin that would have 99% the heat transfer rate of a fin that has infinite length. It is useful to confirm that fin dimensions are not too large.

2.2.3.3 Fin Performance Factor

$$\varepsilon_f = \frac{q_{Fin}}{hA_C(T_b - T_\infty)}$$

Equation 2-5

Essentially, what this provides is a comparison of heat transfer from the fins compared to the flat surface. This value is not an efficiency, it has no upper limit. A value greater than 2 from this factor is expected for extruded fins to be considered worthwhile.

2.2.3.4 Fin Efficiency

$$\eta_f = \frac{\tanh(mL_C)}{mL_C}$$

Equation 2-6

Fin efficiency is a ratio of the estimated heat from the fin over the theoretical maximum that would be seen if the entire fin were temperature T_b. This value, as all efficiencies are, is limited to the range of 0 to 1 and is commonly displayed as a percentage.

2.2.3.5 Total rate of heat transfer from array of fins

$$q_{Total} = N\eta_f hA_{finnedsurfae}(T_b - T_\infty) + hA_{nonfinnedbase}(T_b - T_\infty)$$

Equation 2-7

This simply multiplies the number of fins (N) by the efficiency and heat from each fin and adds it to the heat dissipated by surface exposed between the fins.

2.2.3.6 Total rate of heat transfer from array of fins

$$\eta_o = \frac{q_{Total}}{hA_{totalsurface}(T_b - T_\infty)}$$

Equation 2-8

Similarly to fin efficiency, the total rate of heat transfer calculates the actual heat transfer from the idealized fins over the maximum possible heat transfer that would be seen if all exposed surfaces were at max temperature T_b.

2.3 Module cover design research

This section includes investigation into a number of possible applicable technologies to possibly apply to the project.

2.3.1 Heatsink

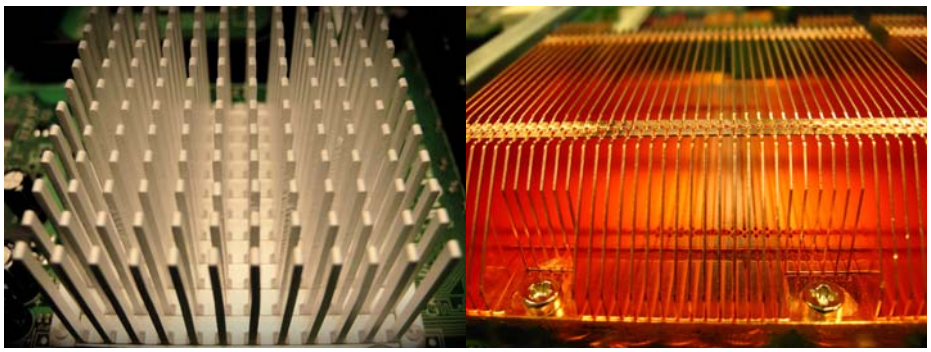

Figure 2-4: Left: an older low capacity aluminum. Right: a much denser copper heatsink. (© jstownsley) (© qfamily)

Traditional finned heatsinks are designed to draw heat away from the component they wish to cool simply through convection. Thin fins increase the overall surface area of the material, allowing greater natural or forced air convection. Heatsinks are made from materials with high thermal conductivities, most commonly aluminum or copper; these materials increase the rate of heat transfer from the component in question to the surrounding air.

2.3.2 Microchannel Heatsinks

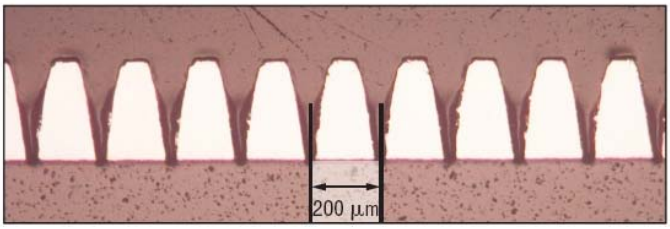

Figure 2-5: A magnified view of a very fine microchannel heatsink. (© Stephen Solovitz)

Microchannel heatsinks operate the same way as conventional heatsinks but contain much thinner fins, sometimes spaced only 100μm apart. (Solovitz) They require forced air convection and offer larger surface area per volume of flow, allowing for improved heat transfer. However as the width of the channels decreases, fiction due to the viscous effects of the air becomes more significant. This increases the pressure drop through the fins and channels requiring greater fan power that in turn increases energy consumption and noise.

2.3.3 Heat Pipes

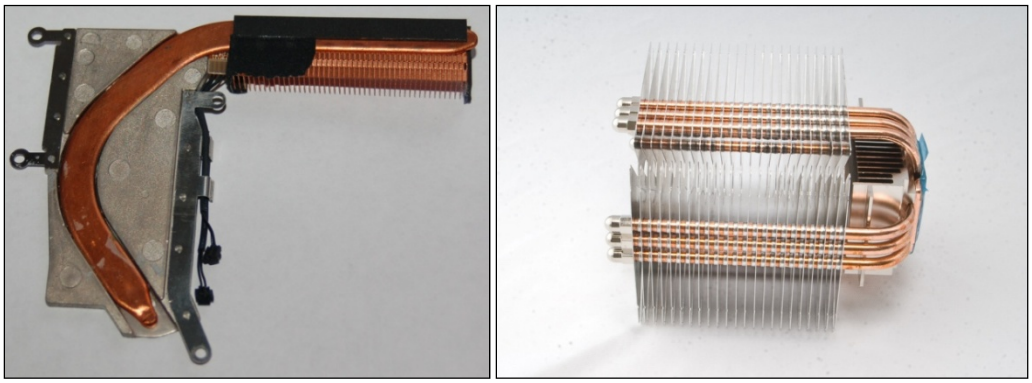

Figure 2-6: Left: a laptop cooling apparatus with a wide heat pipe. Right: a high performance desktop CPU cooler utilizing a large number of smaller heat pipes. (© bolti22) (© fr3d.org)

Although existing for nearly 50 years, one advanced thermal management techniques that has been making a large appearance recently has been that of heat pipe technology. This technology, sometimes called the "superconductor" of heat, has unique thermal properties that allow it to transfer heat from one location to another with very little heat loss. The basic structure of a heat pipe consists of three parts: the container, the wick and the working fluid.

Heat applied to a section of heat pipe container will cause the working fluid in that section to absorb heat, boil into a gas [See (1) in Figure 2-7], and move to a cooler section of the heat pipe (2) where it condenses on the wick (3). The working fluid is then able to travel down the wick via gravity or capillary action of the wick (4). The paired processes of boiling and condensing serve to respectively absorb and give up the latent heats of vaporization (Shankara) that results in the high heat flux properties heat pipes are used for.

The selection of an optimal heat pipe depends greatly on the specifics of the application. Because of this, a number of design considerations must be made when selecting a heat pipe.

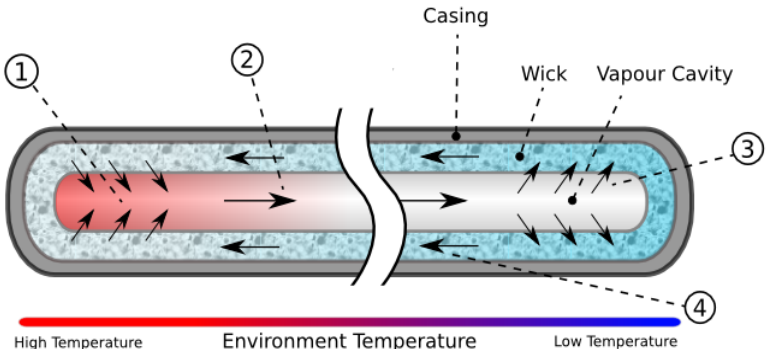

Figure 2-7: Diagram of a typical heatpipe (© novelconceptsinc.com)

The working fluid is one of the most important considerations when selecting a heat pipe, primarily because working fluids only operate properly in a heat pipe within a specific temperature range. Fluids ranging from liquid nitrogen to liquid silver are used in temperature ranges spanning -200 °C to 2000 °C, but for more common temperatures liquid ammonia, water or methanol are often used. (Shankara)

The container has a number of design constraints that are vital to the proper operation of the heat pipe. It must be rigid enough to hold the working fluid at the proper pressures; it must also be made of a thermally conductive material to facilitate heat transfer into the working fluid. The material must have high "wettability," and must be chemically compatible to the wick and working fluid to prevent corrosion. The containers can come in a variety of sizes; when properly designed, larger diameter tubes result in higher heat transfer rates. (Enertron)

Heat pipe wicks are available in a number of different options as well. Sintered metal is commonly used for heat pipe wicks because of its relatively low cost, ease of construction and superior ability to handle bends in the pipe. (Enertron) Wire meshes or even spiral shapes created from stainless steel or copper can also work effectively as wicks for heat pipes. Finally, the actual shape of the containers inner walls can be grooved, serving as a wick as well. Each of these wick solutions has an appropriate application. For example, in a horizontal orientation the groove method is much more effective at longer lengths (200 mm) compared to other wicks but is one of the worst solutions for shorter lengths (125 mm or less).

2.3.4 Heat Spreaders

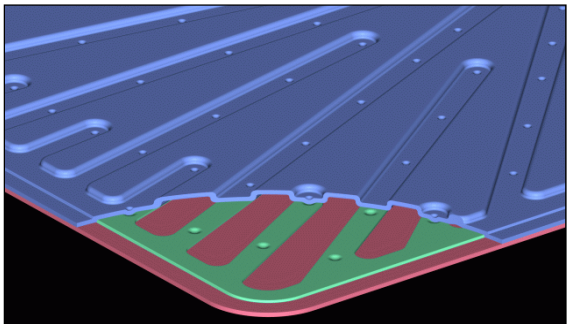

Figure 2-8: A cutaway view of a thin heat spreader from novelconceptsinc.com (©)

Heat spreaders are aptly named; they serve to spread heat from one localized area to the entirety of the heat spreaders surface. These devices are commonly made simply with a slab of high-conductivity material such as copper or aluminum. Need for improvements in this field have provided new solutions that utilize phase change heat transfer much like heat pipes. Very thin liquid filled heat spreaders may even omit the porous wick seen in traditional heat pipes in favor of using the capillary action of close proximity planar walls.

2.3.5 Jet Impingement

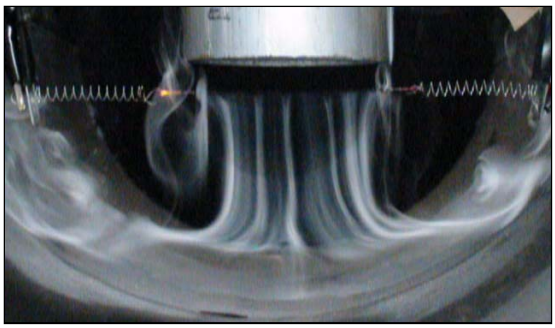

Figure 2-9: Experimental setup featuring jet impingement upon a concave surface. (© S. Sanitjai)

Typically used with liquid fluids to provide extremely high rates of heat transfer from a localized heat source, jet impingement technology also applies when the fluid is air. Submerged jet impingement, which occurs when there is only one type of fluid involved, ejects a fluid through a grid of constrictive cavities upon a higher temperature heat source. The heat transfer rates for these scenarios are typically much higher when using water but impingement using air still provides an improved heat transfer over traditional forced convection. Low jet-to-target spacing and high Reynolds numbers in experimental setups prove the most effective when using air jets. (Glynn)

2.3.6 Synthetic Jet

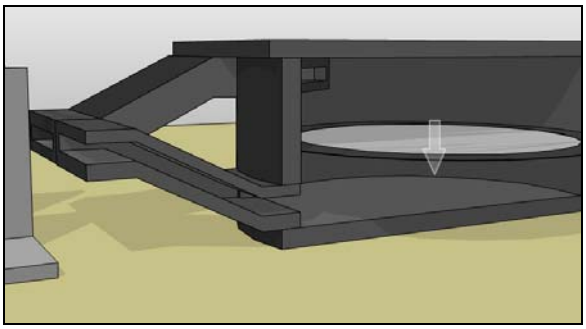

Figure 2-10: A cutaway view of a synthetic jet device from Nuventix (©)

As seen already in jet impingement, jets can be useful in cooling situations. These concentrated bursts of fluid can travel for longer distances without dissipating. A synthetic jet has an added trait that synthesizes surrounding air, resulting in airflow many times greater than the initial jet burst. A specific type of synthetic jet is available commercially as a driven diaphragm device. These devices will oscillate a diaphragm periodically expelling bursts of air which will eventually synthesize much more airflow than that of the original burst. (Shankara) This technology, when combined with other cooling techniques, can increase heat transfer rates by ensuring turbulent flow in forced convection applications and increasing the airflow in cases where only natural convection occurs.

2.3.7 Foam Heatsink Materials

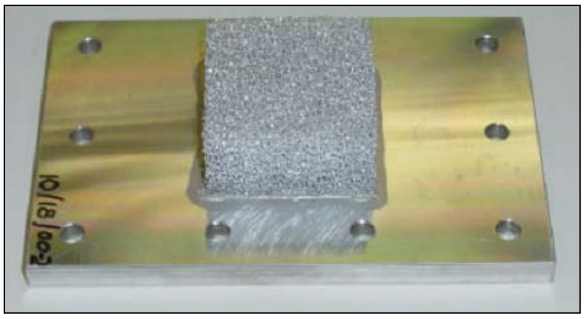

Figure 2-11: A block of aluminum foam (© Klett)

The application of very porous "foam" metal structures as heat transfer elements provides a number of interesting possibilities. While the heat transfer rates for simple foamed aluminum is less than its solid counterpart the material is much less dense and well suited for low weight applications. Developments in carbon foams have produced a workable material with even greater thermal properties. Graphitized foam blocks have thermal conductivities slightly higher than those of solid aluminum blocks but a specific gravity of less than a fourth. (Klett) This fact proves very useful in an environment where weight is an issue. The process of creating graphitized foam from traditional carbon foams revolves around a heating process that expands existing bubbles to facilitate alignment of liquid graphite crystals within the lattice. This process is valuable to increase the thermal properties of the material but is not immediately available commercially.

Manufacturer specifications regarding pressure drops and other mechanical properties can be found in Appendix B.

- **Thickness**

  Past a certain foam thickness, heat transfer will no longer be effective at cooling. Any additional material after this length will not contribute to heat transfer. Large thickness values can potentially be beyond the useful length of foam thus it will be valuable to test different thicknesses.

- **Pores per Inch (PPI)**

  Materials with higher pores per inch have smaller pores. Smaller pores will increase the complexity of the fluid pathway thereby increasing the pressure drop.

- **Density**

  The second variable that must be considered here is the density of the foam. The manufacturer has a number of available aluminum foam densities, all of which are best suited for some particular process. Higher densities of the aluminum foam will provide larger values of heat conduction but can be a detriment to airflow. The team worked together with the foam manufacturer and determined that the best suited density for convective heat exchangers using air as the fluid would be in the range of 10% density.

2.4 Testing rig research

Development of the testing rig involves a non-trivial design process. To gain knowledge regarding the various components of the testing about possible materials and components the following items are brought up for consideration.

2.4.1 Thermal Properties of Insulator Materials

A common term used as a measure of insulation's capacity to slow heat flow is R-value. The R-value is equivalent to the thickness of a material divided by the product of thermal conductivity k and area of the insulator. (Spang) The R value can be described in common terms as the resistance heat encounters when trying to travel through a particular substance. The perfect insulator would have a low k×A value and a very large thickness causing the R-value to be very large.

2.4.2 *Other Properties of Insulator Materials*

Many different types of thermal insulation are designed to perform in a variety of temperature ranges. Some types of materials are capable of withstanding cold temperatures. Rigid Polyurethane Foam, PVC Foam, Cork and Polyimide Foam are examples of such materials. These materials typically have higher R-values than materials that are suited for higher temperatures. Insulators such as Fiberglass and Mineral Wool are capable of withstanding high temperatures typically up to a few hundred degrees Fahrenheit. The last category of insulators actually have the lowest R values but are capable of withstanding much higher temperatures up to 1000°F and beyond; these are made from materials such as Ceramic, Silica, Calcium Silicate, and Millboard. (McMaster-Carr)

Table 2-1: Examples of Common Insulator Materials

Insulation Material	R-value @ 1/2" Thick	R-value @ 1" Thick
Expanding Foam	2.5-3.0	5-6
PVC Foam	2.6-3.0	5.2-6.0
Polystyrene Foam	1.9-2.5	3.8-5.0
Polyurethane Foam	1.7-2.6	3.3-5.3
Bubble Wrap	2.1	4.2
Polyimide Foam	2.1	4.2
Polyethylene Foam	1.9-2.0	3.8-4.0
Mineral Wool	1.9-2.2	3.7-4.3
Foam Rubber	1.9	3.7-3.8
Melamine Foam	1.9	3.8
Cork	1.8	3.6
Cellular Glass	1.7	3.4
Fiberglass	0.8-2.4	1.7-4.8
Silicone Foam	1.3	2.5-2.6
Ceramic	0.4-1.8	0.8-3.6
Silica	0.6	1.3
Millboard	0.5-0.7	1.0-1.4
Calcium Silicate	0.5-0.7	1.0-1.4

2.4.3 *Temperature measurement*

Temperature measurement can vary greatly in complexity. From a simple glass bulb thermometer to wireless infrared emissivity sensors, options for temperature measurement are easily obtained. The most cost-effective and appropriate solution for this measurement in the ranges and environments that the project entails are likely thermocouples. These devices utilize the Seebeck effect, the useful property of dissimilar metals to generate a voltage when attached to a temperature gradient. Using commercially available combinations of metals and standardizing the measurement methodology thermocouples have become cost effective tools to measure temperature (within a moderate range of accuracy) in the industry.

Table 2-2: Common Thermocouple Temperature Ranges (© Omega)

Common Thermocouple Temperature Ranges

Calibration	Temp Range	Std. Limits of Error	Spec. Limits of Error
J	0°C to 750°C (32°F to 1382°F)	Greater of 2.2°C or 0.75%	Greater of 1.1°C or 0.4%
K	–200°C to 1250°C (–328°F to 2282°F)	Greater of 2.2°C or 0.75%	Greater of 1.1°C or 0.4%
E	–200°C to 900°C (–328°F to 1652°F)	Greater of 1.7°C or 0.5%	Greater of 1.0°C or 0.4%
T	–250°C to 350°C (–328°F to 662°F)	Greater of 1.0°C or 0.75%	Greater of 0.5°C or 0.4%

2.4.4 Power to Force Convection

- **Using Fan Curves and Efficiency**

Since one of the main factors in this project is computing the dimensionless ratio of rate of heat transfer (a power term) from a system over the power used to bring about this cooling it is important to understand exactly how to determine the amount of power used to move the air that causes forced convection. The power input into a fan motor can be easily measured using a common voltmeter/ammeter, however this value will be greater than the amount of power actually used to cause convection because of the reality that fans will never be 100% efficient. To more accurately determine power used information regarding efficiency of a fan at a certain operating point must be made available.

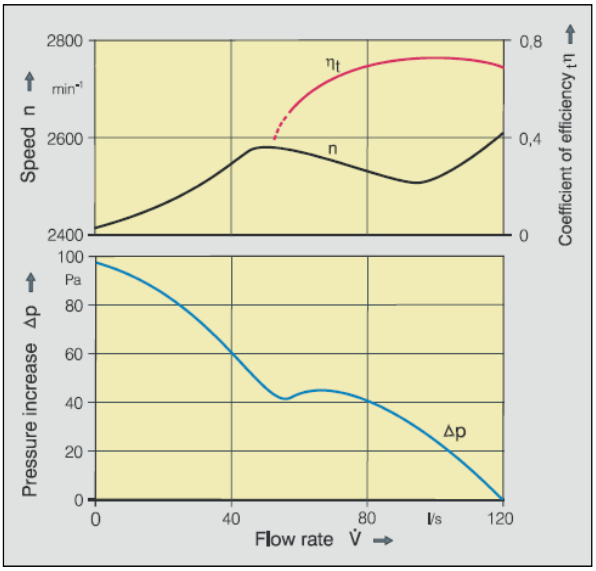

Figure 2-12: Change in speed and efficiency of an axial fan (© EBM Papst)

Figure 2-12 shows the fan curve for a theoretical axial fan and the corresponding rotor speed and efficiency curve. With the knowledge of an operating point (easily determined

by measuring the flow rate) and instrumentation measuring the power used by the fan, calculating the power used to force convection is as simple as multiplying the coefficient of efficiency by the power used.

- **Using Pressure Drop**

Efficiency curves are rarely available for fans, dictating the need to use another method to estimate the power input into the air necessary for forced convection. For a forced air test set-up with a fan placed downstream of the heat exchanger, this can be related to the head loss caused by the tested heat exchangers. A general form of this head loss equation along a single streamline between a distance before heat exchanger inlet to between the heat exchanger and fan is given in Equation 2-9.

$$\left(\frac{P_1}{\rho_1}+\frac{\alpha_1\overline{V_1}}{2}+gz_1\right)-\left(\frac{P_2}{\rho_2}+\frac{\alpha_2\overline{V_2}}{2}+gz_2\right)=h_{total}$$

Equation 2-9

Equation 2-9 can be reduced to Equation 2-10 with the following assumptions:
1. Air acting as Newtonian and incompressible fluid
2. Constant air density, ρ
3. Turbulent flow ($\alpha \approx 1$)
4. Streamline begins in a large reservoir with initial average velocity ≈ zero
5. Neglect entrance losses
6. Neglect changes in height

$$\frac{P_1-P_2}{\rho}-\frac{\overline{V_2}}{2}=h_{HX}$$

Equation 2-10

Head loss can be converted to power by relating it to the mass flow rate of the air shown in Equation 2-11.

$$P_{air}=\dot{m}h_{HX}$$

Equation 2-11

Combining Equation 2-10 and Equation 2-11, a final relationship of power into the air is displayed in Equation 2-12.

$$P_{air}=\dot{m}\left(\frac{P_1-P_2}{\rho}-\frac{\overline{V_2}}{2}\right)$$

Equation 2-12

Therefore, it is shown that the power input to the air is a function of the change in its pressure, average velocity at downstream point, and mass flow rate. The change in static air pressure before and after the test heat exchangers can be estimated by measuring the differential pressure from ambient air to a point slightly downstream of the air flow within the testing rig. A differential monometer can quickly measure this value. The average exit velocity will also need to be measured. The mass flow rate can be determined with this velocity measurement, the cross-sectional area at the location of the velocity measurement, and determining the air density based on air pressure and temperature.

2.4.5 Heaters

It will be necessary to heat portions of the project to simulate actual operating conditions. Creating heat is certainly easier than removing it. Heat generation can be accomplished as easily as passing current through a conductor. This is the basic theory behind resistive heaters, products commonly commercially available in a number of different sizes and ratings.

Figure 2-13: A sampling of resistive heaters available commercially (©Directindustry.com)

Since these devices are merely resistors, any AC or DC power ratings are irrelevant as long as the overall wattage rating falls at or below the value specified by the manufacturer, keeping the power levels below this specification is important to ensure the excess heat does not melt any of the resistive elements. Powering the devices is accomplished by simply attaching in a circuit with a AC or DC power supply of sufficient wattage rating.

3 DESIGN REQUIREMENTS AND SPECS

Per Boeing's need for a more efficient method of electronics cooling, one goal in this project will be to determine the maximum thermal capability of the AECM module with advanced air-cooling. The Sector h team will design and build a prototype to measure the maximum possible wattage each AECM module can dissipate with fan power comparable to the ARINC 600 cooling standard. Form factor changes to the module will be necessary to accommodate airflow and more efficient geometries for convection.

A used a method called Quality Function Deployment (QFD) was used to translate the customer's needs and requirements into engineering specifications. To prioritize these specifications the team looked at how well they correlate to each need. The resulting "house of quality" created from the QFD method is attached as

Appendix C. A summary of specific project requirements is also given in Table 3-1. The proposed product requirements were generated from the current baseline configuration with liquid-cooled cold plates. All of the project specifications and goals are designed for the prototype only and not for final production but should be somewhat indicative of desired performance of a final product.

Table 3-1: Formal engineering project requirements

Spec. #	Parameter Description		Requirement or Target	Tolerance	Risk	Compliance
1	Weight		6.5 lb	Smaller is Better	M	A, T, I
2	Spacing between modules		0.40 in	Smaller is Better	L	A, I
3	Module Dimensions		10.2 by 7.9 in	± 0.1 in	L	A, I
4	Module Thickness		0.69 to 1.50 in	Smaller is better	L	A, I
5	Component Temperatures		105 °C	± 1 °C	L	A, T
6	Flow Rate of Air		5 to 70 CFM (varying)	Smaller is Better	M	T
7	Power Consumption		TBD	Min	H	T
8	Incoming Air Temp	Experimental Temperature	Room Temp (~21)	± 3 °C	L	I
9		Low Short-term	-40	± 3 °C	M	A
10		Low Continuous	-15	± 3 °C	M	A
11		High Short-term	70	± 3 °C	M	A
12		High Continuous	55	± 3 °C	M	A
13		Normal Ground	45	± 3 °C	M	A
14		Normal Flight	30	± 3 °C	M	A
15	Ambient Air Temperature		Room	-	L	I
16	Heat Dissipation		TBD	Min	H	A, T
17	Cover Plate Material		Al 6061	-	L	I
18	Total Prototype Cost		$3,000	Max	H	-

This engineering specification table lists requirements, tolerances, risks and compliances for a series of individual specifications. Requirements or targets are listed with associated risk of completion: L (low risk), M (medium risk), H (high risk). How the team expects to validate these requirements is listed under "compliance" in the form of A (analysis), T (testing), and I (inspection).

3.1 Weight

Prototype weight will be no more than 35% larger than the baseline AECM module weight estimated to be 4.8 pounds. While the goal will be to minimize any changes to system weight, this relatively large increase will make up for construction limitations of the prototype. The overall thickness of the plates will also be increased, increasing weight. Minimizing weight will make the module easier to handle, possibly reduce material costs and increase suitability in an aeronautical environment.

3.2 Module Spacing

In order to maximize the number of AECM modules per volume, the modules should be placed as close together as possible. It is possible that the current spacing of 0.03 inches will facilitate convection based heat transfer between plates. Therefore, the team chose a maximum spacing between the new module form-factor to be 0.40 inches.

3.3 Flow Rate of Air

Flow rates for testing will range anywhere from 5 to 70 CFM, this will enable the team to determine and report upon ideal operating conditions and heat dissipation at various scenarios.

3.4 Power Consumption

The power input required for specific heat dissipation must to measured, and then compared to that heat dissipation. This ratio of power consumption to heat dissipated will be critical in determining the efficiency of the new modules. Ideally, power consumption should be at a minimum, but if a more ideal power consumption ratio occurs at a large power consumption value the larger power consumption may be preferred.

3.5 Intake Air Temperature

During aircraft operation, the incoming air temperature used for cooling will vary greatly. Current testing standards for air temperatures are numbered from 8-13 in Table 1 and must be considered in final analysis. Due to experimental constraints, the team will test the chosen design using room-temperature air only. The intake air temperature will be compared to the component temperature. This change in temperature can be used to roughly extrapolate the equivalent component temperature for all the other intake temperature standards. Equivalent component temperatures will not exceed 105 °C as stated under item 4.

3.6 Heat Dissipation

As a baseline for comparison: an analysis involving a proposed AECM liquid cold plate conduction module yielded a result of 240 watts of heat of dissipation. Though air-cooling could more evenly dissipate the heat over the entirety of the boards and would be able to directly cool the module at all surface locations air simply does not have the heat capacity that liquids do so heat transfer will possibly suffer. The hope is that by using improved air-cooling only, the current ARINC air cooling standard of 140cfm per kW of heat dissipation can be far surpassed.

4 EARLY DESIGN DEVELOPMENT

The selection of general designs to eventually prototype and build required a number of iterations. These iterations are discussed in this section and result in the selection of two basic types of plate. The specific dimensioning and design of these two plates is featured in section 5.

4.1 Idea generation

The team used a few different idea generation techniques to draw out any and all possible ideas relevant to the project. Some of the techniques involved providing a random word or quote to facilitate the production of any possible solutions. The results of these brainstorming sessions were posted on sticky notes and categorized into appropriate logical categories. A picture of this "idea poster" at an early state can be seen in Appendix D.

After the elimination of any irrelevant or unreasonable ideas, the remaining thoughts were clumped into 15 different design solutions. These early design ideas acted primarily as thought-experiments.

4.1.1 Datum

Simple fin heatsink attached via some thermal interface material on both sides of the module, parallel to airflow from top to bottom.

4.1.2 Machined Heatsink Into Module Cover

Module cover features a machined surface that serves as a heatsink. Unlike the Datum, this design does not attach the heatsink to the module cover; the cover itself is the heatsink.

4.1.3 Direct PCB Cooling

Similar to ARINC 600 Specifications with air flowing directly over the PCB, module covers exist to protect circuit boards and incorporate slots to allow airflow to cross over the components.

4.1.4 Heatpipe to Advanced Enclosure Hear Exchanger

Heat pipes mounted to the sides of the modules, drawing the heat to external advanced heat exchangers. Heat dissipation would be excellent, however the boards may be spaced farther apart, and changes in pressure for the heat exchanger may be large. It is also very costly with custom heat pipes.

4.1.5 Wrap Around Heat Pipes

Heat pipes bring heat from opposing sides of the modules and are cooled with heatsinks sandwiched between every-other board.

4.1.6 Add-a-fin setup

Modular fin style allowing for expanded setups for hotter boards

4.1.7 Front Entry Airflow

Similar to baseline. Additional fans provide air flow from front of cabinet, exiting at the top and bottom.

4.1.8 Perpendicular Grooves

Grooves cut into the covers perpendicular to the flow. This potentially increases the heat dissipation while allowing the plates to be closer together. The slots increase air turbulence, increasing convection. It's simplistic design makes it a cheap and durable solution. However, it is not the most effective method of heat transfer within the design matrix.

4.1.9 Synthetic Jet Microchannel

This design entails incorporating some sort of synthetic jet device onto the module cover. The additional convective turbulence should aid the already existing cooling convective flow.

4.1.10 Offset Perpendicular Fins

Offset fins perpendicular to the flow. A modification of number 2, this design should greatly increase heat dissipation, but will also increase the change in pressure, requiring a more powerful fan or blower.

4.1.11 Stacked Fins

This design features microchannels perpendicular to the flow with larger conventional fins on top parallel to the flow. This would likely increase convection, but will be more costly and may take up more space.

4.1.12 Heatpipe Cooled Cold Cabinet with Advanced Heat Exchanger

Modules incorporate heatpipes with high thermal conductivity to transfer heat to the upper and lower surfaces of the cabinet. In this scenario the modules can be very closely spaced but the overall cooling surface area possible is reduced.

4.1.13 Heat Spreader with Heat Sink

Similar to the Datum, this device incorporates a phase-change heat spreader to equalize the temperature across the entire plate, ensuring maximum cooling and reducing possible hot-spots.

4.1.14 Heatpipe heat distribution through fins

Past a certain length, convective fins do not aid significantly in heat transfer. This design incorporates heatpipes along the surface to draw heat out to the farther reaches of the fins, ensuring the whole length of the fin is utilized.

4.1.15 Carbon/Aluminum Foam

This is a possible fin/peg material with higher possible heat dissipation when forced air is used. It may also be applicable to any advanced external heat exchanger that may be used.

4.2 Interim Decision Plan

4.2.1 Interim Decision Matrix

These early design ideas were finally used in a decision matrix with the goal of obtaining a new, reduced set of possible approaches. The decision matrix itself, located below, has a number of categories that were important to the elimination process. Each of these categories were given an importance weighting on a scale of 1 to 10 with 1 meaning less important and 10 meaning most important.

Table 4-1: Interim Decision Matrix

		Heat transfer	Number of Boards	Total Weight	Ease of Manufacture	Compatible with Trays	Durability /Reliability	Pressure Drop	Cost	Audible Noise	Easy to Handle	
	Weight Factor → / **Concept Name ↓**	***10***	***7***	***7***	***6***	***6***	***5***	***5***	***4***	***2***	***1***	**Total Score**
1	**Attach Pre-made Heatsinks**	***D***	-	***A***	-	***T***	-	***U***	-	***M***	-	**0**
2	**Machined Cover Heatsink**	1	0	1	0	0	1	0	0	0	0	**22**
3	**Direct PCB Cooling**	1	2	1	-1	-1	-1	0	-2	1	2	**10**
4	**Heatpipe to External Advanced Heat Exchanger**	2	1	-1	-1	-2	0	1	-2	-1	0	**-3**
5	**Heatpipes Wrapped Around the Module**	0	1	0	-2	0	-1	0	-2	0	-1	**-19**
6	**Add-a-fin setup**	-1	0	-1	-1	0	-1	1	-1	0	-1	**-28**
7	**Front entry airflow**	1	0	0	-1	-1	-2	0	0	-1	0	**-14**
8	**Perpendicular Grooves**	0	0	1	0	0	0	-1	0	1	0	**4**
9	**Synthetic Jet Microchannel**	2	0	0	-1	0	-1	1	-1	0	0	**10**
10	**Offset Perpendicular**	1	0	0	0	0	0	-2	0	0	-1	**-1**
11	**Stacked Fins**	2	0	0	-2	0	0	-1	-1	0	0	**-1**
12	**Heatpipe Cooled Cabinet with Advanced Heat Exchanger.**	2	2	0	-1	0	1	-1	-2	0	2	**22**
13	**Heat Spreader with Heat sink**	2	0	0	0	0	0	0	-1	0	0	**16**
14	**Heatpipe heat distribution through fins**	1	0	0	-1	0	0	0	-1	0	0	**0**
15	**Carbon/Aluminum Foam**	1	0	2	0	0	-1	-1	-1	0	-2	**8**

4.2.1.1 Categories seen in Interim Decision Matrix

- **Heat Transfer**

  Primarily viewed as the ultimate reason for this project, heat transfer is the most important factor, receiving the highest weight of 10.

- **Number of Boards**

  Number of boards refers to the size constraints that are important in an airplane environment. This factor takes into consideration the number of boards that can be installed into a set space.

- **Total Weight**

  Again, weight is also important on an airplane and receives a weight equally important to the "number of boards" category.

- **Ease of Manufacture**

  This factor is included as an early consideration with regards to the eventual construction of the prototype. It is important that the eventual prototyped developed can be manufactured within the resources available to the team.

- **Pressure Drop**

  Refers to the expected pressure drop across the boards. This is a fairly important consideration to make when realizing the eventual module installation would require airflow to pass from one bank of modules to another.

- **Compatible with Trays**

  A number of designs would require modifications to the insertion and removal process of the boards themselves. This factor takes into account how easily the boards could be managed in this manner.

- **Durability / Reliability**

  A few of the early designs include moving parts which should be seen as possible sources of failure, this factor accounts for this possibility.

- **Cost**

  It should be noted that the cost in this decision matrix refers to the probable costs of the prototype only. No considerations are made for possible eventual production as this falls outside of the scope of this very heavily research based project. This is why cost receives a somewhat lower weighting.

- **Audible Noise**

  More of an aesthetic rather than performance based category, it is important to keep noise within reasonable limits for devices such as these.

- **Easy to Handle**

  This factor accounts for any sharp edges or operator safety factors when removing or installing the modules.

4.2.2 Interim Designs (5 chosen designs)

Finally the decision matrix was used to eliminate unsuitable design ideas. Each concept design was weighed against a datum design for each category. If the concept improved upon the datum it would receive a positive value, if it was worse, it would receive a negative value, if it neither improved nor detracted from the datum overall, a zero value was reported. These values ranged from –2 to +2 to provide a bit of flexibility to account for one particular design being much worse or better in a particular category when juxtaposed with other designs. The end result of the decision matrix was an overall score that factored in weights and gave a total score; it is these values that were used to choose the interim 5 concepts that are discussed in further detail.

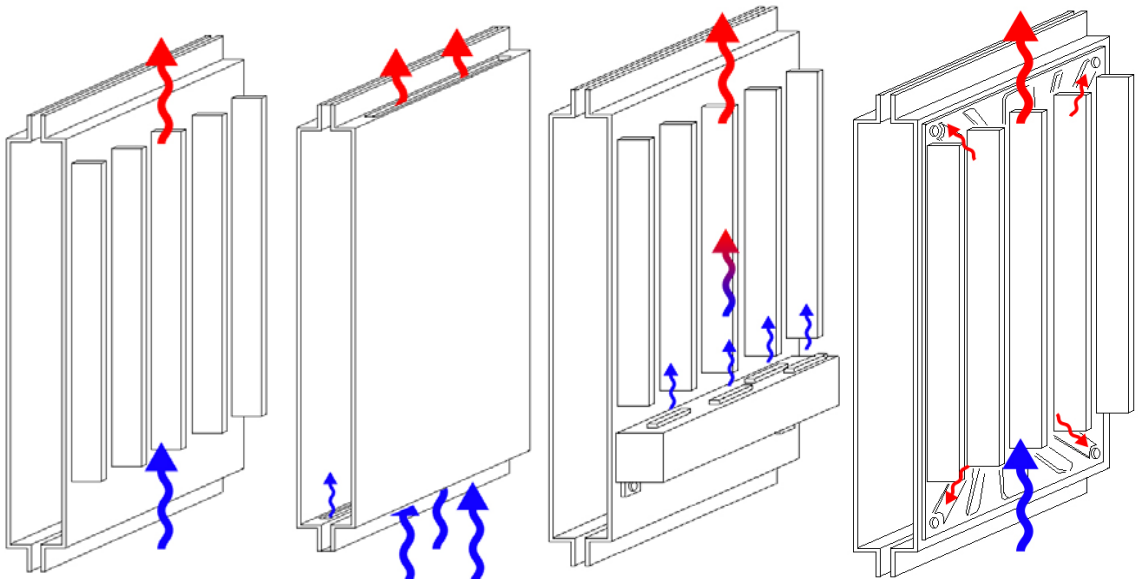

Figure 4-1: A) Machined Heatsink Into Module Cover. B) Direct PCB Cooling C) Synthetic Jet Microchannel D) Heat Spreader with Heatsink*

**These figures are basic representations of the encompassing idea, they are not meant to represent an actual finalized design and are not by any means to scale or fully representative of the proper device.*

4.2.2.1 Machined Heatsink into Module Cover (Figure 4-1A)

This concept involves directly machining conventional fins, pegs, or other geometry into the aluminum module covers. Air would be forced over the plates directly between the modules from the top to bottom of the cabinet. This would eliminate any contact resistances created by attaching heatsinks or other cooling device. The fins or other chosen geometry would increase the area in contact with the flow, increasing heat transfer compared to blowing the air over a flat place. This will not be the most effective method of heat transfer when compared to more advanced techniques however, this simplistic design will be a cheaper alternative to the other designs, be easier to

manufacture, have increased reliability and medium pressure drop, resulting in cheaper operating costs.

4.2.2.2 Direct PCB Cooling (Figure 4-1B)

Holes along the top and bottom edges of the module open only when the module is engaged with the cabinet. This should have minimal effect on current electronic shielding, however changes in effective shielding must still be considered in the analysis. The air will flow from the bottom directly over the PCB. This may increase heat transfer by eliminating the thermal resistances of the many layers of material between the boards and airflow. Increase backpressure is possible depending on air inlet and exit geometries. Cost and reliability could be an issue in the complexity of this system, although space can be conserved by allowing the modules to be densely packed together, without requiring space for airflow between them. The team chose to continue exploring this design because of the uncertainty and possibility of greatly increased heat dissipation.

4.2.2.3 Synthetic Jet Microchannel (Figure 4-1C)

Microchannels parallel to direct air flow over the AECM modules would be machined or attached to the aluminum module covers. Supplemental jets will be placed upstream to increase turbulence and assist in airflow over the plates. They may be located directly on the modules or on the cabinet as deemed necessary. The channels would increase the exposed surface area and stimulate turbulent, highly convective flow. This would increase heat transfer at the expense of increased backpressure. Synthetic jets will assist in mixing even more. The jet will need to be powered by an electrical system, increasing power consumption. However, they may greatly increase heat transfer. The team will need to weigh the benefits of increased heat transfer to increase power consumption and may also discover that replacing the microchannel with thin conventional fins will be more cost effective.

4.2.2.4 Heat Spreader with Heatsink (Figure 4-1D)

A thin phase-change heat spreader (as seen in Figure 2-8) would be placed on both sides of the modules to more evenly distribute the heat to attached traditional heatsinks. Air is then forced over the sinks as described in section 4.2.2.1. Results would be similar to the aforementioned design, however the heat spreader would more evenly distribute the heat away from problem areas, increasing the efficiency of an attached custom heatsink. If the heat spreader is not directly integrated into the module increased thermal contact resistance may be an issue, but modern thermal grease and other bonding materials might allow for a net increase in heat dissipation.

4.2.2.5 Heatpipe Cooled Cold Cabinet with Advanced Heat Exchanger

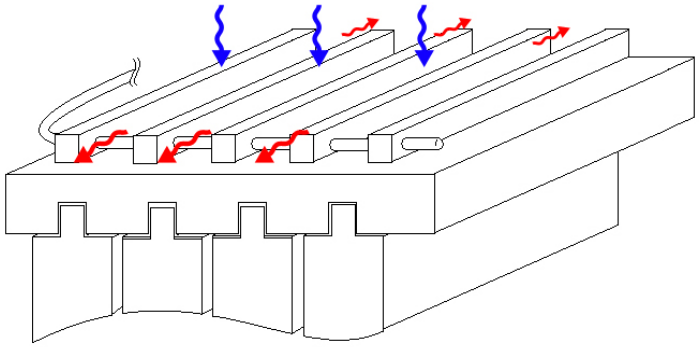

Figure 4-2: Interim Design: Heatpipe Cooled Cold Cabinet with Advanced Heat Exchanger

Heat Pipes imbedded into the top and bottom cold plates could be used to replace the current liquid-cooled system. The heat pipes would then be connected to an external advance microchannel heat exchanger. Heat pipes have proven to be an excellent method of heat transfer in personal computer applications, and will likely be just as effective on an industrial scale. They will provide high heat transfer between the boards and heat exchanger(s), and allows the boards to be very close together, resulting in significant space saving. An external heat exchanger will allow for less restricted designs and improved heat dissipation. Increased prototype cost will be an issue. Overall system weight may also increase.

4.3 Obtaining Current Designs

Discussion and considerations regarding the 5 chosen interim designs have been made since the development of the interim report. This section will cover some of the deliberations made regarding these choices and the reasoning behind the selection of the final two module form-factors.

4.3.1 Accepted Designs

4.3.1.1 Machined Heatsink Into Module Cover (Figure 4-1A)

The first of the five interim design choices: Machined Heatsink Into Module Cover needs little modification from the form presented above in 4.2.2.1. It should be understood that the possible specifics of this have been expanded to include any sort of possible geometry, as long as the geometry is homogenous with the material of the module cover. In other words, the final design(s) for this module cover form factor could make use of any sort of thermal transfer geometry including but not limited to: aluminum foams, extruded pins, machined or cast geometry, fins and any combination of the aforementioned geometries. Details of this design can be seen in section 5.1.

4.3.1.2 Sandwiched Foam Plates

This design did not exist during the interim decision making processes but is included in this the final stage because of the high surface area and cooling properties of the aluminum foam material. Details of this design can be seen in section 5.2.

4.3.2 Rejected Designs

4.3.2.1 Direct PCB Cooling (Figure 4-1B)

The design featured in 4.2.2.2, Direct PCB Cooling, was realized to offer little, if any, advantage with regards to heat transfer rates over the ARINC 600 specification and furthermore would require significant chassis modifications. Because of these severe limitations it has been eliminated as one of the options for further development.

4.3.2.2 Synthetic Jet Thin Channel (Figure 4-1C)

It has been determined that the synthetic jets should not be located on the module itself. This causes a problem in the areas directly beneath the synthetic jets lacking cooling and hurts the modularity of the panels because of the external power leads the synthetic jets would require. Furthermore, the synthetic jets have a very short effective cooling length. The cooling advantages provided by the inclusion of synthetic jets would only exist for roughly 1" of the module length.

4.3.2.3 Heat Spreader with Heatsink (Figure 4-1D)

Enough analysis has not been made to determine whether or not localized hot spots (which would be reduced with an effective phase change heat spreader) are a problem. If it is determined that the inclusion of a heat spreader would be beneficial, this option may remain as a possible future implementation, otherwise- it does not provide any advantage over a solid plate heat spreader which is present in every other design.

4.3.2.4 Heatpipe Cooled Cold Cabinet with Advanced Heat Exchanger (Figure 4-2)

The idea behind this design was to mimic the liquid-cooled AECM module modeled in the report prepared by Robert Wong. It has been discarded because it doesn't utilize the main advantage of convective cooling in this setup: the large hot planar surfaces of the module. Thermal dissipation rates could not be expected to ever reach the 240W seen in the liquid cooled scenario because of the significantly lower heat capacity of air.

5 HEATSINK DESIGN DEVELOPMENT AND DETAILS

5.1 Air Flow through Machined Aluminum Fins

5.1.1 Manufacturing Considerations

Other manufacturing techniques would be highly appropriate for a finned module plate. Similar products on the market today are often die-cast or extruded; processes not appropriate for prototyping. The possibility of using a investment casting method with a rapid prototyped model was considered too time consuming and costly, especially considering the mating surfaces would still require substantial machining. This left the most obvious and original idea of manufacturing remaining: CNC machining. Machining down to expose extruded fins suffers from limitations in dimensions of the fins, if the fins are machined too thin or too long they might fail during the machining process. Experimentation in the machine shop and experience of the laboratory technicians dictated that a thickness dimension of 1/16 inch should be acceptable with an extruded length of roughly 1/2 inch.

5.1.2 Extruded Fin Design Development

Intuitive knowledge dictates that extruded fins used for cooling purposes should be as long and thin as possible, but further analysis helps to confirm any lingering questions regarding this assumption. To analyze the fin design a simple program was written in MatLab to evaluate a large number of possible fin scenarios to determine design that would produce the maximum possible theoretical cooling as well as calculate efficiencies of the various designs. This analysis uses equations defined in Section 2.2.3 and assumes the fins are simple extruded rectangular prisms and that the system has a constant convective heat coefficient. The source code for this program is found in Appendix M.

To alleviate any unit problems in calculations all variables in the program were converted into SI units.

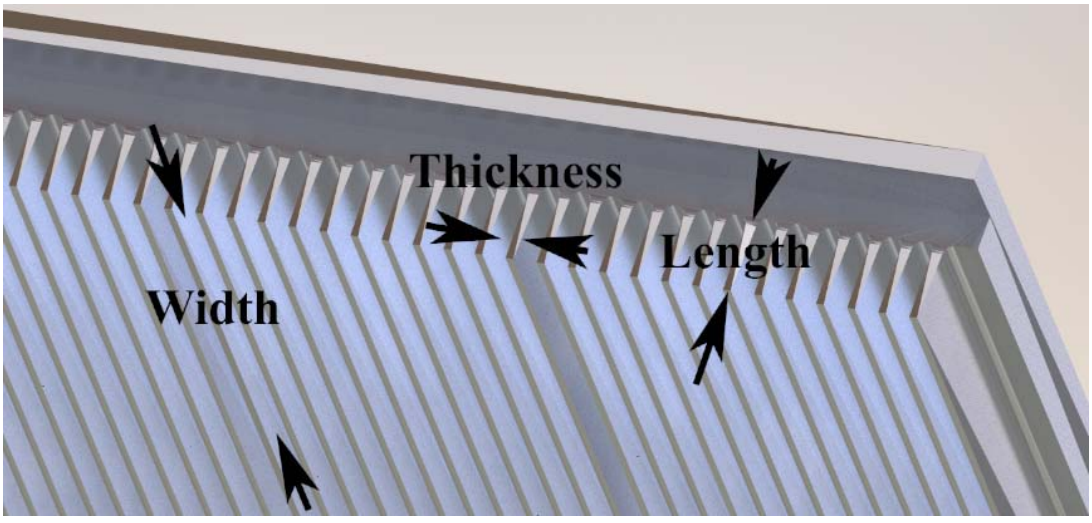

Figure 5-1: Width, Thickness and Length of fins as used in the MatLab program

5.1.2.1 Givens, Constants and Assumptions

This section establishes constants to be used later in the program. They include:

- **Width of fins: 7.120in**

- **Thermal conductivity of 6061 Aluminum: 180 W/m*K**
- **Assumed convection heat coefficient h of: 40 W/m^2*K**

  This is the most problematic assumption made in the program. h values would certainly change slightly with different fin designs but determining closed form solution for the exact values is difficult if possible.

- **Temperature at the base of the surface: 105 °C**
- **Temperature of the fluid: 70 °C**
- **Spacing between fins required for manufacturing: 1/8 in**

  The space between fins was assumed to be 1/8 inch to accommodate the milling bit that would fit between the fins.

5.1.2.2 Settings for loop resolution

This section defines the upper and lower limits for dimensions on both the thickness and extruded length of the fins. As stated in Section 5.1.1, thicknesses should be less than 1/16 inch and lengths no longer than 1/2 inches. Respectively, these are the minimum and maximum values set for these variables. The matching extreme values were selected within reason and a resolution of 0.01 inch to assure a large but not extreme sample size was used for analysis.

5.1.2.3 Create all possible scenarios

By far the most difficult section to program, this section creates a large array with every possible scenario of length versus thickness that is later used for calculations. This is accomplished by setting an initial value of length and proceeding through every possible size of thickness. The length is then incremented by one resolution step and thickness again runs through its values. This process is repeated until the length reaches its maximum value and all combinations are seen in the array.

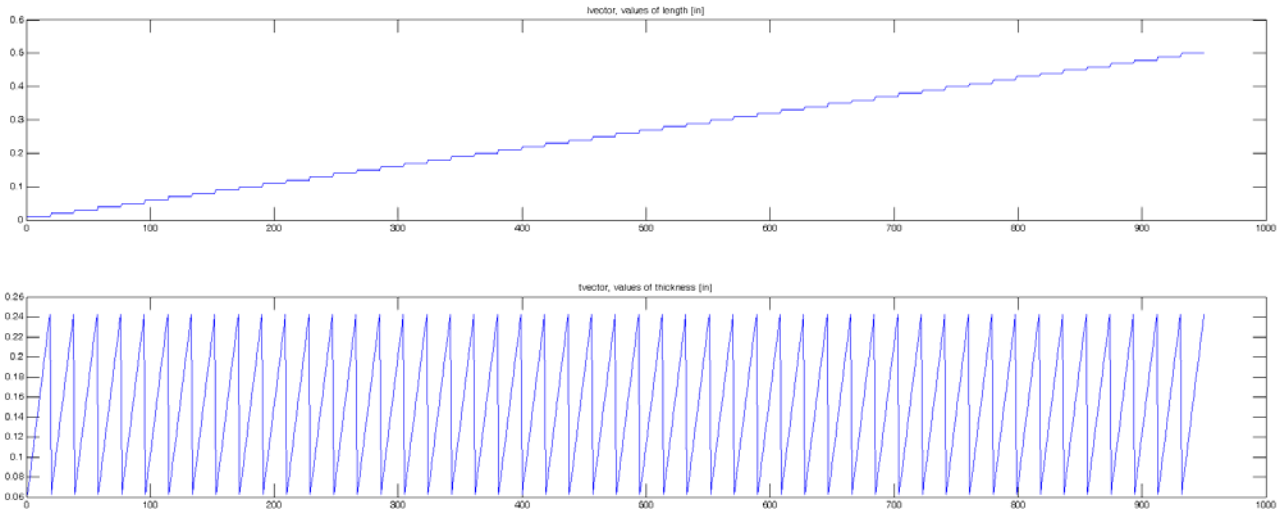

Figure 5-2: Plots showing the two varying values of length and thickness

The difficulty in this section came from a confusing result that caused a spike in the length vector when using a stepper index number for both length and thickness. This was finally fixed by entirely re-coding the section using a single stepper index to increment the array location.

5.1.2.4 Number of fins that will fit

Very straightforward, this code simply finds the number of fins that will fit on the plate it takes into consideration the thickness, the spacing between modules and the width of the plate.

5.1.2.5 Infinitely long fin

One value that is readily determined is the heat transfer from a fin of infinite length. With this knowledge it becomes possible to calculate the length of a fin that would transfer 99% of the heat from the infinite fin. It was important to find these values to ensure the fins were not extravagantly long.

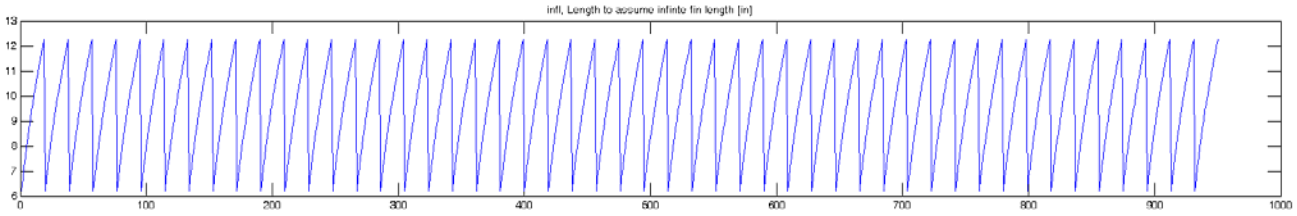

Figure 5-3: Plot showing lengths of fins to produce heat transfer rates 99% of an infinite length fin

The maximum length of 1/2 inch does not even come close to approaching the 6 inch minimum result of this calculation. This makes it clear that the fins will have fairly high efficiency there is no need to worry about too long of a fin.

5.1.2.6 Heat transfer from one fin

This value is used both as a stepping stone for the total heat transfer from the surface and as an important factor in the fin performance factor and fin efficiency calculations.

5.1.2.7 Fin performance factor

A fin performance factor above 2 is necessary. Any less than that and it is not worthwhile to add extruded surfaces at all.

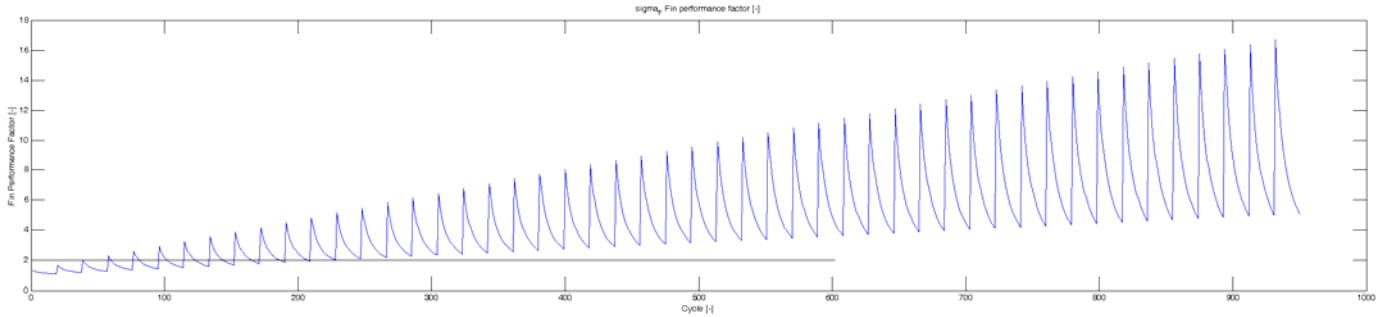

Figure 5-4: Fin performance factor spanning all size combinations

The results show a performance factor ranging from roughly 1 to as high as 16, the largest value occurs at the start of the last length setting which denotes the configuration with the longest and thinnest fins. Any value above the 250th cycle has a performance factor above 2. This number can be referenced in the length array and indicates that the fins should at least be 0.13 inches long.

5.1.2.8 Overall Surface Efficiency

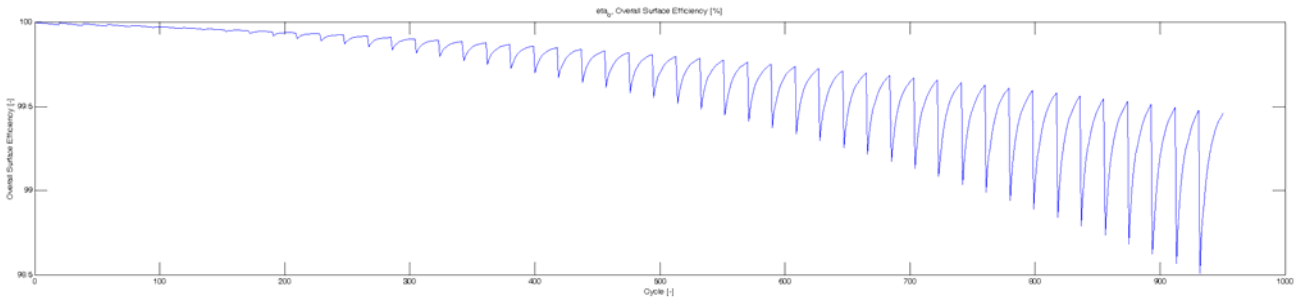

Figure 5-5: Overall Surface efficiency

As expected, the surface efficiency decreases as the length of fins increases. The absolute values are all very high however. The worst case still has 98.3% efficiency. This indicates that efficiency is not necessarily an important factor in this particular design.

5.1.2.9 Total Heat Transfer from Surface

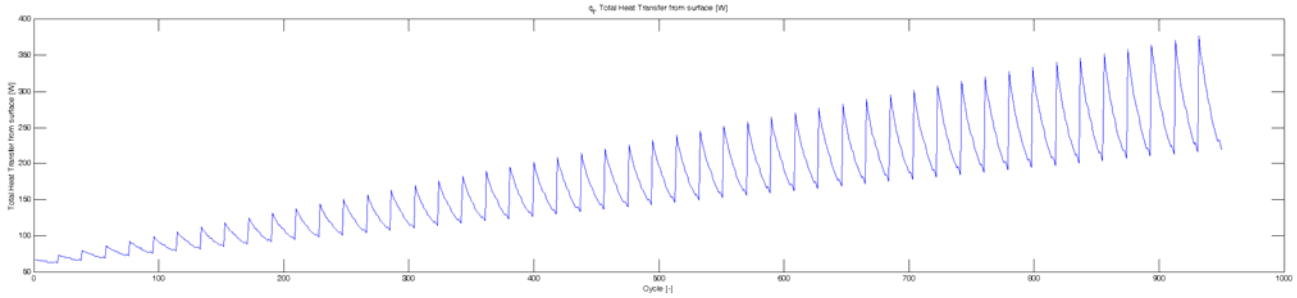

At 376.15 Watts, the maximum calculated heat transfer rate from this simulation occurred at the point with the longest length and smallest thickness. This configuration also has the highest performance factor making it an easy choice.

5.1.2.10 Selection of dimensions

The program provided indication that the fins should be made as long and thin as possible within the ranges specified by manufacturing constraints.

While in hindsight this is fairly obvious, it is important to validate and ensure there are no major problems in efficiency or performance factors.

5.1.3 Finned Plate Design Details

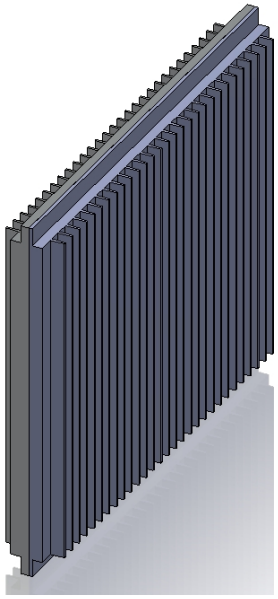

Figure 5-6: Model of Machined aluminum plates with extruding fins. The plates are separated into two halves.

This design makes changes to the AECM specifications that occur only on the outermost face. These fins will extrude outward from the face.

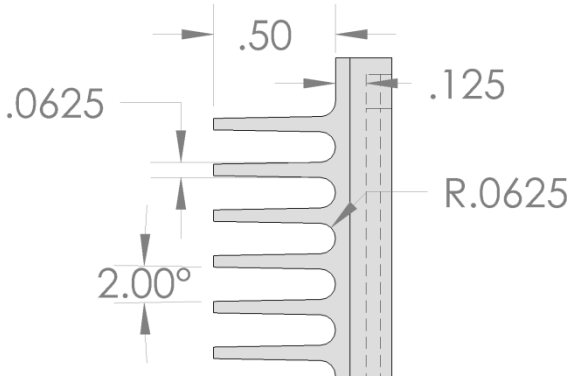

Figure 5-7: Actual fin dimensions in inches. Fins repeat 49 times; Drawing not to scale.

As seen in Figure 5-7 the extruded length was kept at (0.50) inches. The fin thickness at a nominal depth is 1/16 (0.0625) inch and to preserve quality when machining the plate thickness between therm-a-gap and fins was increased to 1/8 (0.125) inch. The 1/8 round at the base of the trough is introduced to reduce stress concentrations and for aesthetic and ergonomic purposes. A slight 2° taper is introduced to help add surface area to help offset the lost surface area introduced by rounding the trough. The plate supports 49 extruded fins along its length. Each model would feature 98 fins total. The fins are offset from the edge so that they can "mesh" if desired.

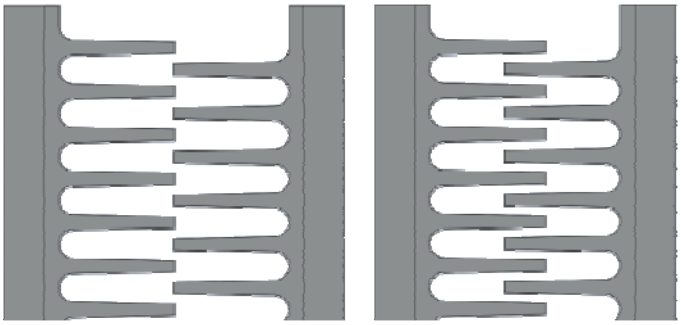

Figure 5-8: Illustration of fin "meshing."

5.2 Air Flow through Aluminum Foam

5.2.1 Foam Block Design Development

5.2.1.1 General Design

Section 2.3.7 overviews basic information regarding selecting the density and PPI of the porous foam material. The dimensions were chosen to account for a variety of possible configurations while still fitting within the project specifications.

- **Materials**

  The materials chosen were selected to minimize pressure drop. The two smallest pore per inch values available from ERG Aerospace were 5 and 10 PPI. 10% Density was chosen to ensure proper thermal conductivity and provide reasonable structural rigidity. The material

- **Dimensions**

  The foam blocks are sized to fit within the confines of the testing plates. Two thicknesses are used to determine how cooling capabilities change with this variable.

  Final dimensions are: 0.624"x6.994"x9.324" and 0.874"x6.994"x9.324".

- **Mating**

  Ideally, the foam blocks would be brazed to the actual plate surface. Another lesser possibility is brazing the blocks to a flat aluminum sheet and affixing the sheet to the plate. The next best possibility, the choice made for this experiment, involves including a layer of therm-a-gap between the foam aluminum and the flat plates. The malleability of the therm-a-gap affords a decent thermal connection as the foam will cut into the material providing a solid thermal conduction path.

- **Cut Channels**

  In an effort to reduce the large pressure drop likely experienced by the various foam blocks, channels are created to reduce the path through which the air must travel through the foam.

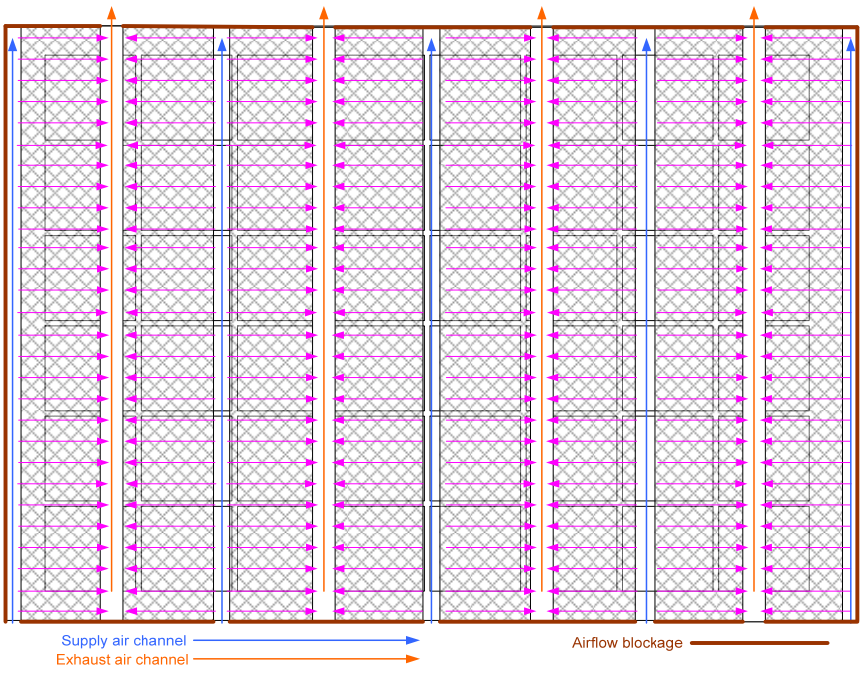

Figure 5-9: Theoretical air flow through one example of aluminum foam channels. (© Charlie Kusuda)

These channels are designed to reduce the pressure drop seen in the system. Appendix N shows the results of a rudimentary CFD analysis used to decide between two methods of channels. This analysis used the testing geometry along with assumed values for the porous material used to mimic the aluminum foam. Leaving a bit of material instead of butting the edge of the channel next to the exit reduced the pressure build up at the end, a desired result, by a slight 0.26 inches of water. The pressure reduction was expected to be seen as a reduction of the air travelling through the channel and "compacting" into the end of the channel. The decision to cut the foam in a zig-zag pattern was partially driven by this, but less so than the desire to manufacture the channel foam blocks in a manner that did not require later alignment and assembly.

5.2.1.2 Specific Block Setups

- **Uncut Thick foam 5ppi**

  This setup serves as a baseline.

- **Uncut Thin foam 5ppi**

  This setup is included to determine how important the foam thickness is. Similar cooling compared to thicker 5ppi would indicate that the material in the middle of the thicker foam does not contribute greatly to heat transfer.

- **Uncut Thick foam 10ppi**

  This setup should result in the largest pressure drop and is likely to provide the largest overall value of cooling. It will be valuable to directly compare to the uncut thick 5ppi foam.

- **Cut Thick Foam 10ppi**

  The large pressure drop likely experienced by the uncut thick 10ppi foam make this block a good candidate for channels.

- **Cut Thin Foam 5ppi**

  The large pressure drop likely experienced by the uncut thick 10ppi foam make this block a good candidate for channels.

6 TESTING VALIDATION

This section covers the various aspects of testing the module covers. Obtaining the desired result of heat dissipated per power input to force convection requires measuring and interpreting a number of factors that are discussed below.

In summary, the testing procedure for this set of engineering specifications will be to vary the heat output of the heating elements until a steady state temperature is reached that corresponds to the proper delta T between plate temperature and room temperature.

6.1 Factor of Performance

Developing some sort of standard to compare performance between designs is important. The absolute heat transfer rates of the devices tested will vary greatly, even among the same configuration, because the data will be recorded at greatly different flow rates. The Factor of performance serves to process the data and return a number that can be used to compare the efficiency of the various devices.

It is defined as the ratio of heat dissipation to power used to force convection. Symbolically:

$$F_P = \frac{q_{fins}}{P_{convection}}$$

Equation 6-1

- **Heat transfer from fins: q_{fins}**

  This is the amount of heat the configuration can handle without surpassing the delta T (difference between electronic component and incoming air temperature) of 35 °C.

- **Power used to force convection: $P_{convection}$**

  This is the power used to draw the air through the system. It will include the losses inherent in the testing setup, however these losses are consistent among the various configurations and of very small values compared to the losses seen through the plates; this small discrepancy is assumed to be negligible.

6.2 Measured Data (Testing Variables)

The testing devices must be able to measure important experimental data while allowing change to a number of independent variables. These testing setup variables are derived from Table 3-1 as appropriate; these are: heat generation, spacing between modules, intake air temperature (interpreted as Delta Ts), and the power used to force convection of the air.

6.2.1 Heat generation [W]

- **Strip Heaters**

  The testing rig must incorporate an element that simulates the heat output of a possible electronic system. Ideally, the wattage output can be varied precisely to simulate a wide range of possible electronic boards, the goals of this project call to maximize heat

transfer, not to design around a specific given heat output. Flexible Silicone heaters are well suited for this purpose.

- **Adjustable Power Supply**

Figure 6-1: Variable Autotransformer (Attributed to C J Cowie)

Using DC lab heaters simplifies the process of recording the amount of heat introduced to the system. If the comparatively small heat losses in the wires leading to the devices are neglected, it is safe to assume that the heaters are 100% efficient. That is, the power input to the strip heaters is exactly equal to the heat output. The corresponding power input can be altered using a device known as a variable autotransformer . These devices allow the user to finely adjust AC voltage output from 0V up to levels often as high as 140V.

- **Measuring Wattage**

A watt meter that compensates for the complexities of AC power generation will be attached to the Variable Autotransformer to provide reliable data regarding power input to the heaters. To account for the losses in the Variac device, the wattage measured using this device is reduced by 5% before entering the calculations; this assumes a Variac efficiency of 95%.

6.2.2 Spacing between Modules [in]

The design for the testing rig should allow for adjustments in the spacing between the modules within a certain range. This variable adjustment is important beyond simply accommodating heatsinks of differing sizes; it will be a variable that is tested when optimizing the final design. Different sized gaps between the paired module plates will greatly alter the pressure drop and consequently the power consumed to overcome the pressure drop. Being able to vary this distance enables optimization of this factor.

6.2.3 Intake and Exhaust Air Temperature [°C]

In the real-world scenario the electronic devices operate at a maximum temperature of 105°C. The corresponding cooling air acts at temperatures ranging from as low as -40°C and as high as 70°C. This corresponds to a maximum delta T of 145°C and a minimum delta T of 35°C. Since heat transfer due to convection is a linear function of delta T, it will be assumed for the purposes of this project that using delta Ts between ambient room temperature and the steady state temperature of the plates is appropriate and sufficient.

6.2.4 Plate Temperature [°C]

Steady state temperatures at various locations can be measured using a number of thermocouples. These devices would likely be fed into a data collection device that can provide digital logs of data over a period of time. The data will likely be a voltage readout which can be calibrated to be interpreted as temperature in a proper unit scale.

6.2.5 Flow velocity [Ft/min]

Flow velocity, ultimately used as a factor to determine mass and volumetric flow rates, will be measured using a rotary vane anemometer device. The measurement of velocities using this device obtains an average velocity that can be readily used in calculations. The measurement of flow velocity will occur at a significant length after any airflow interruptions to encourage measurement of a fully developed velocity profile. Power in Watts is read directly from the watt meter output.

6.2.6 Pressure Drop[inH2O]

A measurement of pressure drop caused by the heat-sink is valuable to calculate the power used to force convection. This value is ultimately used in the power ratio between heat removed and power used to force convection.

6.3 Validation

The design verification testing plan is seen below in Table 6-1. This plan helps to ensure that the engineering specifications seen in Table 3-1 are validated during testing. Sample types are as follows: A: concept verification, B: design verification.

Table 6-1: Design Verification Plan

Item No	Specification or Clause Reference	Test Description	Acceptance Criteria	SAMPLES TESTED	
				Quantity	Type
1	Module Weight, spec # 1	Weight both module plates with PCB, Therm-a-gap, and heaters	6.5 lb max	1	B
2	Module Dimensions, spec # 2, 3, 4	Measure Module Dimensions	See Spec #'s 3, 4, 5 (inches)	1	B
3	Junction Temperature to incoming air temperature difference, spec # 5, 11	Measure difference between Component Temperatures at heater/PBC interface and incoming air temperature. The critical temperature is 35°C above inlet temperature.	Steady state change in temp equal to 35°C, and max junction temp of 105°C if incoming air temp can reach 70°C	13 + 1 locations	B
4	Flow Rate, spec # 6	Set flow rate to compare to measured heat dissipation	Variable from 5-70 CFM, choose 4 to test at	4, one test each at dif. rates	A
5	Power Consumption to Resistance Heaters, spec # 16	Measure power to heaters at each flow rate	Unknown, want max possible Watts	1 per flow rate	A
6	Air Exit Temperature, spec #16	Measure air exit temperature at the anemometer at each flow rate at steady state. Alternative method to calculate heat dissipation to air with flow rate, specific heat, and temp change of the air.	Unknown, want max possible to increase heat dissipation to air	average of 2 readings per flow rate	A

7 TESTING RIG DESIGN DETAILS

Now that the general schematics for the module plates are established, the important task of developing a testing platform must continue. This device must be able to measure important experimental data while allowing a varied number of independent variables. The designed testing rig consists of three separate subassemblies and one component for insulation shown in Figure 7-1.

(1) Blower and Duct Manifold Assembly, T200
(2) Insulated Half Module Assembly, T300
(3) Cork Board and Fiberglass Insulation
(4) Bottom Cover Assembly, T400

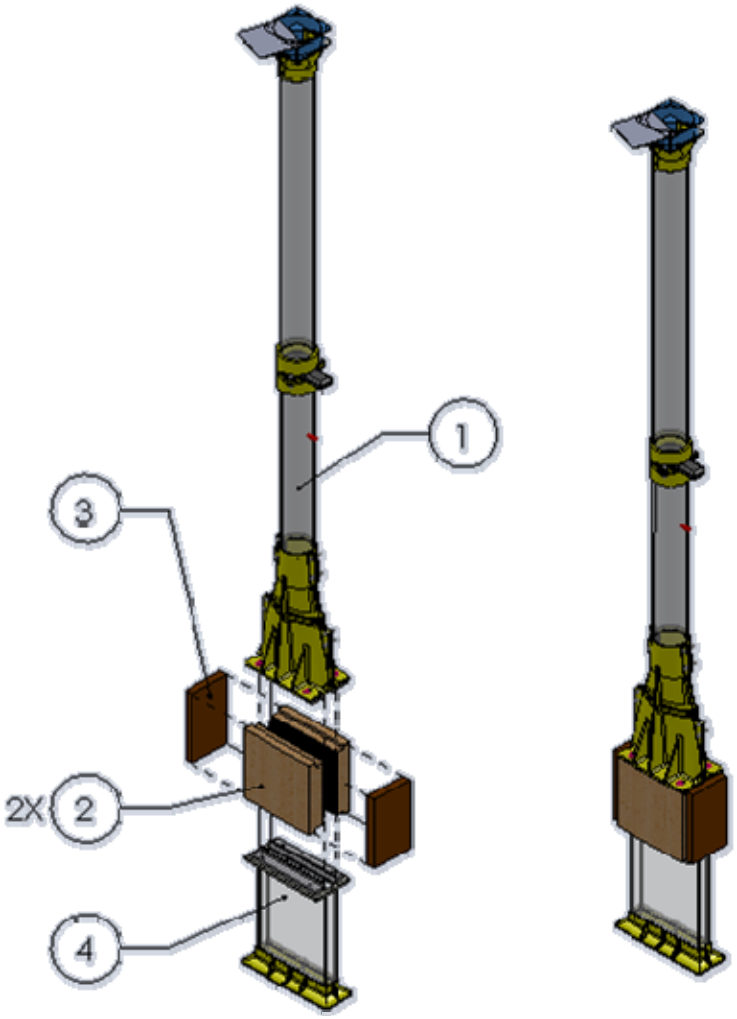

Figure 7-1: Overall Testing Rig Assembly. Subassembly descriptions are listed below.

Relying on the symmetry of the AECM modules, air will be blown between two module plate halves. Measuring the total heat dissipation from both halves will provide the equivalent heat transfer to the flowing air for a single module. Heaters will be used to

simulate electronic component heat dissipation. Thermocouples will constantly monitor the components temperature at multiple locations, and will also be used to measure the average intake and exit air temperatures. The power input to the heaters, volumetric flow rate and pressure drop in the system will all be recorded as well for power measurements.

The half module assemblies will be insulated on all four sides with 2" of cork board and fiberglass material as necessary to ensure that the heat dissipation is transferred only to the air flow and not escaping to the surrounding environment. Cork from McMaster-Carr was chosen due to its low cost, rigidity for clamping, and high thermal resistance (see Table 2-1 for thermal resistances of insulating materials). While plastic and fiberglass insulations have higher thermal resistances than cork, cork can withstand much higher temperatures rated up to 266°F. Its glass transition temperature is much lower, meaning it is very unlikely that it will deform or melt. The cork is shown in brown on Figure 7-1. The duct manifold up until the anemometer and lower air intake is insulated with fabric insulation to further reduce heat escaping from the system (insulation not shown in the assembly).

The insulated module assemblies will be held in place to the blower manifold and bottom intake cover with light clamping pressure provided by long bar clamps. An overall supporting structure of the test rig is not shown in the assembly for simplicity. The rig will support the structure horizontally, mounting to the rapid prototyped lower connector, air reducer, and fan connectors.

Descriptions of sub-assemblies and their components are listed in the following subassembly section along with reasoning behind their selection. Each sub-assembly is represented by its respective drawing number located in Appendix F.

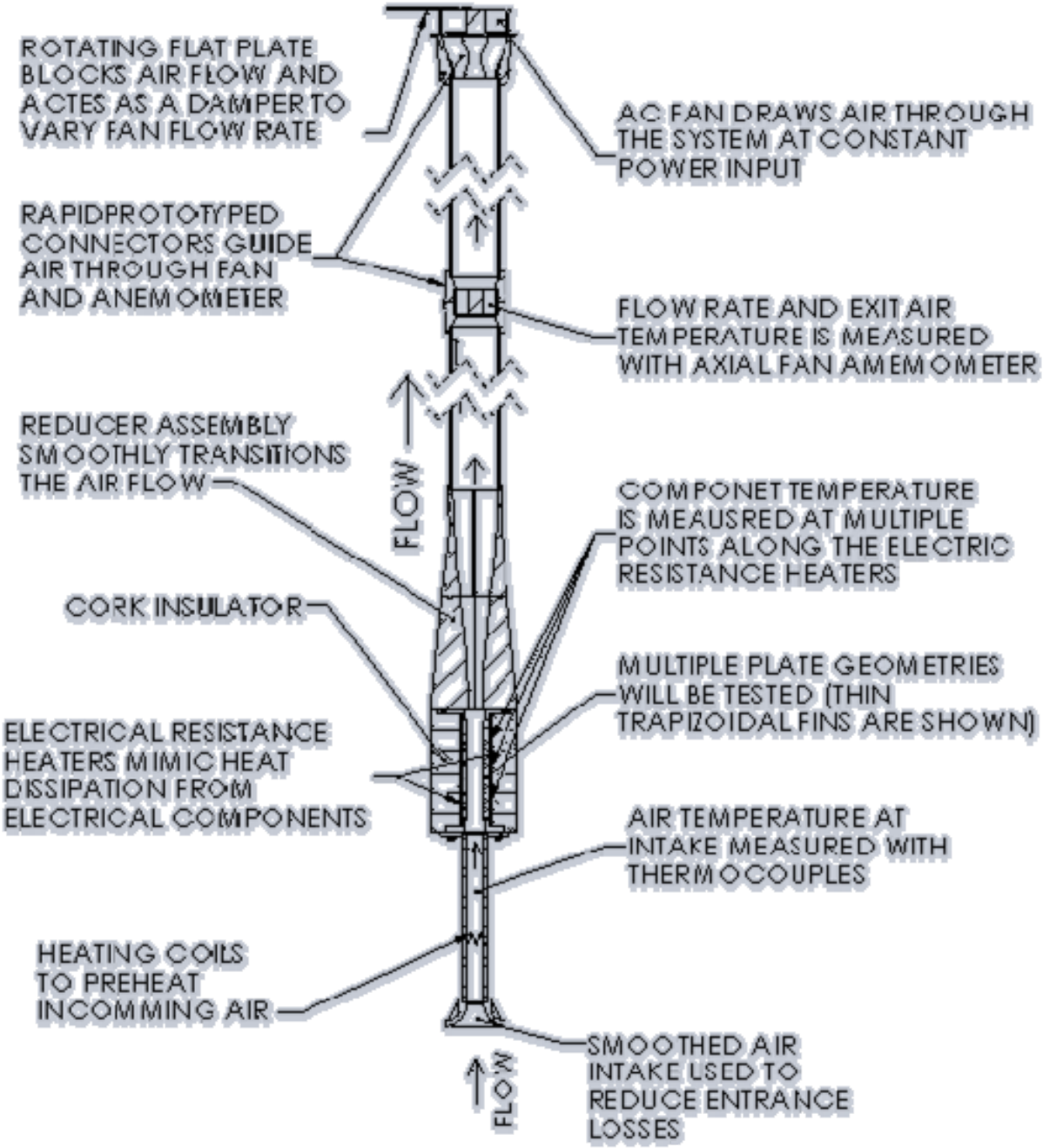

Figure 7-2: Cross-Section of the flow through the test rig assembly, with brief system notes.

7.1 Duct and Fan Assembly, T200

This assembly has three main purposes: It guides the airflow evenly from the module plates through the fan, it controls the spacing between the two modules, and it houses important testing components: the rotary vane anemometer capable of measuring average air flow rate, thermocouples for exit air temperature, the differential pressure manometer, the system fan, and a damper to control air flow rate.

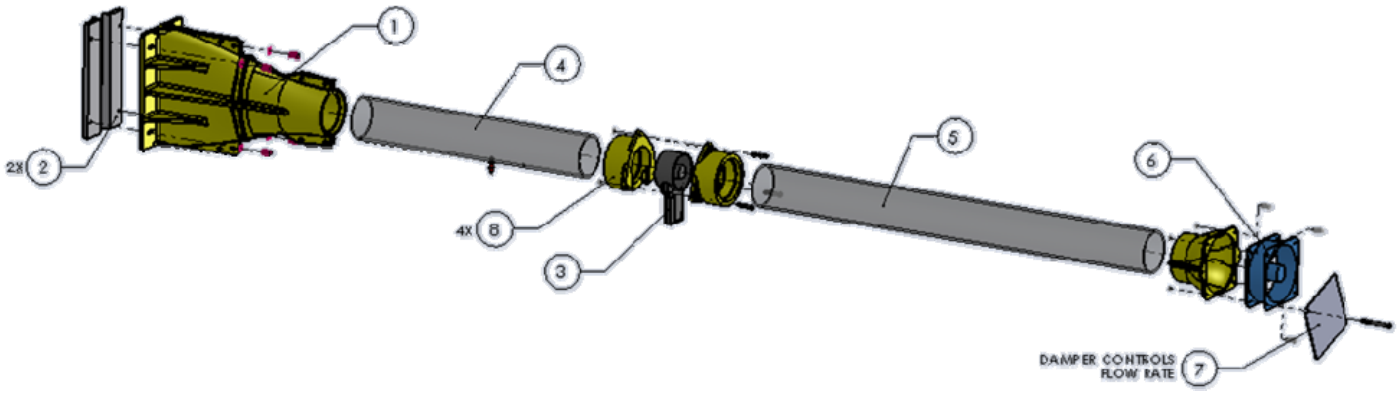

Figure 7-3: Blower and Duct Assembly (Drawing T300)

7.1.1 Air Duct Reducer, T301 (1)

This manifold gradually guides the air flow from the modules' rectangular cross-section to the thermocouples, mass flow measuring device, and fan. Due to its complex geometry, it was rapid prototyped from ABS material at Cal Poly. This left a rough surface on the interior of the manifold. Therefore, it was necessary to sand the interior of it to reduce as much resistance to the flow as possible. The 16" tall manifold was too large for available rapid prototyping; therefore, it was printed in 4 separate parts. In Figure 7-4, sections 1 and 3 are mated together using epoxy. The interior is smoothed with 220 grit sand paper. Sections 2 and 4 are assembled similarly. The halves are then bolted together and taped to prevent air leaks. Simple lap joints at all connecting surfaces ensure proper alignment and structural support.

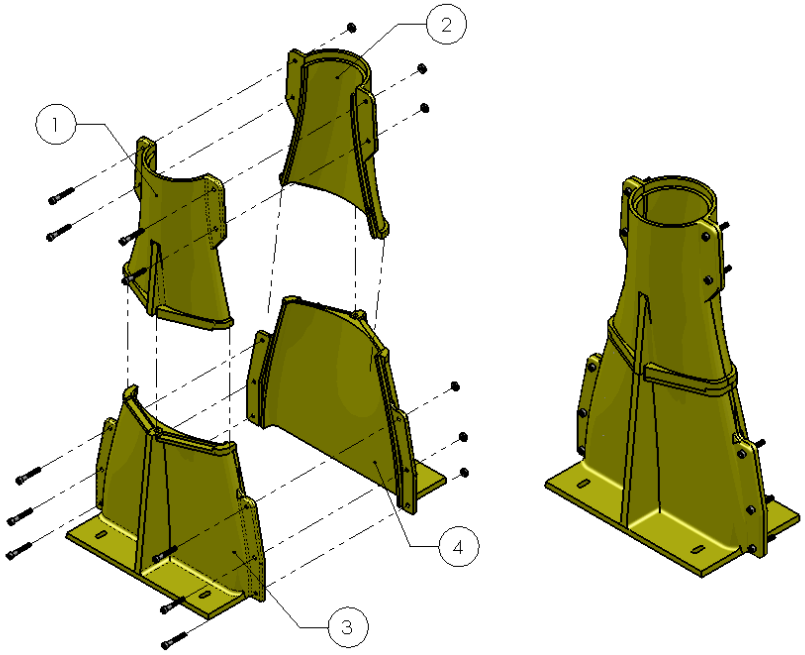

Figure 7-4: Air Duct Reducer (T301) shown in an exploded view and in its assembled form. Washers are not shown for simplicity.

The manifold also supports the AECM module sub-assemblies. The four slotted bolt holes connect the manifold to the upper module brackets. The slots allow the distance between the brackets to change for different module plate geometries and to optimize heat dissipation with changing spacing.

Because the module halves will be clamped against the upper module bracket, the clamping force will be transferred directly to the four bolts (5). Washers will help to dissipate the stresses over a larger area (6). The design of the manifold should be adequate to support the clamping forces introduced around the slotted bolt holes

7.1.2 Upper Module Rails, T302 (2)

These machined aluminum rails support the pressure directly from the module plate assemblies as described above. Holes are tapped along the top surface for ¼"-20 attachment bolts.

7.1.3 Rotary Vane Anemometer – Air Flow Rate and Temperature Measurement (3)

Measuring mass flow rate is critical in determining system performance compared to the ARINC air cooling standard. A radial vane anemometer from Omega was chosen to measure the flow rate. Pitot-static probes and hot wire anemometers were also considered. Both would measure the velocity profile of the flow from a series of points. However, inaccuracies of meaning velocity locations and the amount of time required to measure the average velocity prompted the decision to use a simpler rotary vane device.

The selected anemometer directly calculates the flow rate with a similar accuracy of ±2%, very reasonable for this purpose and useful for setting fan speeds. The actual data used will be the velocities provided by the device because that measurement features higher precision. The device also measures average air temperature with accuracy ±0.1 °C, useful for informally checking exit air thermocouple measurements.

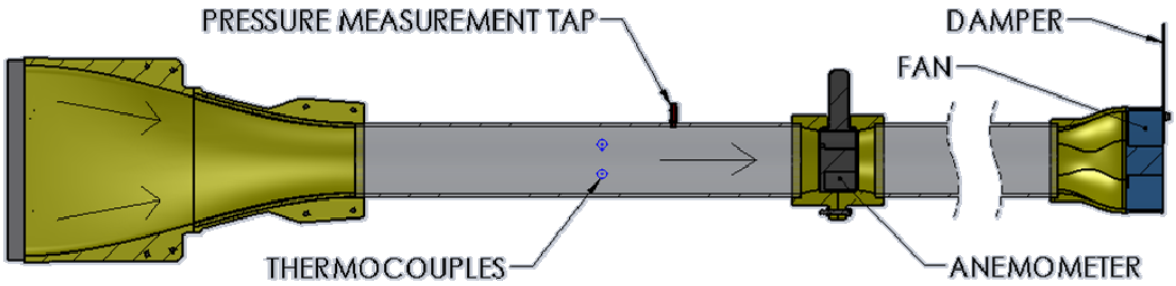

Figure 7-5: Reduced section view displaying basic components of the duct assembly.

7.1.4 Acrylic Pipe (4 and 5)

Stock acrylic pipe with an inner diameter of 3 1/8" (closest to the anemometer diameter of 2 7/8") connects the system components. Using the pipe to increase the duct length develops the flow before entering the anemometer and again between the anemometer and the fan. Because the anemometer does not directly measure the velocity profile of the fluid a fully developed upstream flow is not necessary; meaning a length of 10 diameters is not required.

7.1.5 System Fan (6) and Custom Damper (7)

The fan is a key component to the system, providing the air flow necessary for convection heat transfer. The fan selected is 119mm in diameter and is capable of 70 cfm at 3 inches of water. The high strength and small size of this fan allows for it to fit in the assembly properly yet still provide enough flow through the porous aluminum blocks. A data sheet for the EBM Papst fan is shown in Appendix O.

A damper will provide the ability to block airflow thereby reducing the flow rate. It must be located after the fan to ensure the head loss it contributes is not added to the losses associated with the rest of the setup. The damper is a simple hinged plate.

7.1.6 Custom Pipe Connectors - Anemometer and Fan (8)

In order to properly transition the air flow through the anemometer and fan, custom fixtures have been created. These were rapid prototyped in house. The connectors enclose the devises and are bolted together. They are affixed to the acrylic tubes using epoxy which forms a leak proof bond.

7.2 Insulated Module Half, T300

This assembly contains the plate designs listed in Section 5 which are tested in an arrangement that could resemble a final AECM module. The module plates will be interchanged over the insulated module half assembly for testing: finned aluminum plate and blank plate for aluminum foam configurations. They will not be permanently connected, but rather held on with the clamping force mentioned earlier regarding the entire test rig assembly. However, the blank PC board, electric resistance heaters, and Therm-a-Gap interface material are adhered in layers to the insulating cork, all shown in Figure 7-6.

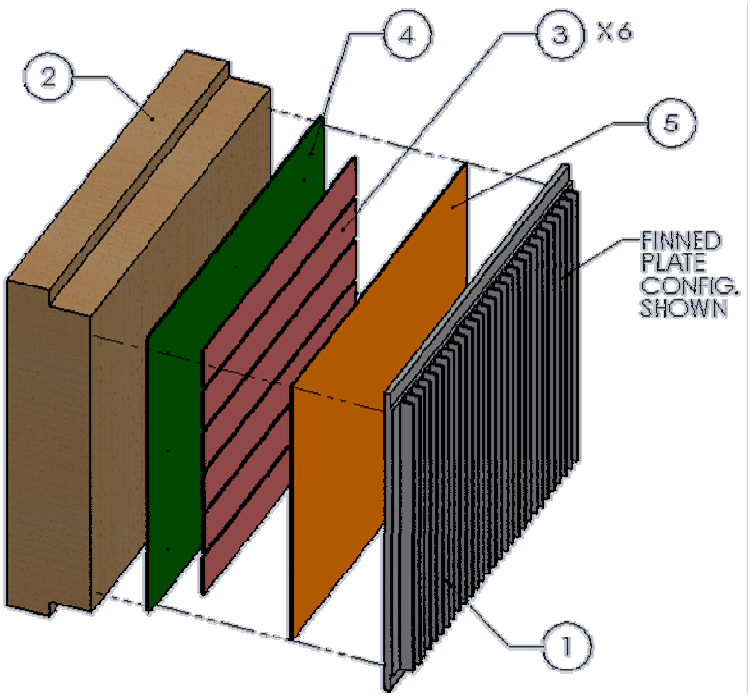

Figure 7-6: Insulated half of an AECM module. (Drawing T300) The machined fin plate concept is shown.

7.2.1 AECM Module Plate Designs (drawings M01 & M02)

The plates will be inserted into the Insulated Module Half Assembly for testing. They serve to simulate the actual FR4 PCB in the AECM analysis as well as serve as a mounting point for the adhesive strip heaters.

7.2.2 Semi Rigid Cork Board, T202 (2)

Because of the reliance on the symmetry of the AECM modules for testing, it is important to ensure no heat escapes from the outer edges of the testing rig. As stated earlier, this cork board makes an ideal insulator for this setup because of its high thermal resistivity and resistance to higher operating temperatures.

7.2.3 Electric Resistance Heaters, Omega SRFG-108/5-P (3)

The test rig design calls for twelve DC Voltage Flexible Silicone-Rubber Heat Strips ordered from Omega. These strips would be arranged six per module and fill most of the

PCB surface. The dimensions of commercially available strip heaters do not fit precisely and the gaps between the six heaters located on each side mimic the spacing between the chips seen on the AECM model. These strips feature adhesives which aid in mounting them onto the PCB; this initially directs the heat outward towards the insulation but will not affect the eventual steady state results.

The specifications state the strips have a maximum operating temperature and output of 149°C (300°F) this specification is safely above the maximum possible operating temperatures seen in the test setup. The strips have a watt density of 5 W/sq.in., this density corresponds to a maximum output of 240 Watts per module half. This value, coincidently, is the calculated maximum wattage of heat transfer for both halves of the AECM liquid cooled module; it should be safe to assume that using air cooling to dissipate heat will become inefficient well before the maximum overall output of 480 watts is reached.

7.2.4 Blank PC Board, T203 (4)

To complete the simulation of the actual AECM module operating conditions a plate that mimics a blank PC board is included in the side panels as well. Beyond simple simulation purposes, this plate also serves as a secure mounting platform for the adhesive on the heating strips, as a protective layer between the heating elements and the cork insulation, thermocouple connections, and as yet another layer, albeit thin, of insulation. The board is a dual copper side blank FR4 board with a thickness approximately half of the board used in the AECM thermal model.

7.2.5 Therm-A-Gap Pad, T201

Due to the soft nature of the silicone heater strips the interface between the heaters and the module plates is likely be far superior to what would be exhibited by a direct connection between PCB elements and the plate. However, to increase test accuracy, the interface between the heating pads will be interrupted using a pad of thermal interfacing material. Therm-a-Gap is the commercial name of the material used in the AECM specifications and an identical 0.040” sheet will be used in the test to help match the simulation.

7.3 Bottom Cover Assembly, T400

This assembly is designed to regulate the spacing between the module halves and provide an attachment for the air intake duct. It is critical that the cross-sectional area of this opening match the mating sides as closely as possible to reduce resistance to air flow.

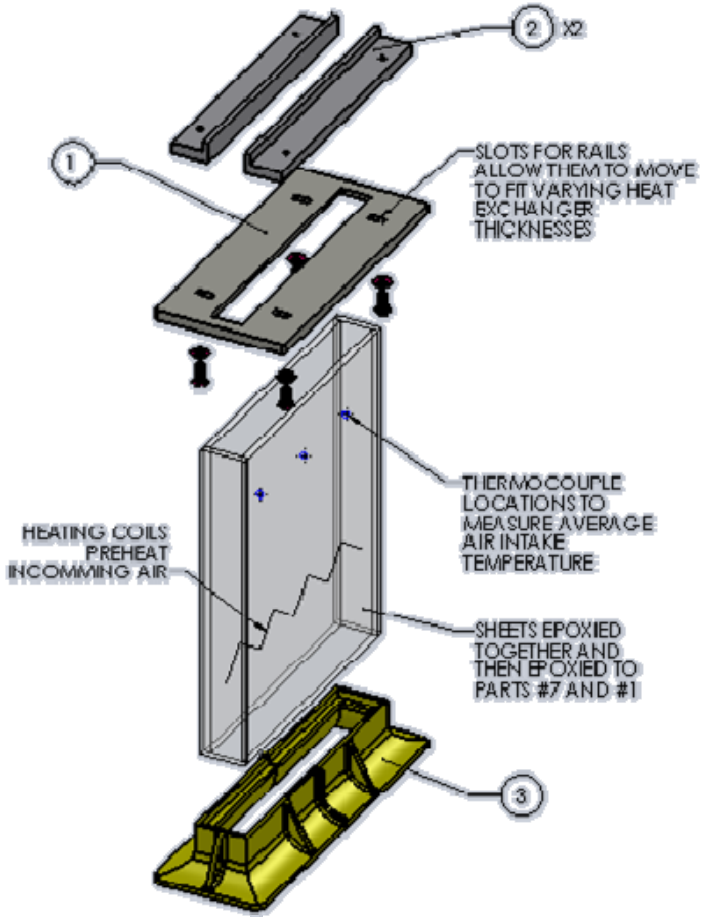

Figure 7-7: Bottom Cover Assembly (Drawing T400)

7.3.1 Lower Plate Connector, T401 (1)

This machined aluminum component connects the two module assemblies together at a variable distance apart just as the air duct reducer (drawing T301) does for the top section of the test rig. The connector will support the clamping force due to the bar clamps as well. Therefore, it must to strong enough to resist any reactive stresses, choosing to machine this out of aluminum will provide more than adequate strength.

7.3.2 Lower Module Brackets, T402 (2)

This bracket serves an equivalent purpose as the Upper Module Bracket (drawing T302) described in section 7.1.2.

7.3.3 Inlet shroud T402 (3)

This device is meant to smooth transition from external to internal flow. Neglecting this section would cause a significant pressure drop. To accommodate the rapid prototyping manufacturing process this shroud is designed to be fabricated in two halves which can subsequently be permanently affixed together.

7.3.4 Inlet Air Preheating Coils

This section includes heating coils extracted from a commercially available hair dryer. Current will be sent through the device using a Variac and adjusted to reach the appropriate inlet temperature for testing.

8 MANUFACTURING

8.1 Finned Heat Exchangers

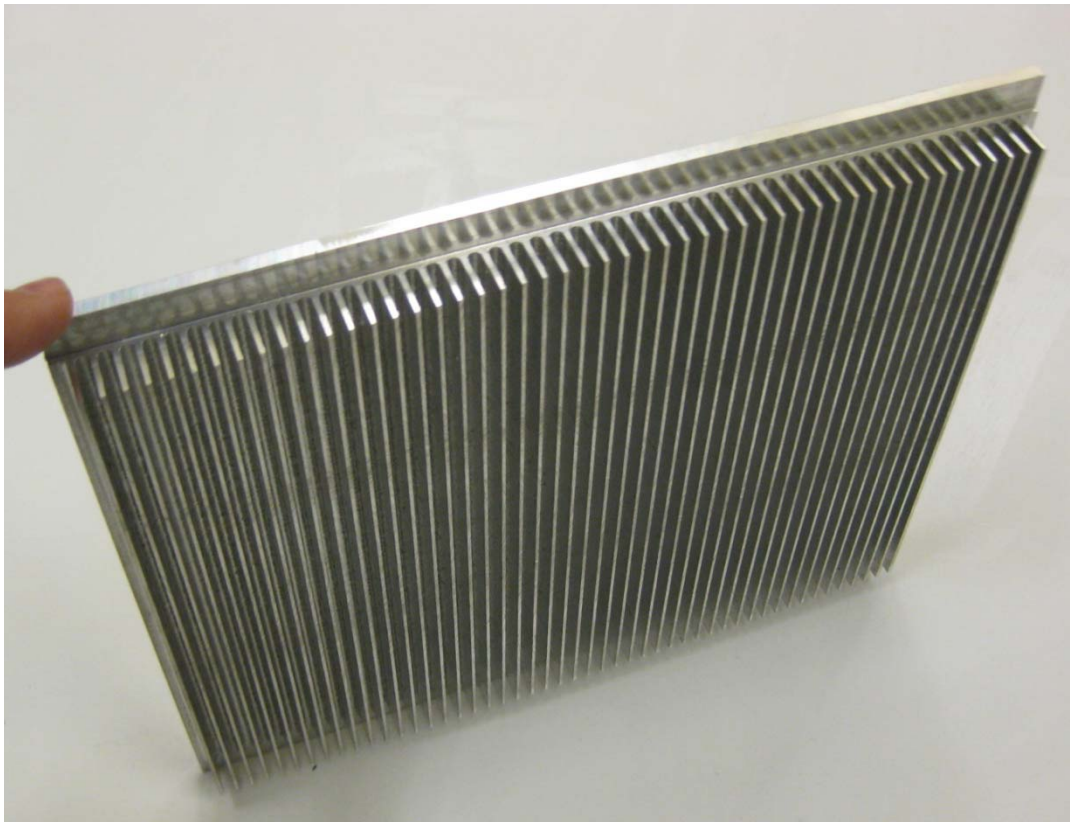

Figure 8-1: Finished finned plate

8.1.1 Stock Sizing

The CNC mill requires a precisely sized piece of stock to ensure the program matches reality when machining. To reduce the amount of material required to be removed, the stock was first cut using a horizontal band saw. Standing tall in a vice, the stock was then

faced using the flat face of a large end mill. After sizing these two parallel edges precisely the proper distance apart, the stock was oriented parallel to the ground and mounted in the vice. The final shaping was accomplished using the sides of an end mill, removing material until the block was of proper size.

8.1.2 CNC Mill

CNC milling was performed by student technicians in the on-campus Mustang '60 lab using a HAAS brand mill. The procedure for the finned plate included two steps. The first step removed material from between the fins. Each trough took approximately 20 passes, the small depth cuts were chosen to prevent end mill failure, a large concern because of the small 1/8 bits used. Finally, a special 2 degree taper 1/8 ball end mill took an additional 3 passes per trough to provide the contour shown in the model. The second CNC program step required flipping the plate around to mill the troughs required for the Therm-a-Gap and FR4 boards.

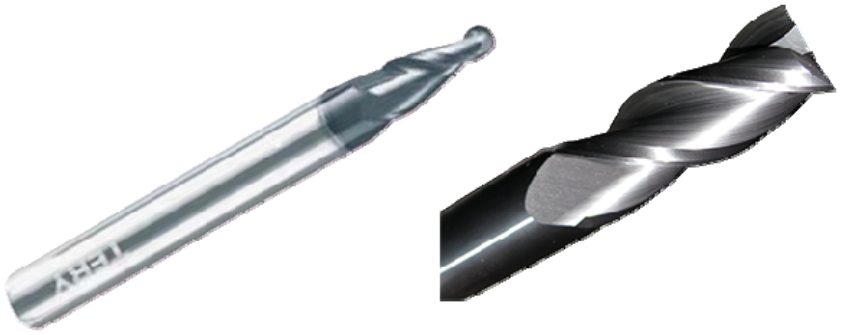

Figure 8-2: Example of Milling Bits used for finned plate Left: Taper ball end mill. Right: Flat endmill.

Figure 8-3: HAAS CNC Mill in Mustang '60 Lab

8.2 Foam Heat Exchangers

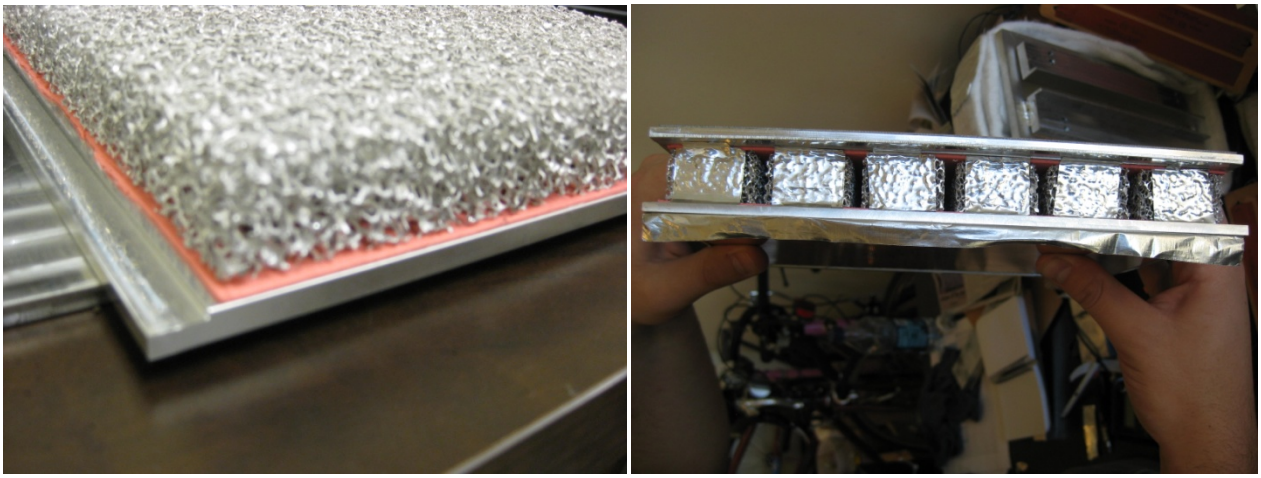

Figure 8-4: Left: Half Foam block and plate assembly. Right: Full Assembly with channels.

8.2.1 Plate

The initial CNC run on the first plate was run without cutting the stock material to size. The program would simply run from the center of a significantly larger plate and size the sheet itself. This proved problematic due to the chatter experienced with the thin plate. When it came time to face the side that mated with the foam the plate had become so distorted that the resulting surface was quite poor and misshapen. The attempts to alleviate this resulted in the plate having a number of defects on the surface and an overall thinner profile than expected. The second plate was attempted after making proper stock sizing cuts prior to running the CNC mill and experienced no significant flaws in manufacturing.

Figure 8-5: The finished plates mounted in rig. Note slight manufacturing errors in near plate.

8.2.2 Foam Block

The foam blocks arrived from ERG cut to proper dimensions with acceptable tolerances.

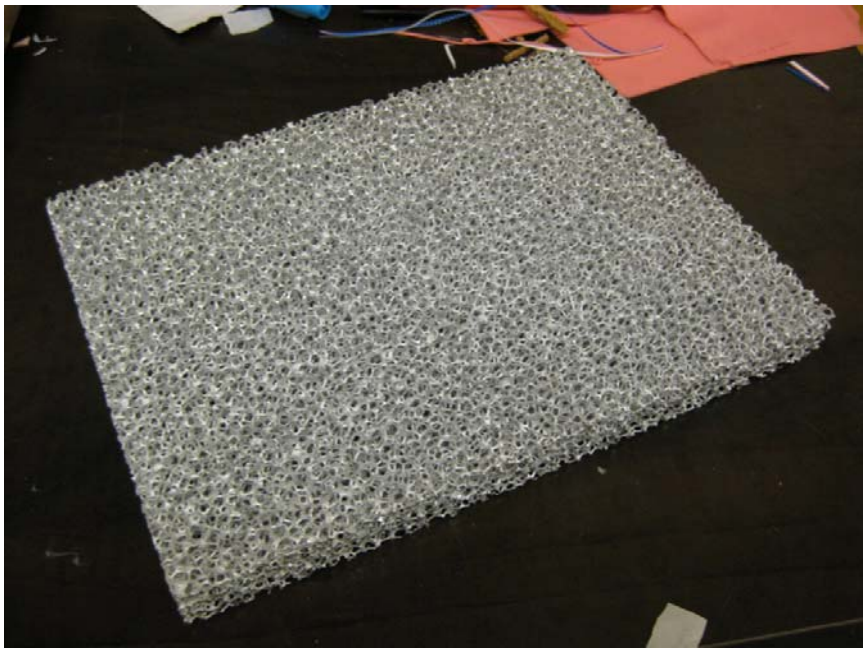

Figure 8-6: Foam Blocks as shipped from ERG

Cutting the blocks was as simple as taping a 1:1 scale drawing of the desired channels onto the block and running it through a vertical band saw. After the two cuts on each side of a channel were made the piece would be extracted using pliers, provided it had not already been removed by the force of the cutting teeth.

Figure 8-7: Foam Blocks after cuts performed on band saw

8.2.3 Mating

Working with the Therm-a-Gap material was more difficult than expected. Contact was minimized to prevent oils from skins reducing its performance but handling and manipulating the material could be compared to working with sheets of silly-putty. Patience and persistence were required to align the material to the plates. The Therm-a-Gap has one side with a fine cloth meshing. The other side lacks this feature and is better suited for mating on rough surfaces. Thus, the cloth side was always mated to the plate and the opposite would slightly embed into the pores of the aluminum foam, ensuring good thermal contact.

Keeping the plates aligned when combining all layers required some quick troubleshooting. An alignment method involving some straight edged aluminum scraps proved useful for this purpose.

8.3 Test Rig

8.3.1 Wiring

The resistive heating strips were wired in parallel to reduce the overall resistance and thus the need for a extremely high voltage power supply. The heaters were plugged into the Variac which was in turn plugged into the watt meter.

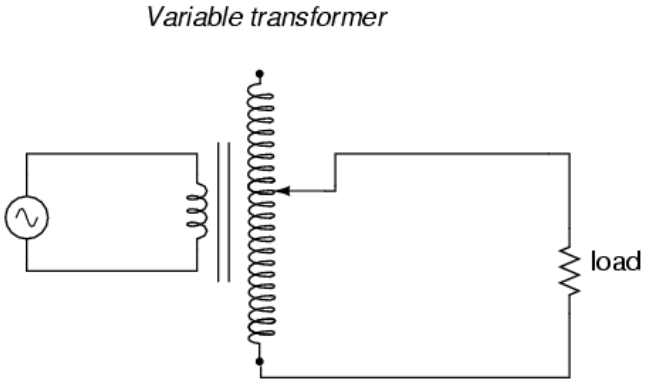

Figure 8-8: Simple Wiring Diagram of Strip Heaters (© Tony R. Kuphaldt)

20 feet of lamp wire, purchased from Home Depot, worked wonderfully to stitch the heaters together. A quick calculation in-store confirmed the wires would handle the current with a factor of safety larger than 4, more than adequate for electronic circuits.

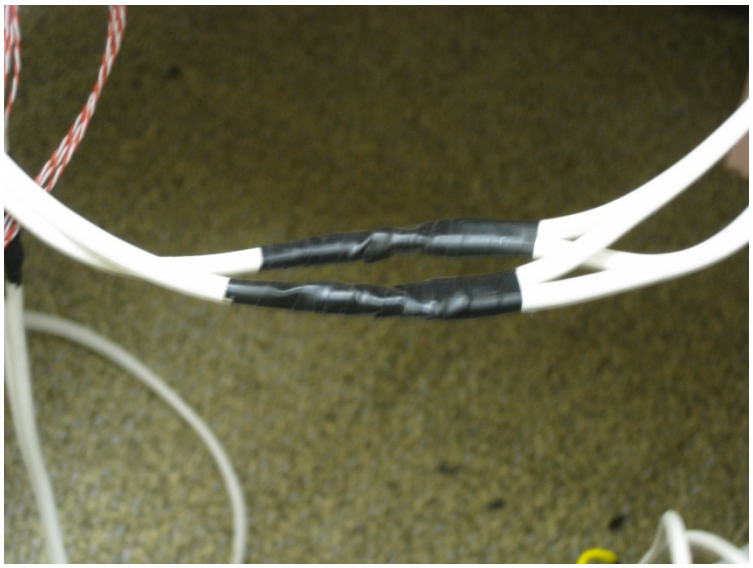

Figure 8-9: Photo of final wrapped soldier joints

A quick "power-up and touch" test confirmed that all heaters were wired and working.

8.3.2 Blower and Duct Manifold Assembly, T200

- **Outlet Shroud**

Figure 8-10: Assembled outlet shroud with a first layer of insulation

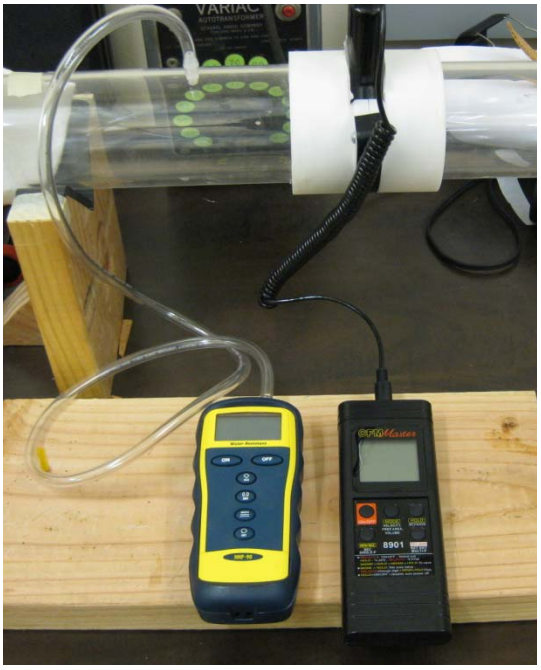

Figure 8-11: Pressure manometer and anemometer mounted in the T200 Assembly

- **Rails**

  This section involved milling and tapping to fabricate the rails designed to slide along the outlet shroud. Roughly 7 hours in the shop using the a Ganesh brand mill (1/2 endmill) produced acceptable parts.

Figure 8-12: Machining the aluminum upper rails

- **Fan and Damper**

  A simple damper was fabricated from a thin sheet of aluminum. Tightening the nuts provided enough strength to hold the damper rigid while testing.

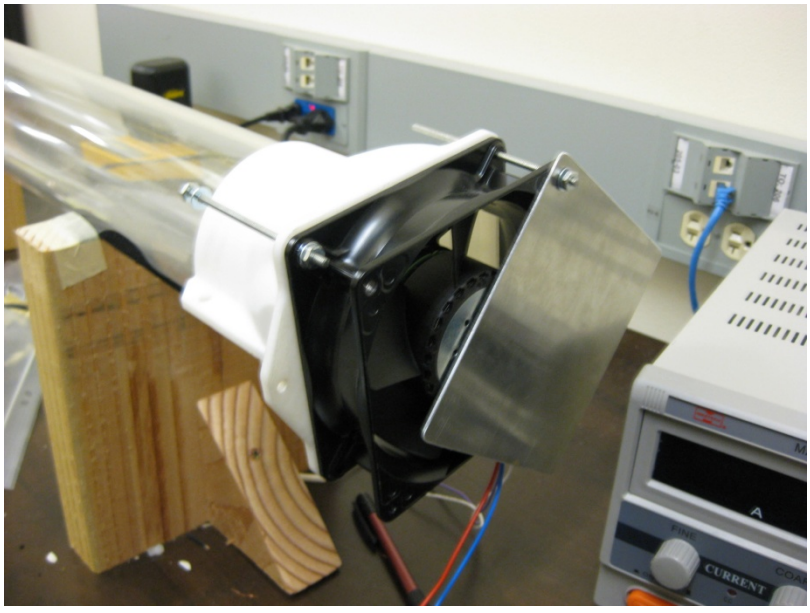

Figure 8-13: Simple flap damper used to reduce air flow

8.3.3 Insulated Half Module Assembly, T300

- **PCB**

  The PC boards arrived from the manufacturer with the main dimensions already cut to proper dimensions with an acceptable tolerance. All that was required in terms of manufacturing was the simple process of rounding the edges using a belt sander so the boards would fit in the rounded corners of the module slots.

Figure 8-14: Thermocouple and wire through-holes drilled

Figure 8-15: PCB with rounded corners

- **Heaters**

  Mounting the heaters required only simple alignment before they were ready to peel and stick to the FR4 boards. Protective gloves were worn to prevent oils from staining the copper boards.

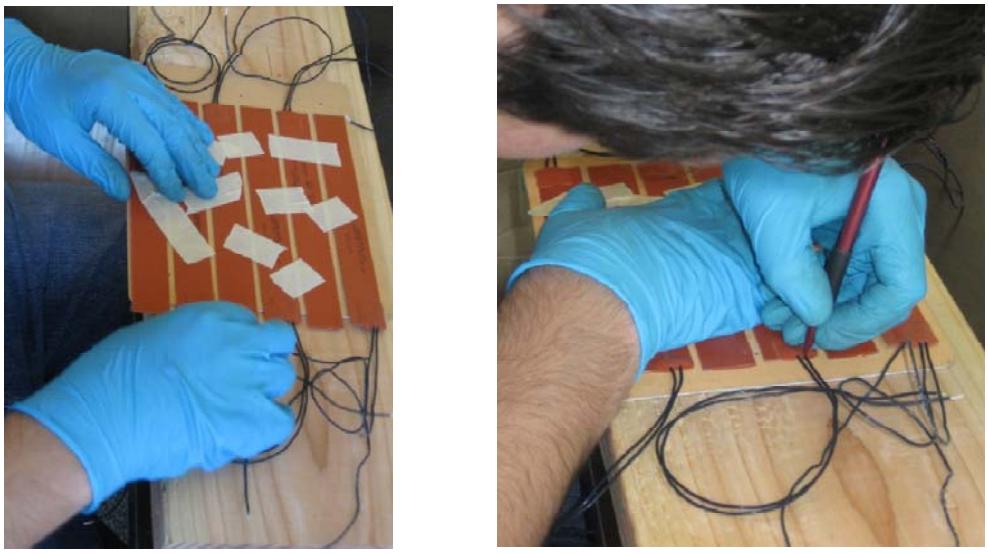

Figure 8-16: Left: Initial alignment of heaters onto FR4 board. Right: Marking positions once mounted

- **Cork insulation**

  Cork insulation was cut to size using a vertical band saw.

Figure 8-17: Example blocks of cork

- **Therm-a-Gap**

  Therm-a-Gap was cut to size using a sharp razor blade.

Figure 8-18: Cutting the Therm-a-gap using razor blade

8.3.4 Bottom Cover Assembly, T400

Figure 8-19: Aligning lower plate connector for fastening to inlet assembly

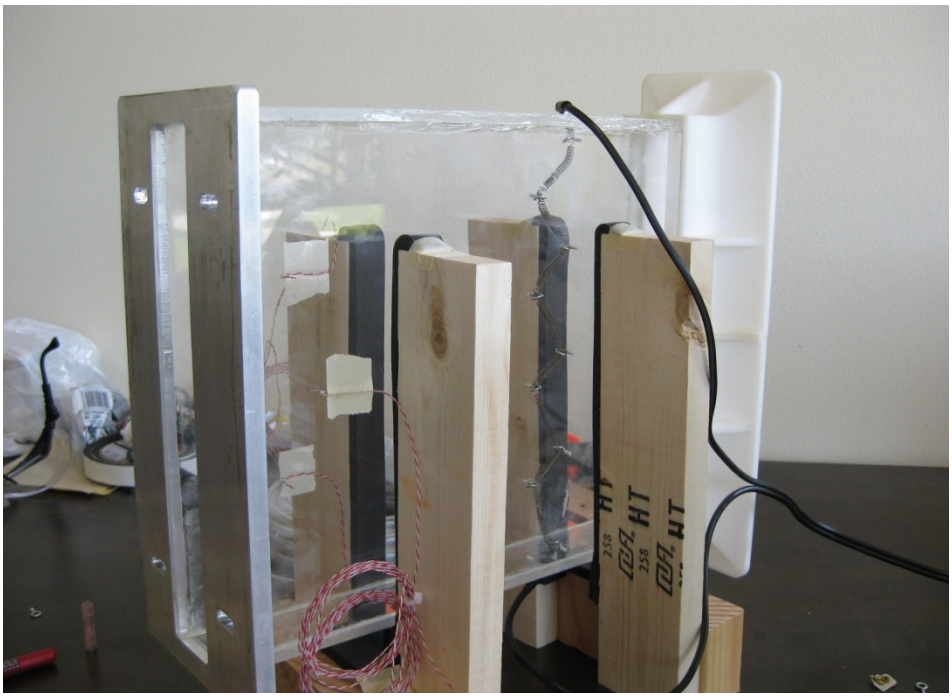

Figure 8-20: Finished assembly. Note installed thermocouples and inlet heaters

8.3.5 Scaffolding

Some simple scaffolding was built from wood to cradle the testing rig.

Figure 8-21: Scaffolding to support length of testing rig

8.4 Pre-testing assembly

8.4.1 Arranging Plates and Therm-a-gap preparation

The strip heaters each feature a small plateau protrusion where the wires connect to the internal heating elements. This protrusion does not actually produce heat. While the Therm-a-Gap is designed to distort to fill gaps this protrusion is beyond the material's ability to do so. Mating an unmodified sheet of Therm-a-Gap over the protrusion would cause a poor thermal interface between the surrounding areas. To provide the best mating surface between the heaters and the plates, small squares were cut with a razor blade and removed from the Therm-a-Gap.

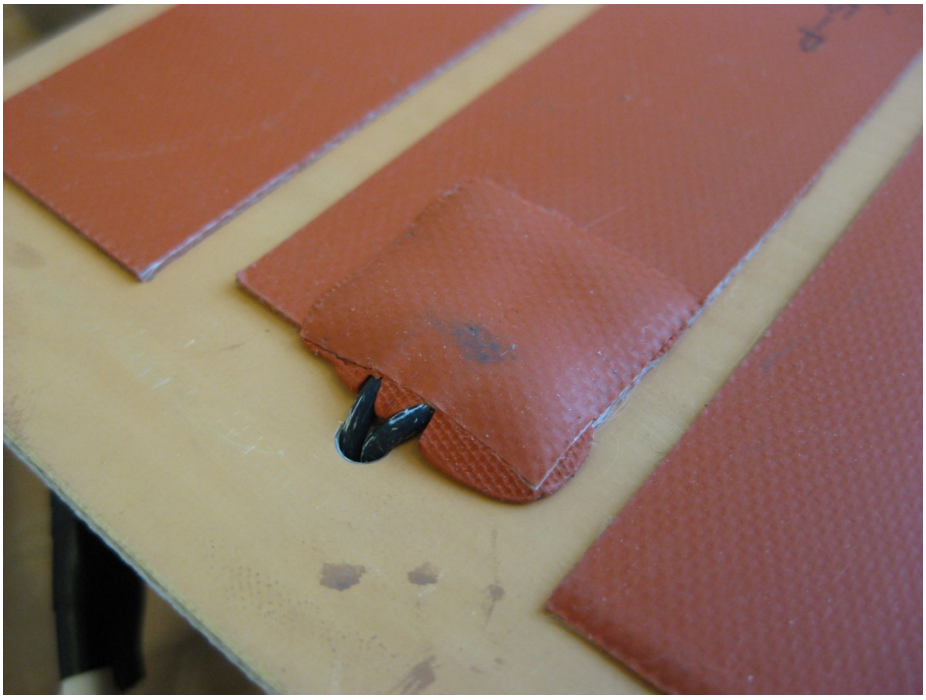

Figure 8-22: Small but significant heater protrusions

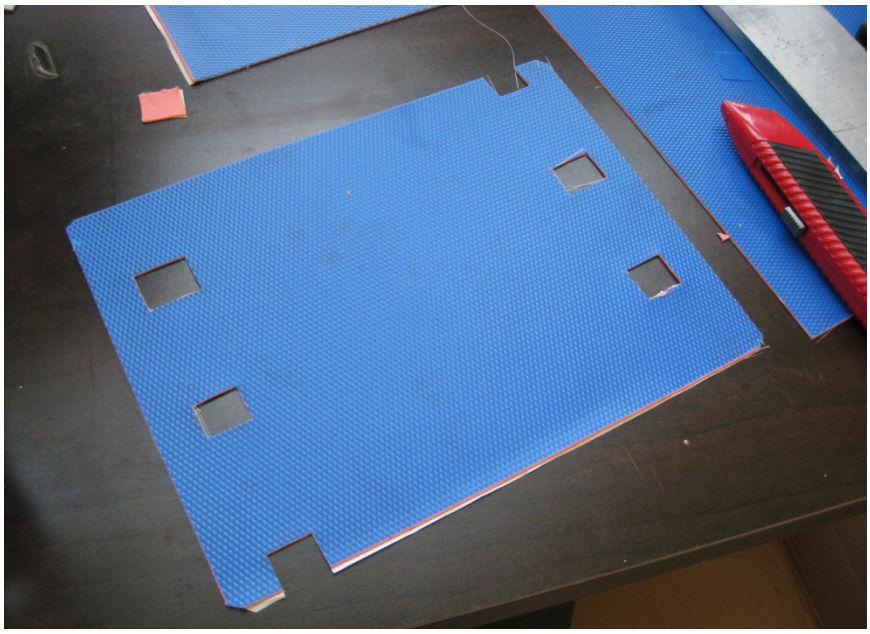

Figure 8-23: Therm-a-Gap cut to accommodate heater protrusions

8.4.2 Sealing Leaks

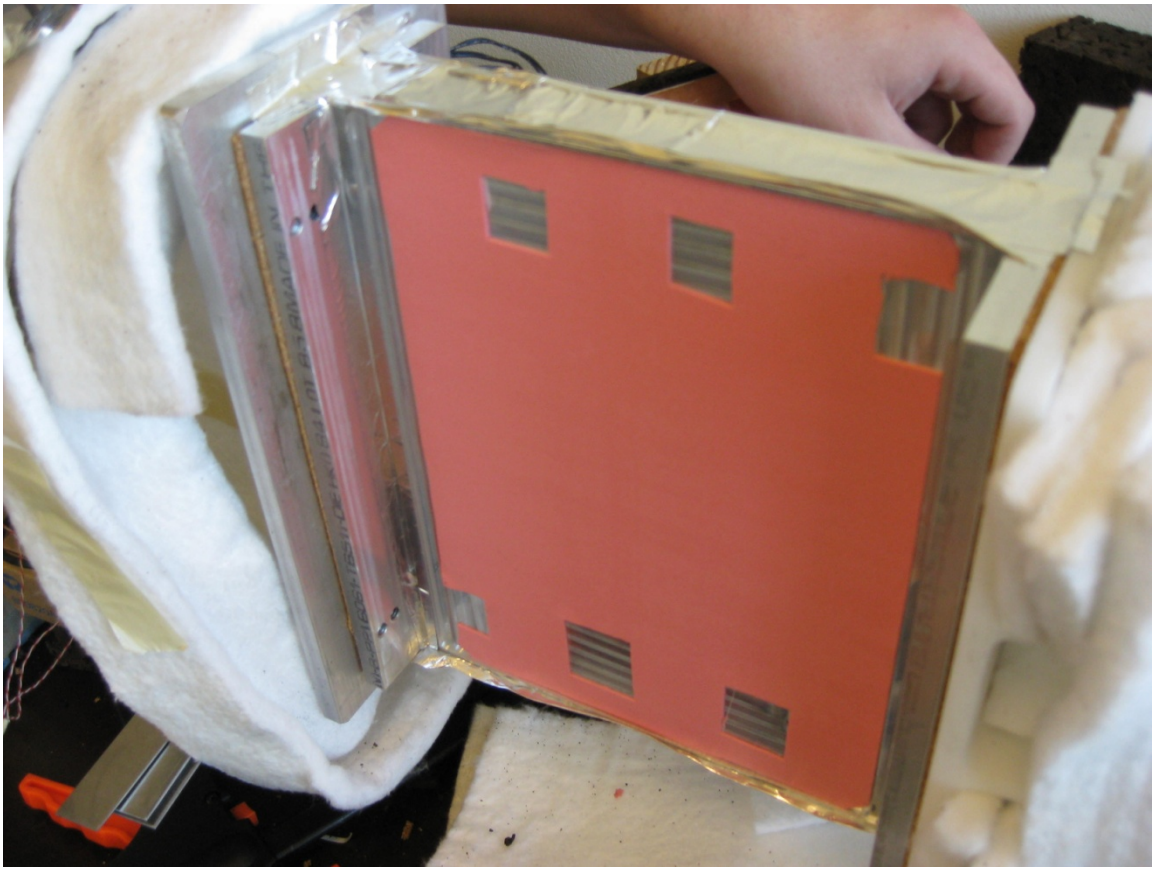

Figure 8-24: Adhesive backed aluminum tape used to prevent air gaps near rails

8.4.3 *Insulating*

Thick fabric insulation acquired from another Boeing team blanketed the assembly to reduce heat loss.

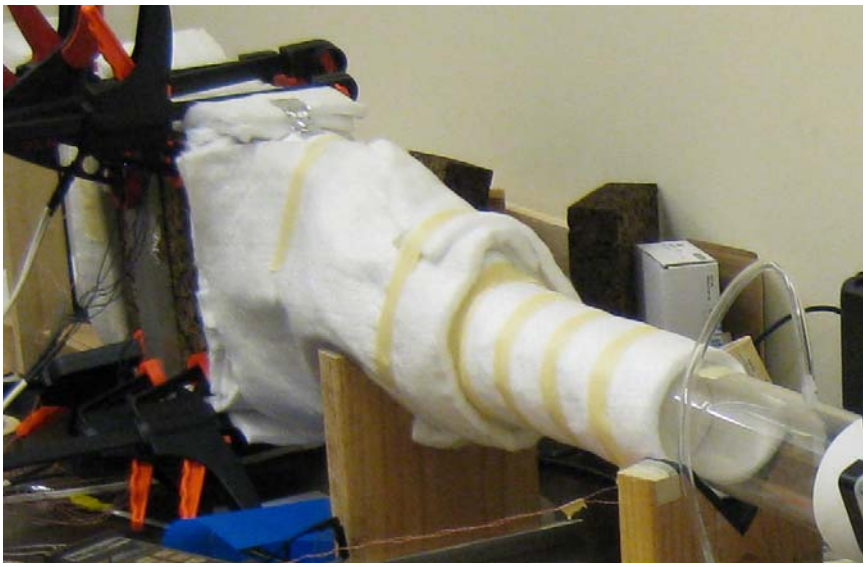

Figure 8-25: Insulation wrapped around rig during testing

8.4.4 *Clamping*

Six clamps were used to hold the assembly. The two central clamps exerted pressure at the center of the boards ensuring a good thermal connection inside.

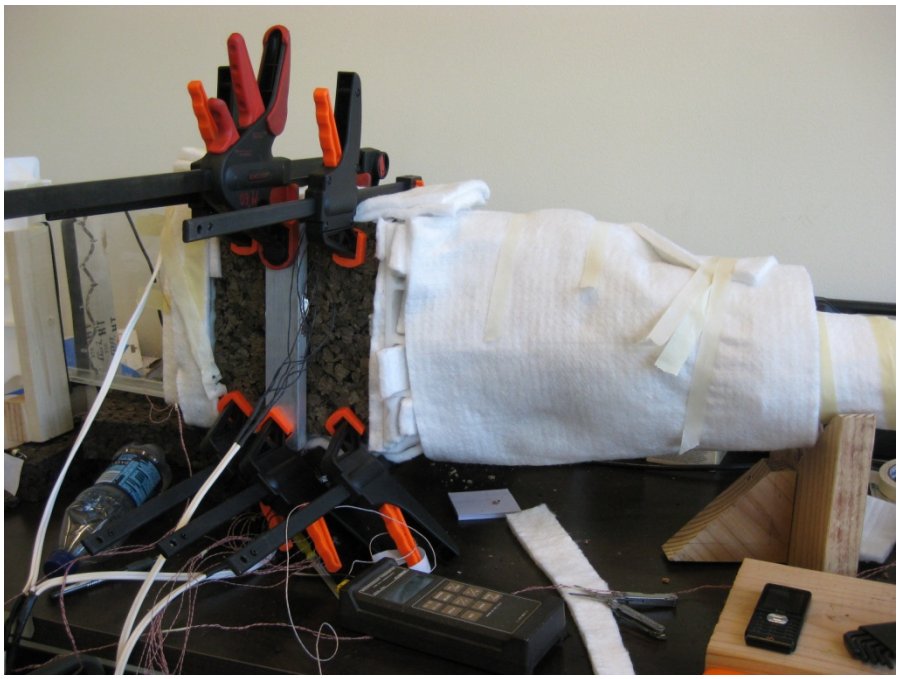

Figure 8-26: Arrangement used to clamp assembly together.

8.5 Budget

The technical specifications called for a budget of $3,000. This amount was generated by an earlier guesstimate and has served as a guideline for component selection but has now been determined to be insufficient. The current required totals are seen in Section 8.5.1 but still fall well below one fourth of the $25,000 amount allocated for all of the Boeing senior project teams.

For sake of clarity the entire bill of materials has been separated into three sections which, together, compose Appendix G. The first section details the prices of the components that are required to manufacture the testing rig, the second section details the pricing of the actual AECM modules and the final section details prices of purchased lab equipment to necessary for certain measurements.

8.5.1 Grand Total

An overall estimate of 16% has been added to account for additional costs associated with tax and shipping.

The grand total is larger than the earlier estimate of $3,000. A great deal of effort was made in choosing appropriate products (especially lab testing equipment) that do not bring the totals exceedingly high but have accuracy and quality appropriate for this project.

Table 8-1: Bill of Materials: Grand Totals

Testing Rig Sub Total	704.99
Module Plates Sub Total	1789.14
Lab Equipment Total	1051.12
Subtotal:	$3,545.25
Addl: 16% For tax and shipping:	$312.38
Grand Total:	**$3,857.63**

9 TESTING

9.1 Testing Procedure

Once the testing rig was entirely assembled and ready for testing (See Section 8.4) the testing process commenced. Each test took 3 or 4 hours to completed. An estimated total of 20 hours were spent over a number of days to complete the testing. Discomfort from long exposure to the noise produced by the fans was alleviated by wearing protective headgear.

9.1.1 Confirming Steady State

The creation of a testing layout in Lab View helped immensely to gauge when steady state had been reached. The running plot seen in Figure 9-1 would provide a visual

indication of steady state, but additional time after visual confirmation was always provided. Adjustments would be made using the Variac until the hottest thermocouple reached 35°C above ambient air. This value usually ranged between 56°C and 57°C. After each adjustment the temperatures would change fairly rapidly but a "buffer" time of 6 minutes was added to ensure temperatures had settled. Each data point took about 5 adjustments before the delta T was within the desired tolerance.

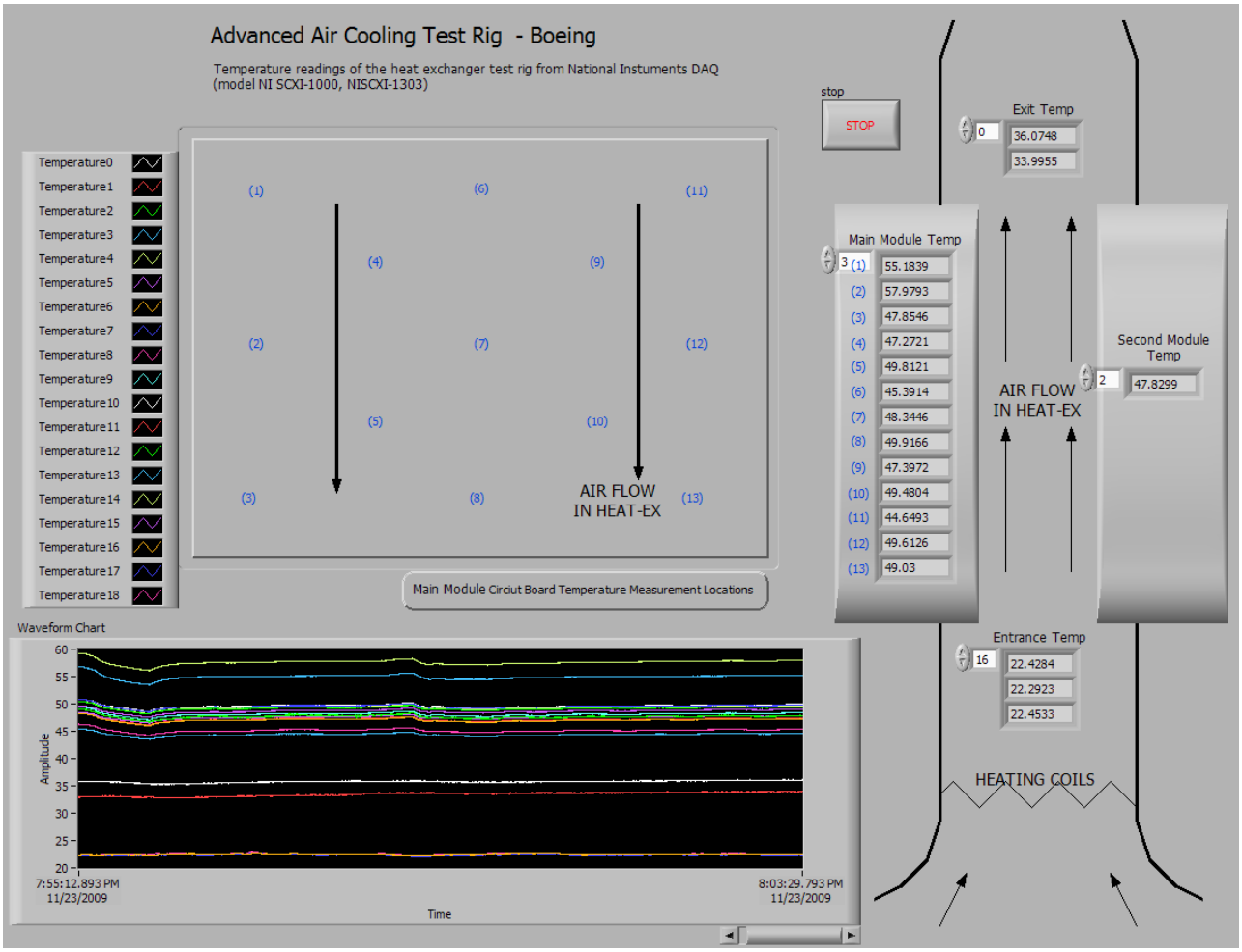

Figure 9-1: Screenshot of Lab View Showing plot of temperature trend. Testing 10PPI Thick at 70CFM

9.1.2 Recording Data

Once steady state was reached a screenshot of the Lab View window was taken and the values were read from the various instruments. The values from the screenshot were then recorded onto a spreadsheet. This method of taking a snapshot allowed simultaneous recording of each fluctuating value. To account for the natural fluctuation a second set of screenshots and instrument values were recorded 5 minutes later.

Figure 9-2: Recording data during a loud experiment

9.2 Individual Design Testing Results

9.2.1 Finned Plate

Raw testing data and preliminary result calculations can be found in Appendix H: Experimental Results – Aluminum Finned Plates.

Table 9-1: Heat Dissipation and Power Ratio based on various flow rate for the finned plate configuration.

Flow Rate (CFM)	72	50	31	16
Heat Dissipated (W)	**167**	**153**	**133**	**105**
Power Ratio	**58**	**146**	**466**	**3039**

9.2.2 Uncut 5ppi 0.87" Thick Alum Foam

Raw testing data and preliminary result calculations can be found in Appendix I: Experimental Results – 5ppi Solid Aluminum Foam.

Table 9-2: Heat Dissipation and Power Ratio based on various flow rate for the solid 5ppi 0.87" thick aluminum foam configuration.

Flow Rate (CFM)	72	50	31	9
Heat Dissipated (W)	**283**	**246**	**186**	**73**
Power Ratio	**12**	**29**	**98**	**1318**

9.2.3 Uncut 10ppi 0.87" Thick Alum Foam

Raw testing data and preliminary result calculations can be found in Appendix J: Experimental Results – 10ppi Solid Aluminum Foam..

Table 9-3: Heat Dissipation and Power Ratio based on various flow rate for the solid 10ppi 0.87" thick aluminum foam configuration.

Flow Rate (CFM)	43	50	30	15
Heat Dissipated (W)	**301**	**266**	**210**	**130**
Power Ratio	**21**	**32**	**114**	**459**

9.2.4 *Cut 10ppi 0.87" Thick Alum Foam*

Raw testing data and preliminary result calculations can be found in Appendix K: Experimental Results – 10ppi Channeled Aluminum Foam.

Table 9-4: Heat Dissipation and Power Ratio based on various flow rate for the channeled 10ppi 0.87" thick aluminum foam configuration.

Flow Rate (CFM)	73	51	31	16
Heat Dissipated (W)	**310**	**266**	**206**	**129**
Power Ratio	**15**	**40**	**130**	**565**

9.2.5 *Uncut 5ppi 0.64" Thick Alum Foam*

Raw testing data and preliminary result calculations can be found in Appendix K: Experimental Results – 10ppi Channeled Aluminum Foam.

Table 9-5: Heat Dissipation and Power Ratio based on various flow rate for the solid 5ppi 0.64" thick aluminum foam configuration.

Flow Rate (CFM)	50	31	14
Heat Dissipated (W)	**262**	**203**	**134**
Power Ratio	**14**	**47**	**320**

9.3 Overall Results

Experimentally determined cooling characteristics for all 5 heat exchanger configurations based on flow rate is shown below in Figure 9-3. This plot is designed to be used as a selection tool for choosing an appropriate starting design point AECM air cooling. Given a desired heat dissipation, one can select the most effective option with highest Factor of Performance.

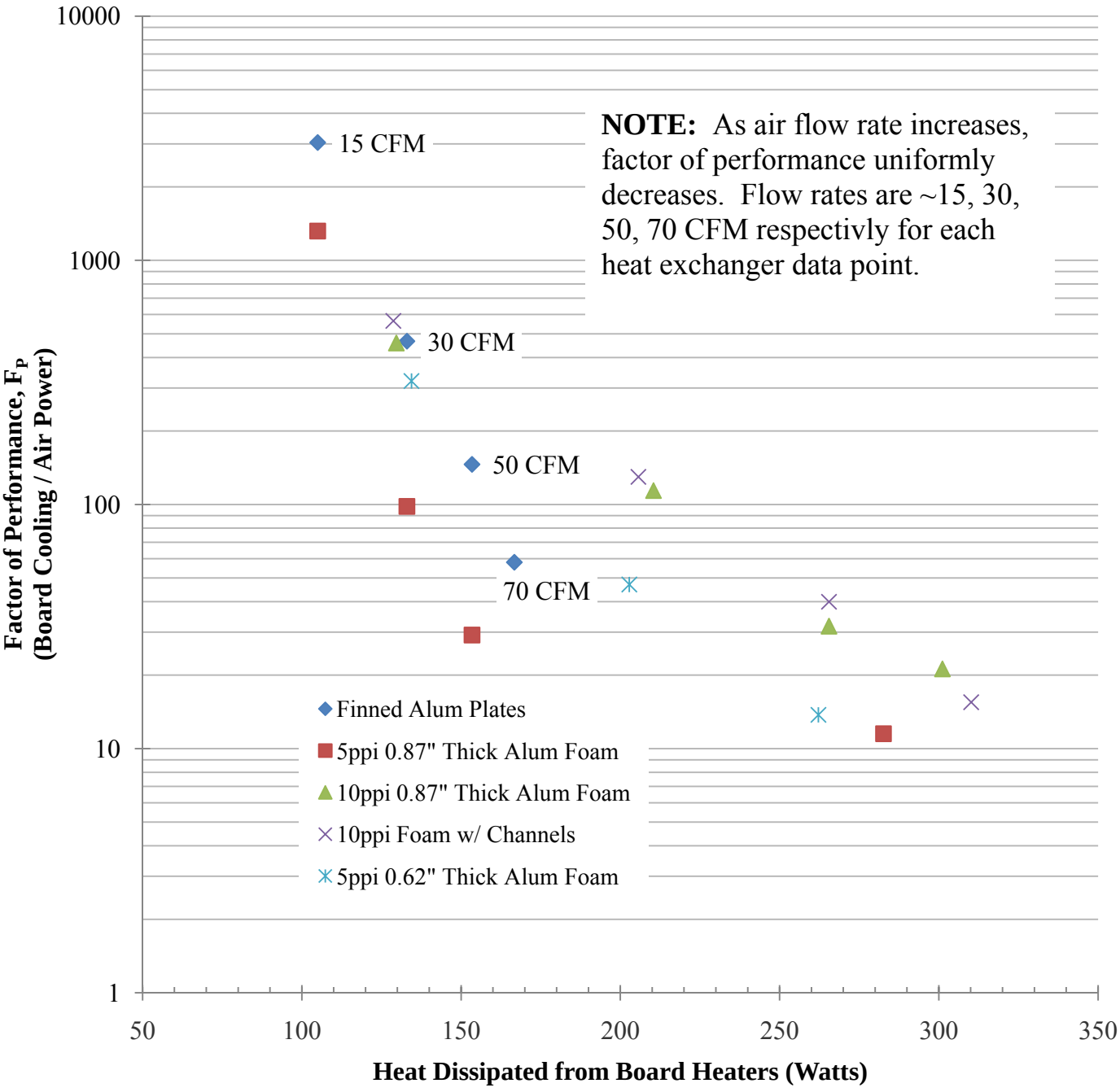

Figure 9-3: Plot of all reduced results

9.4 Specification Verification

Since the project primarily focuses on testing, specifications of the test rig and testing procedures are given below in Table 9-6.

Table 9-6: Testing Specifications: Original design specifications for testing of air cooling modules. Whether these specifications were realized or not during testing is also shown with explanations.

Spec. #	Parameter Description	Requirement or Target	Tolerance	Is specification met in Testing for all Configurations?
1	Spacing between modules	0.40 in	Smaller is Better	**Yes**
2	Plate Dimensions	10.2 by 7.9 in	± 0.1 in	**Yes**
3	Module Thickness	0.69 to 1.50 in	Smaller is better	**Yes**
4	Module Weight	6.5 lb	Smaller is Better	**Yes**
5	Max Component Temperatures	105 °C	± 1 °C	**No**
6	Worst Case Incoming Air Temp	70 °C	± 3 °C	
7	Flow Rate of Test Air	5 to 70 CFM	Smaller is Better	**Yes**: Tested at 15, 30, 50, and 70 CFM
8	Power Consumption	TBD	Min	Found from change in air pressure and velocity.
9	Heat Dissipation	TBD	Min	Found from power into test strip heaters at steady state.
10	Total Prototype Cost	$3,000	Max	**No**: $3800

* Specification numbers 5 and 6 were not able to be realized. Located at the air intake, an air heating device was designed and built to preheat the air to 70 °C, simulating the worst case intake air temperature to all testing. Three equally spaced thermocouples placed down-stream of the heater, before entering the heat exchangers, were used to get an accurate idea of the temperature distribution of the air. However, after prolonged testing, the device failed to give accurate and repeatable temperature measurements. The temperature distribution of the air was extreme, varying by as much as 34 °C between thermocouples. Temperature measurements taken over a period of time under constant flow rate are given in Figure 9-4.

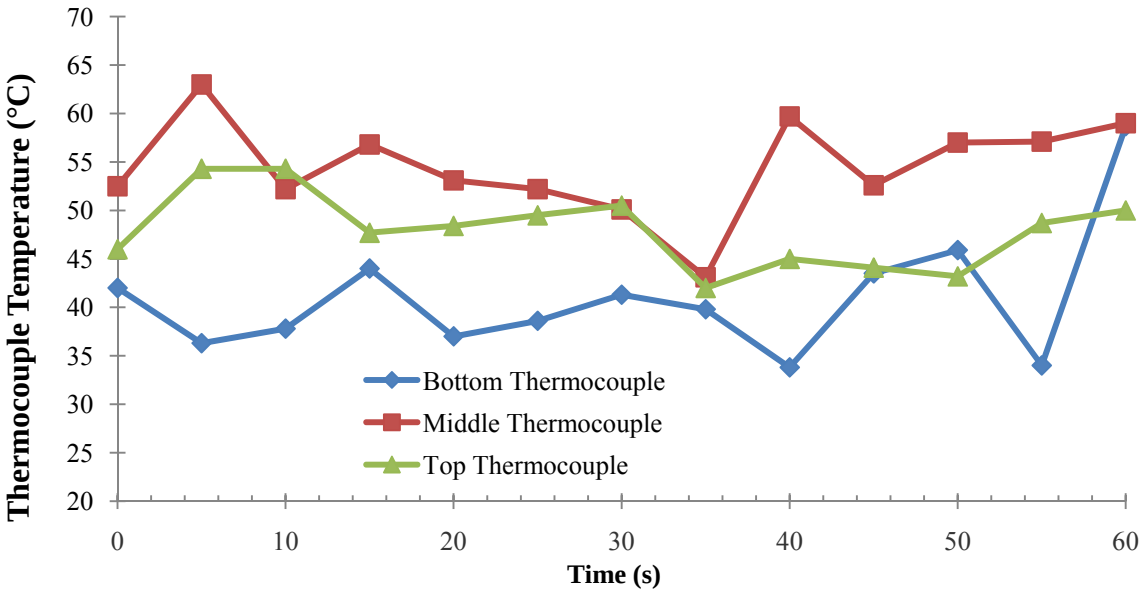

Figure 9-4: Erratic air intake thermocouple temperature readings over a period of one minute with intake air heater on.

The following is a list of additional justifications to remove the air intake heaters from the testing procedure:

1. Inconsistent temperature readings for individual thermocouples. Large standard deviations (each about 6° C).
2. During initial testing, the heaters began to show signs of imminent failure. Noticeable stresses and minor cracking began to form in the acrylic at the heaters location after prolonged operation.
3. The amount of time to adjust the incoming air temperature for each test run would be much too high.
4. Each test configuration would lack consistent temperature measurements, and therefore, be difficult to compare to one another.

To replace the inlet heater system, an alternative method to simulate the worst case scenario conditions was created. The difference in temperature between the intake temperature, 70 °C, and the not-to-exceed board temperature, 105 °C, would remain constant at a change of 35 °C. Therefore, the air intake temperature was measured during eat run to be about room temperature with very accurate stability. Therefore, max component temp was set at intake temp plus the original temperature change of 35 °C. This assumes a linear relationship in temperature. Even if this assumption is inaccurate, the tests can still be adequately compared to each other.

10 CONCLUSIONS

10.1 Results Discussion

10.1.1 Overall results

Experimentally determined cooling characteristics for all 4 heat exchanger configurations based on flow rate are seen in Figure 9-3. This plot is designed to be used as a selection tool for choosing an appropriate starting design point for AECM air cooling. Given a desired heat dissipation, one can select the most effective option by choosing a nearby result with the highest Factor of Performance.

10.1.2 Errors in testing and possible improvements

- **Calculated Heat transfer inversion**

  The heat transfer from the plates as was calculated using the energy balance equation for the air was expected to yield lower results than the power into the heaters. This expectation accounts for heat loss through insulation to the surrounding environment. The actual results did not yield this result, instead the calculated heat transfer was significantly and uniformly higher.

  Using the 5PPI thick foam configuration as an example; at a measured flow rate of 72CFM the heat transfer calculated from the energy equation was 463 watts, the power input into the heaters was 283 watts. This resulted in a 64% discrepancy. Other tests yielded similar discrepancies.

  The source of this discrepancy might be attributed to a poor flow rate measurement. The relatively inexpensive anemometer was designed for use in HVAC situations where it would be inserted into a duct of uniform size. The device likely measured flow velocity accurately but errors in calibrating the cross sectional area may have caused improper volumetric flow rate calculations. This error, when introduced to the mass flow rate and eventual heat transfer equations, might cause the inversion error seen in the results.

  It is likely that the actual flow rates were significantly lower than the measured flow rates. In the aforementioned 5ppi thick configuration a 40% decrease in flow rate gives the calculated heat transfer a nearly equivalent value as the power input.

  Utilizing a more appropriate flow rate measurement device would help to confirm these assumptions. A hot-wire anemometer, coupled with a longer outlet tube to ensure fully developed flow would be a possible future improvement.

- **Thermocouple #4**

  Without exception, thermocouple #4 dictated the upper temperature limit. This thermocouple was at the lowest middle location on the circuit board, a location unlikely to see the hottest temperatures. Additionally, this thermocouple always reported values greater than 2 °C above the average board temperature.

- **Heating incoming air**

  The failure of the inlet pre-heater occurred too late in the quarter to allow any redesign. Implementing a working pre-heating system would help to more accurately represent the worst-case-scenario environments seen in actual implementation.

10.2 Recommendations and Real-World Application Considerations

10.2.1 Safety

Actual future implementation of AECM modules introduces a small number of safety considerations. Caution should be used when handling the sharp edges of the aluminum foam and finned plates. Heat exchangers in use will often reach temperatures high enough to cause significant burns. Warnings posted regarding these possible hazards should be adequate to assure safe use of the modules.

10.2.2 Reliability

The static nature of the module covers dictates little expectation of mechanical failure. The cyclical heat stresses acting on the plates are negligible. The most likely cause of failing to reach performance expectations would be chronic particulate buildup. The foam heat exchangers would be especially susceptible to this. The porous nature and small flow channels inherent in the material would easily collect dust. Filtering to ensure particulate-free air through the cooling system would help alleviate this problem.

Failures in air forced convection systems when air cooling are less likely to cause catastrophic failure when compared to liquid-cooled systems. Air cooled module plates in still air will experience significant cooling via natural convection causing slower rates of temperature increases when compared to liquid-cooled modules.

10.2.3 Manufacturing

The prototype nature of this project restricted the possibility of certain manufacturing techniques. Alternative methods of manufacturing, including metal extrusion and die-casting would allow for significant decreases in cost and increases in finned plate densities. A finished product could be expected to see higher cooling performances than the devices tested in this project.

The cooling performance of the foam configurations would be significantly increased if the aluminum foam blocks were brazed to the module covers. This manufacturing technique, while expensive on a small scale, would likely see drastic reductions of cost if mass produced.

10.3 Comparison to Existing Systems

10.3.1 Liquid-cooled AECM Model

The liquid cooled AECM module model predicted a heat transfer rate of 240 watts. This value falls in the upper range of the values obtained experimentally using air cooled plates. The comparison between the two systems beyond the simple juxtaposition of heat transfer rates requires the calculation of factors of performance for the liquid cooled module, a result not obtainable without additional testing. Further analysis of results from other AECM research projects might allow for a more direct comparison.

10.3.2 ARINC 600 Standard

Direct comparison to the ARINC standard is not possible at present. The data provided is lacking information regarding incoming air temperature and maximum operating thresholds. The pressure drops at similar CFM rates for the AECM air cooled designs are comparable to those reported for the ARINC standard.

With additional details regarding the ARINC 600 cooling standard a direct comparison would be easily obtained.

10.4 Final Thoughts

The heat dissipation seen from the heat exchanger plates is competitive with the liquid-cooled module plates and deserves further investigation. The added benefits of natural convection and the weight savings of air cooling further endorse this conclusion.

Bruno Caulk and Kevin Whipp would like to thank Boeing for the exciting opportunity to help develop new technologies. Thanks to Sarah Harding for her support and organization help. Special thanks go to Charlie Kusuda for his valuable advice, time dedicated to helping the team and eager involvement.

We have learned a great deal of real-world problem solving and project organization and see this project as an invaluable contribution to our engineering education.

Bruno Caulk Kevin Whipp

11 APPENDIX A: WORKS CITED

"About Selecting Thermal Insulation" McMaster-Carr 6 March 2009 < http://www.mcmaster.com/#about-thermal-insulation/=x5t34>

Enertron "Selecting a Heat Pipe" Enertron Total Thermal Management Solutions 26 January 2009 <http://www.enertron-inc.com/enertron-products/heat-pipe-selection.php>

Engelhardt, Andreas "Pushing the Boundaries of Heat Pipe Operation" Electronics Cooling 25 January 2009 <http://www.electronics-cooling.com/html/2008_nov_a3.php>

Glynn, Colin; O'Donovan, Tadhg and Murray, Darina B. "Jet Impingement Cooling" Centre for Telecommunications Value-Chain-Driven Research, Trinity College, Dublin <http://www.ctvr.ie/docs/PHO_Pubs/UKHeatTransfer%20Sept2005.pdf>

Graphite Foams" Oak Ridge National Laboratory June 16, 2001 <http://www.ms.ornl.gov/researchgroups/CIMTECH/FOAM/foams.htm>

"HEAT SPREADERS" Novel Concepts, Inc. 26 January 2009 <http://www.novelconceptsinc.com/heat-spreaders.htm>

Laider, Keith, J. *The World of Physical Chemistry*. Oxford University Press, 1993

Klett, James; Stinton, Dave; Ott, Ron; Walls, Claudia "Heat Exchangers/Radiators Utilizing"

Kusuda, Charles "Alternative Equipment Cooling Method Study" Digital file prepared for presentation at Cal Poly University, San Luis Obispo, January 2009

Mahalingam, Raghav; Heffington, Sam; Jones, Lee and Williams, Randy "synthetic jets for forced air cooling of electronics" Nuventix Inc. May 2007 <http://www.nuventix.com/technology/papers/>

Shankara Narayanan K.R. "What is a Heat Pipe" CheResources 25 January 2009 <http://www.cheresources.com/htpipes.shtml>

Solovitz, Stephen A.; Stevanovic, Ljubisa D. "Microchannels Take Heatsinks to the Next Level" Power Electronics Technology 1 November 2006 <http://powerelectronics.com>

Spang, Bernhard Dr. "U in Heat Exchangers" CheResources March 2009 < http://www.cheresources.com/uexchangers.shtml>

Vita Standards Organization "Mechanical Specifications for Microcomputers Using REDI Conduction Cooling Applied to VITA 46" 29 December 2006

Wong, Robert S "Maximum Heat Dissipation for an Advance Equipment Cooling Method (AECM) Electronics Module" Boeing 3 November 2008

12 APPENDIX B: DUOCELL ALUMINUM FOAM INFO

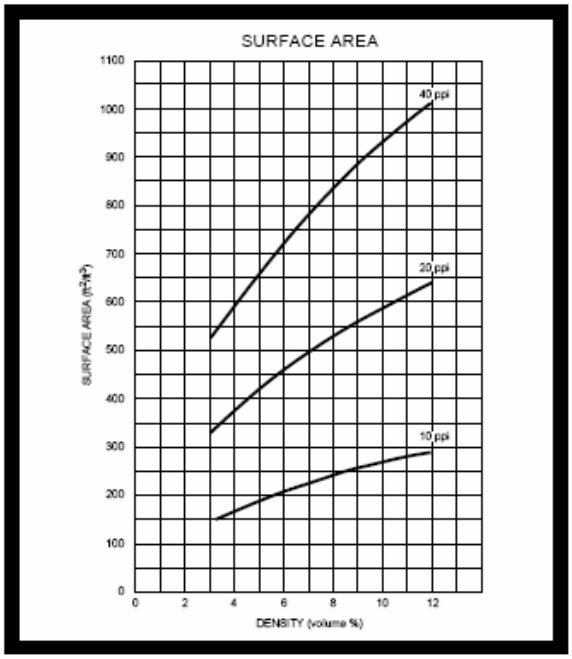

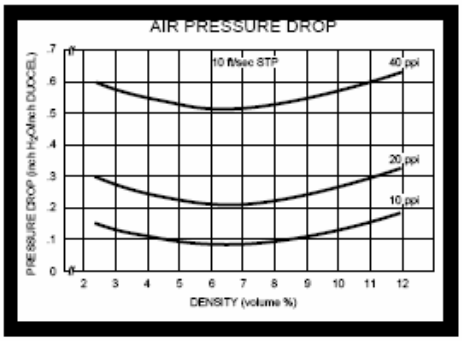

DUOCEL...true foam metal

Duocel is a true metal skeletal structure. It is not a sintered, coated, or plated product. Its purity is typically that of the parent alloy metal, with no voids, inclusions, or entrapments. There are other products that look like Duocel, but the similarity stops with the appearance.

Duocel is manufactured by directional solidification of metal from a super-heated liquidus state in an environment of overpressures and high vacuum. The resulting material has a reticulated structure of open, duodecahedronal-shaped cells connected by continuous, solid metal ligaments. The solid-metal ligaments routinely test to 99 percent purity of the parent alloy (to AMS specifications), are not porous, and approximate single strand drawn wire.

The matrix of cells and ligaments is completely repeatable, regular, and uniform throughout the entirety of the material. Duocel is a rigid, highly porous and permeable structure and has a controlled density of metal per unit volume.

Duocel is available in production in 6101 and A356 aluminum alloys and in vitreous or glassy carbon. Other aluminum alloys, other metals, ceramics and composite materials are available on special order.

Density of metal and cell size (expressed as pores per inch) can each be varied independently to tailor the properties of the material to meet specific design requirements. Density is continuously variable from 3 percent to 12 percent. Cell size can be 5, 10, 20, or 40 pores per inch (ppi). (Mean cell sizes of .170", .080", .040", or .020".)

Duocel is manufactured in billet form in the following dimensions and then is furnished to the dimensions specified by the customer. Larger sizes are available on special order.

	Nominal (in.)
Length	16
Width	12
Thickness	4

The material is supplied as a finished end-item product to the requirements of the customer. ERG's engineering and manufacturing departments will assist you in determining how Duocel should be fabricated to meet your needs.

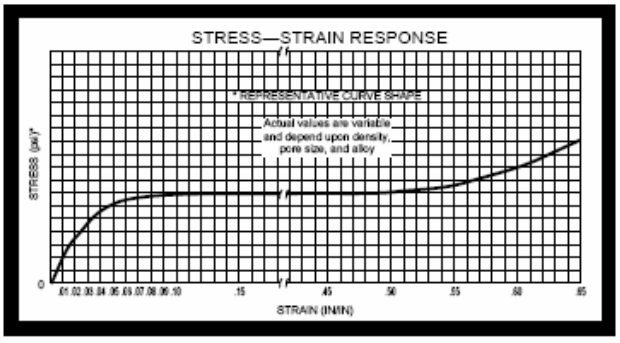

The "dual personality" material

ERG's exclusive manufacturing process gives Duocel a unique "dual personality." On the one hand, it has all of the properties of the metal of which it is made, such as corrosion resistance, intrinsic strength, electrical and thermal conductivity, acceptance of coatings, and others. On the other hand, it has the advantages offered only by Duocel: low density, high strength to weight, high porosity, extremely large surface area, and more.

If a design calls for aluminum for its electrical properties, for example, you can have those properties with Duocel. As a bonus, you save weight (and money). Or, if weight is the critical factor, as in a heat exchanger for airborne equipment, Duocel will do the job at a fraction of the weight of a solid aluminum part.

But don't think of Duocel as just a replacement material for existing parts. Think of it as a new basic material — one with its own set of unique properties, one that opens up a whole new way of designing.

The Duocel structure provides several unique mechanical properties:

1. Independently variable porosity from 5 to 40 pores per inch.
2. Independently variable density from 3 to 12 percent.
3. High (and variable) surface area to unit volume.
4. High strength-to-weight ratio.
5. Completely isotropic load response.
6. Variable stress-strain characteristics.

The accompanying graphs show some of Duocel's general properties. ERG's engineering department has extensive research and engineering data for specific applications of Duocel, such as heat transfer, energy absorption, and structural applications. We will be pleased to furnish this data to you and to answer your questions about the suitability of Duocel for your application.

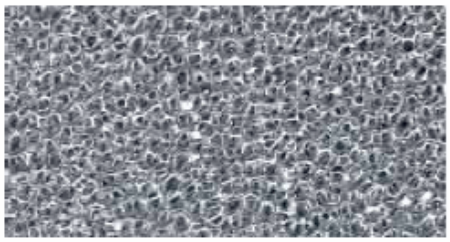

40 pores per inch

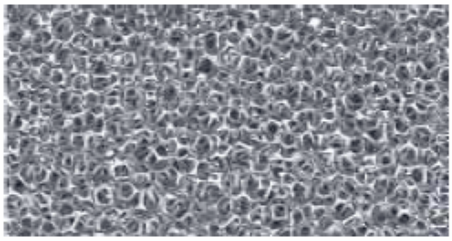

20 pores per inch

10 pores per inch

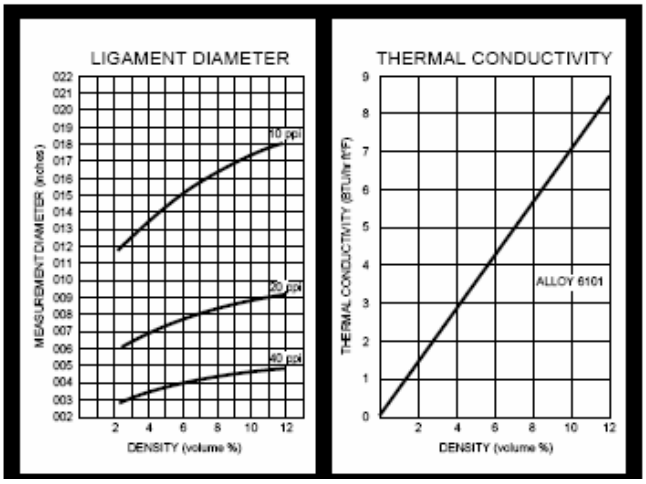

Fabrication properties and processes

Duocel can be cut, turned, milled, ground, lapped, drilled, rolled, and finished with special machine-shop equipment to normal tolerances. Through forming, Duocel can easily conform to complex shapes. Any bonding technique that can be used for the parent metal can be used for Duocel. It can be vacuum- or dip-brazed, epoxied, or adhesion bonded. Unlike other similar materials, Duocel can be brazed to metals, forming an integral metal-to-metal bond. Duocel can also be heat treated, anodized, alodine coated, or metal plated. It accepts colors, finishes, platings, and coatings just as the parent metal does.

13 APPENDIX C: HOUSE OF QUALITY (QFD)

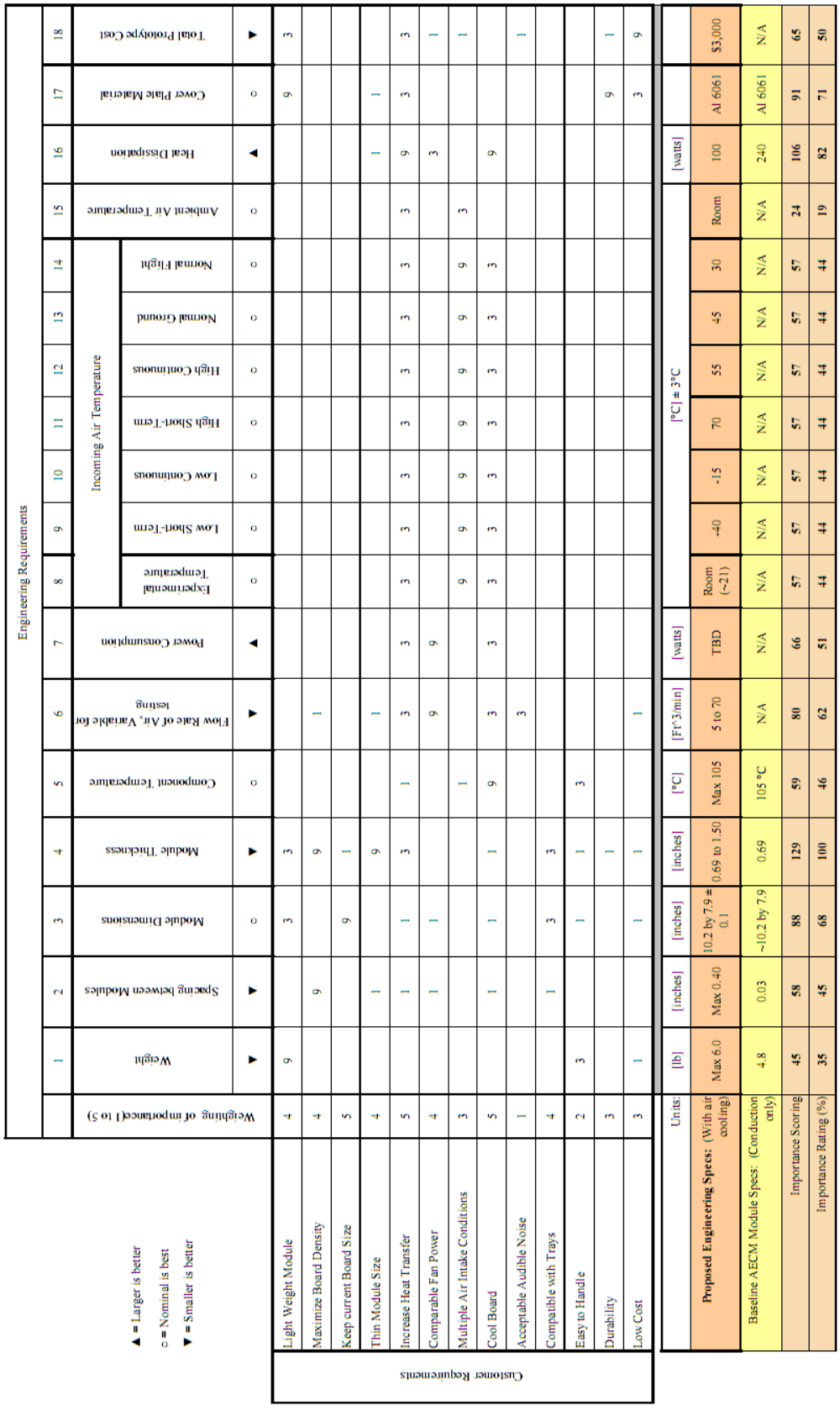

Customer Requirements	Weighting of importance(1 to 5)	1 Weight ▼	2 Spacing between Modules ▼	3 Module Dimensions ○	4 Module Thickness ▼	5 Component Temperature ○	6 Flow Rate of Air, Variable for testing ▼	7 Power Consumption ▼	8 Incoming Air Temperature: Experimental Temperature ○	9 Incoming Air Temperature: Low Short-Term ○	10 Incoming Air Temperature: Low Continuous ○	11 Incoming Air Temperature: High Short-Term ○	12 Incoming Air Temperature: High Continuous ○	13 Incoming Air Temperature: Normal Ground ○	14 Incoming Air Temperature: Normal Flight ○	15 Ambient Air Temperature ○	16 Heat Dissipation ▲	17 Cover Plate Material ○	18 Total Prototype Cost ▼
Light Weight Module	4	9		3	3													9	3
Maximize Board Density	4		9		9		1												
Keep current Board Size	5			9	1														
Thin Module Size	4		1		9		1										1	1	
Increase Heat Transfer	5		1	1	3	1	3	3	3	3	3	3	3	3	3	3	9	3	3
Comparable Fan Power	4		1	1			9	9									3		1
Multiple Air Intake Conditions	3					1			9	9	9	9	9	9	9	3			1
Cool Board	5		1	1	1	9	3	3	3	3	3	3	3	3	3		9		
Acceptable Audible Noise	1						3												1
Compatible with Trays	4		1	3	3														
Easy to Handle	2	3		1	1	3													
Durability	3				1													9	1
Low Cost	3	1		1	1		1											3	9
	Units:	[lb]	[inches]	[inches]	[inches]	[°C]	[Ft^3/min]	[watts]	Room (~21)	-40	-15	70	55	45	30	Room	[watts]		
	Proposed Engineering Specs: (With air cooling)	Max 6.0	Max 0.40	10.2 by 7.9 ± 0.1	0.69 to 1.50	Max 105	5 to 70	TBD	N/A	N/A	N/A	N/A	N/A	N/A	N/A	N/A	100	Al 6061	$3,000
	Baseline AECM Module Specs: (Conduction only)	4.8	0.03	~10.2 by 7.9	0.69	105 °C	N/A	N/A	N/A	N/A	N/A	N/A	N/A	N/A	N/A	N/A	240	Al 6061	N/A
	Importance Scoring	45	58	88	129	59	80	66	57	57	57	57	57	57	57	24	106	91	65
	Importance Rating (%)	35	45	68	100	46	62	51	44	44	44	44	44	44	44	19	82	71	50

▲ = Larger is better
○ = Nominal is best
▼ = Smaller is better

14 APPENDIX D: IDEA POSTER

15 APPENDIX E: FOAM PRESSURE DROP CALCS.

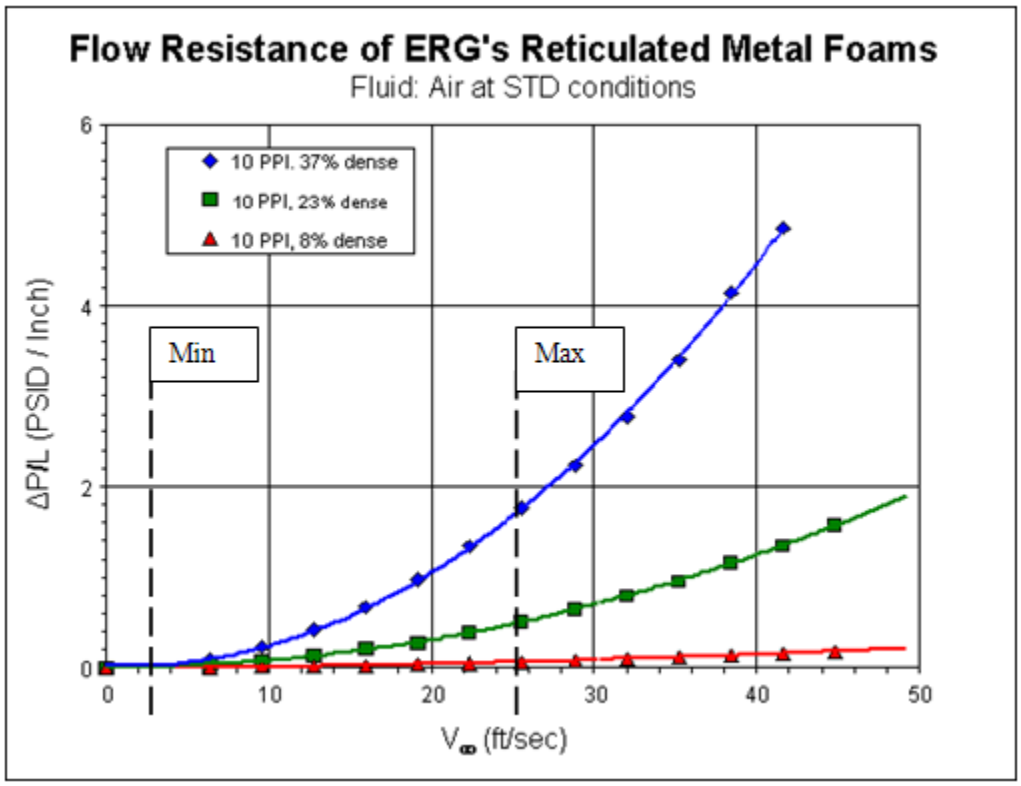

Assume:

- Max flow rate of 70 cfm, through 9" wide aluminum foam, 3/4" thick.

- Using 10 PPI (pours per inch), 8% dense foam (red line in chart above),

  8% dense foam is recommended by ERG Aero for use in air cooled heat exchangers.

  - Air travels over 7inches of alum foam

Maximum Average Velocity:

$$\overline{V}_{\max} = \frac{\dot{V}\left[\frac{ft^3}{\min}\right]\left[\frac{1\min}{60s}\right]}{A\left[in^2\right]\left[\frac{1\,ft}{12in}\right]^2} = \frac{70}{9*0.75}\left[2.4\frac{ft}{s}\right] = 24.9\,ft/s$$

- The minimum velocity can be calculated similarly to be 2.49 ft/s
- Both velocities are represented by the vertical dashed line on the above plot

Pressure Drop over 7 inches of foam:

- Measuring from max velocity line intersecting red line

$$\Delta P \cong \left(0.12\frac{psi}{inch}\right)(7.0inches) = 0.84\,psi = 23inH\,2O$$

- If 20 PPI, 8% dense foam used (plot shown below):
-

$$\Delta P \cong \left(0.2\frac{psi}{inch}\right)(7.0inches) = 1.4\,psi = 39inH\,2O$$

-

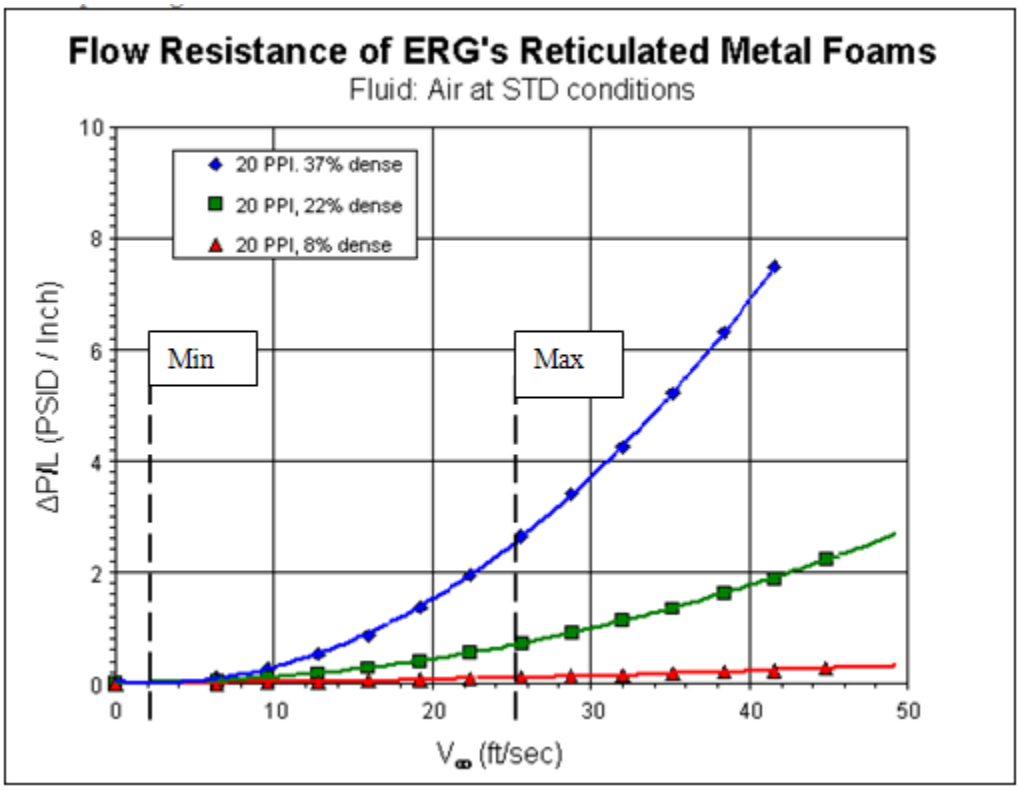

16 APPENDIX F: DRAWING LIST

All necessary custom parts with drawings to create custom parts and assemblies are included in this section. Each one appears in the following order:

16.1 T100 MAIN TESTING RIG

16.2 T200 MODULE HALF ASSEMBLY

- T203 PC BOARD
- M01 DESIGN CONFIG #1 – MACHINED ALUMINUM FIN GEOMETRY

16.3 T300 BLOWER AND DUCT ASSEMBLY

- *T301 AIR REDUCER - Split into 4 parts for Rapid Prototyping
- T302 UPPER RAILS
- *T304 ANEMOMETER CONNECTOR HALF
- *T306 FAN CONNECTOR HALF

16.4 T400 BOTTOM COVER ASSEMBLY

- T401 LOWER RAILS
- T402 LOWER MODULE CONNECTOR
- T403 AIR INTAKE

* Drawings are not included due to their simplicity.
** Parts with be rapid prototyped at Cal Poly and only include critical dimentions.

REVISIONS			
REV.	DESCRIPTION	DATE	APPROVED

NOTES

1. THIS ASSEMBLY DOES NOT INCLUDE A STAND TO SUPPORT THE TESTING RIG. IT ONLY DISPLAYS THE BASIC ELEMENTS AND GEOMETRY REQUIRED FOR TESTING.
2. ALL THERMOCOUPLES AND NESSESARY WIRES ARE NOT SHOWN FOR SIMPLICITY.

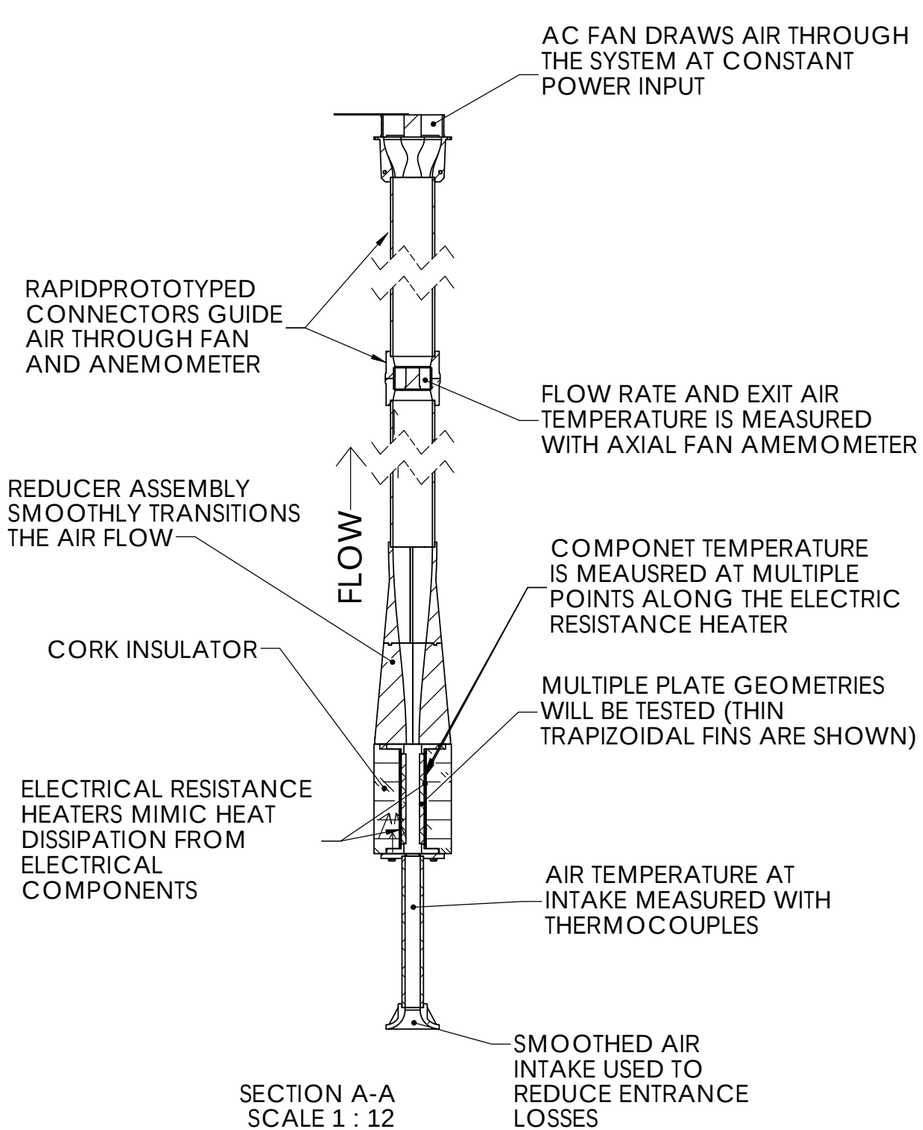

SECTION A-A
SCALE 1 : 12

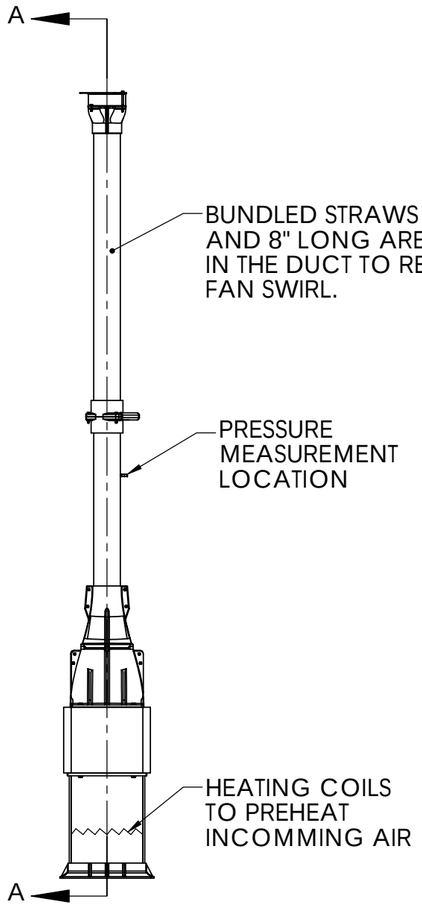

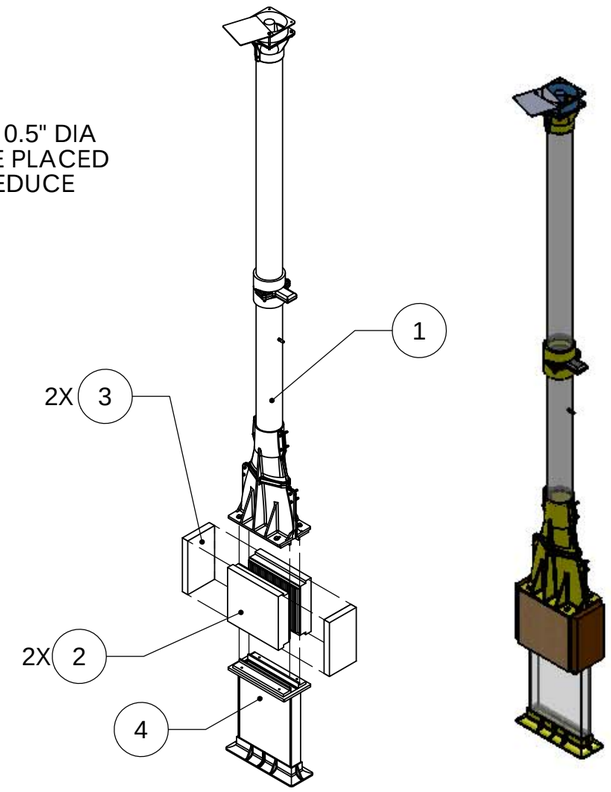

ITEM NO.	PART NO.	Description	VENDOR	QTY
1	T300	BLOWER AND DUCT ASSEMBLY		1
2	T200	INSULATED MODULE HALF ASSEMBLY		2
3	T101	Semi Rigid Cork Board Insulation (MCMASTER: 9354K12)	MCMASTER_CARR	2
4	T400	BOTTOM COVER ASSEMBLY		1

	NAME	DATE
DRAWN	BRUNO	3/10/09
CHECKED		
CHECKED		

MATERIAL: N/A
FINISH: N/A

NEXT ASSY	USED ON
APPLICATION	

UNLESS OTHERWISE SPECIFIED:
DIMENSIONS ARE IN INCHES
TOLERANCES:
FRACTIONAL: ±1/8
ANGULAR: ± 3°
.XX ±.01
.XXX±.005

SECTOR

Senior Project
In Partnership with Boeing
Cal Poly
Mechanical Engineering Dept.
San Luis Obispo, CA
Bruno Caulk and Kevin Whipp

TITLE:
AIR COOLING TESTING RIG

SIZE	DRAWING NO.	REV
B	T100	D

SCALE: 1:20 | SHEET 1 OF 1

REVISIONS			
REV.	DESCRIPTION	DATE	APPROVED

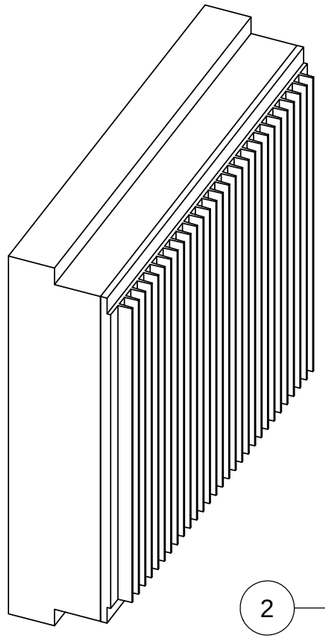

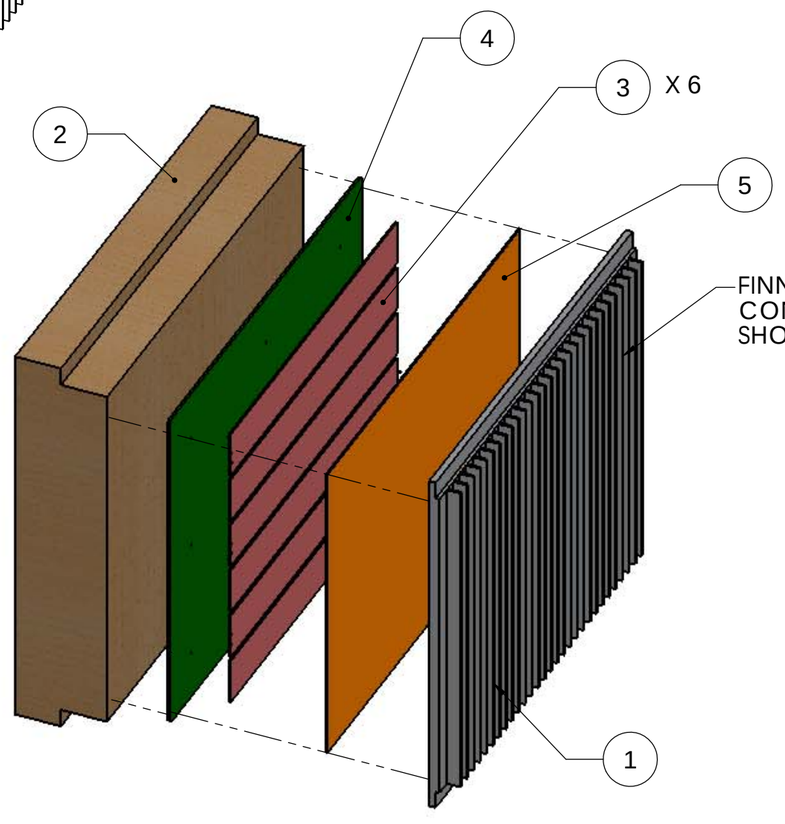

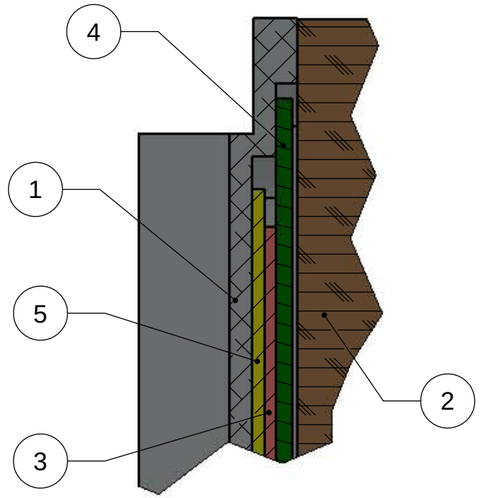

DETAIL A
SCALE 2 : 1

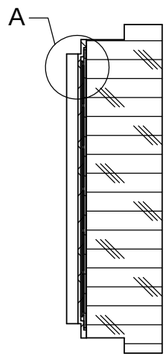

SECTION A-A
SCALE 1 : 4

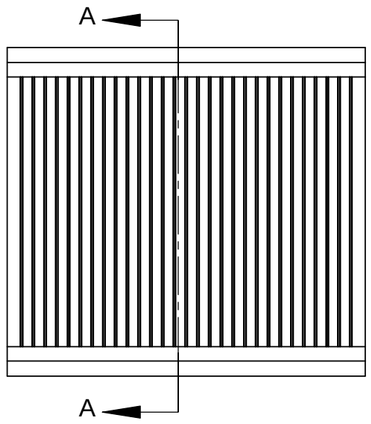

ITEM NO.	PartNo	Description	VENDOR	QTY
1	MXX	ALUM PLATE WITH 3 CONFIGS: M01, M02, M03		1
2	T202	Semi Rigid Cork Board Insulation (MCMASTER: 9354K12)	MCMASTER-CAR	1
3	SRFG-108/5-P	1"x8" SILICONE HEATER 5 W/Sq in. w/ ADHESIVE	OMEGA	6
4	T203	PC BOARD	TBD	1
5	T201	0.040 in thick, Therm-a-gap material Type A PSA (CHOMERICS: 69-12-20684-A580)	CHOMERICS	1

	NAME	DATE
DRAWN	BRUNO	3/10/09
CHECKED		
CHECKED		

MATERIAL

FINISH

T100	
NEXT ASSY	USED ON
APPLICATION	

UNLESS OTHERWISE SPECIFIED:
DIMENSIONS ARE IN INCHES
TOLERANCES:
FRACTIONAL: ±1/8
ANGULAR: ± 3°
.XX ±.01
.XXX ±.005

SECTOR

Senior Project
In Partnership with Boeing
Cal Poly
Mechanical Engineering Dept.
San Luis Obispo, CA
Bruno Caulk and Kevin Whipp

TITLE:
INSULATED MODULE HALF ASSEMBLY

SIZE	DRAWING NO.	REV
B	T200	B
SCALE: 1:3		SHEET 1 OF 1

NOTES:

REVISIONS				
ZONE	REV.	DESCRIPTION	DATE	APPROVED

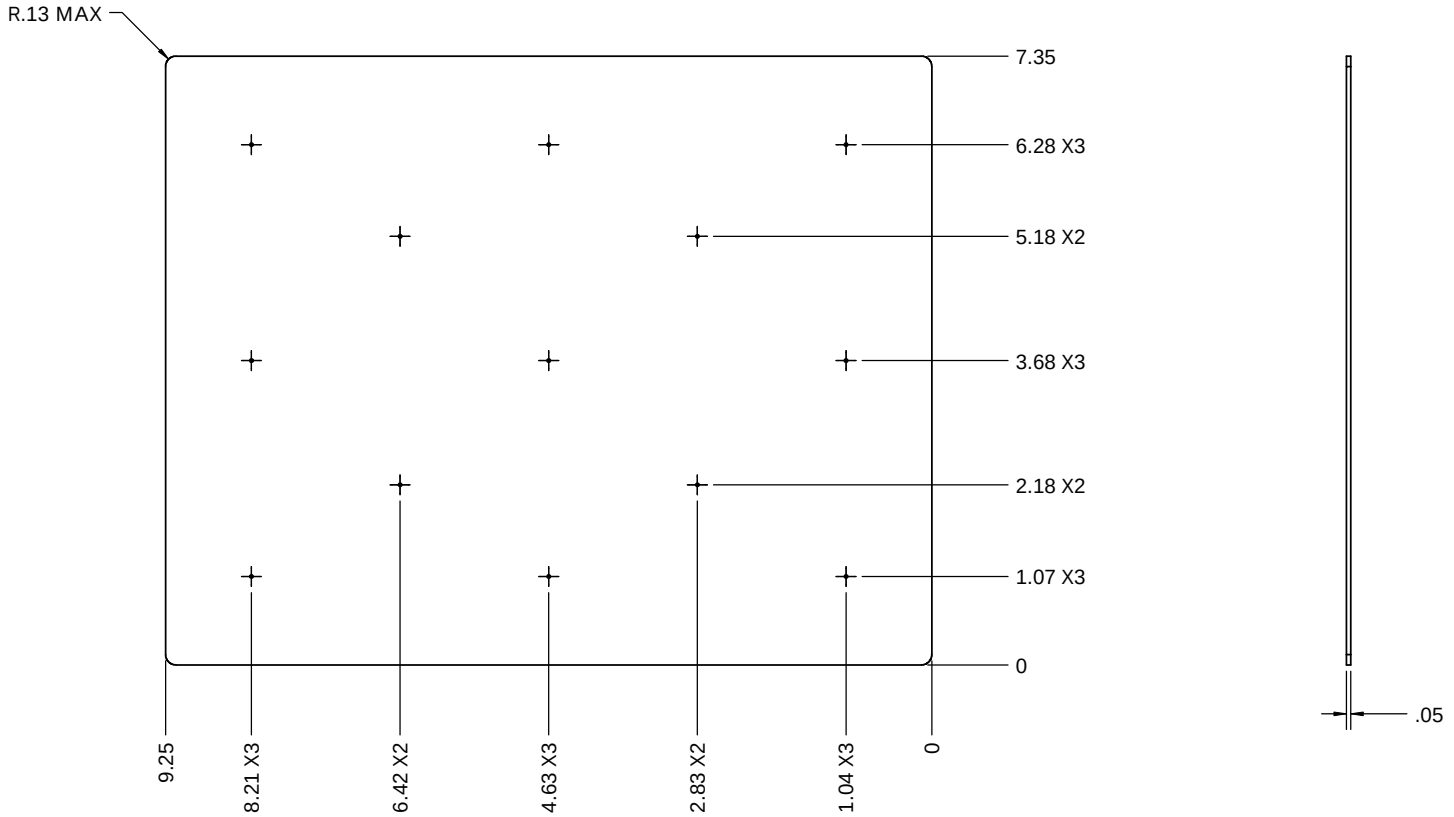

	NAME	DATE
DRAWN	BRUNO	4/30/09
CHECKED		
CHECKED		

MATERIAL

FINISH

T400

NEXT ASSY | USED ON

APPLICATION

UNLESS OTHERWISE SPECIFIED:
DIMENSIONS ARE IN INCHES
TOLERANCES:
FRACTIONAL: ±1/8
ANGULAR: ± 3°
.XX ±.01
.XXX±.005

Senior Project
In Partnership with Boeing
Cal Poly
Mechanical Engineering Dept.
San Luis Obispo, CA
Bruno Caulk and Kevin Whipp

TITLE: PC BOARD

SIZE B | DRAWING NO. T203 | REV A

SCALE: 2:3 | SHEET 1 OF 1

NOTES:

1. PART TO BE MACHINED WITH CNC ON THE CAL POLY CAMPUS
2. BASE DIMENTIONS MATCH THAT OF THE BLANK MODULE PLATE, M02. FINS ARE JUST AN ADDITION TO THE TOP OF THE PLATE.
3. FOR TESTING, POCKET WILL HOUSE BLANK CIRCUIT BOARD, THERMOCOUPLE ARRAY, HEATER STRIPS, AND THERM-A-GAP CONDUCTIVE INTERFACE MATERIAL.
4. DIMENSIONS ARE TYPICAL FOR A TOTAL OF 49 VERTICAL FINS.

REVISIONS		
REV.	DESCRIPTION	DATE
A	INITIAL RELEASE	

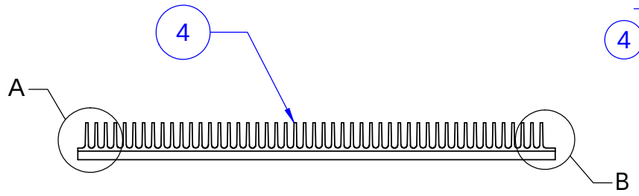

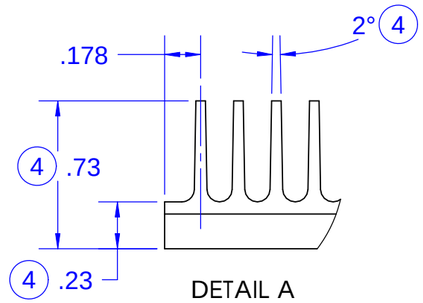

DETAIL A
SCALE 4 : 3

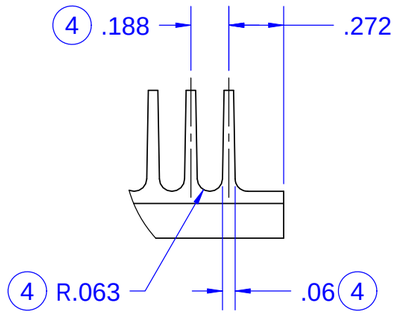

DETAIL B
SCALE 4 : 3

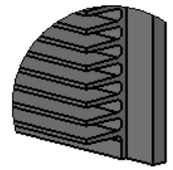

DETAIL C
SCALE 2 : 3

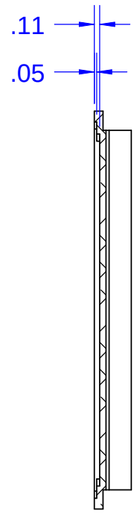

SECTION N-N

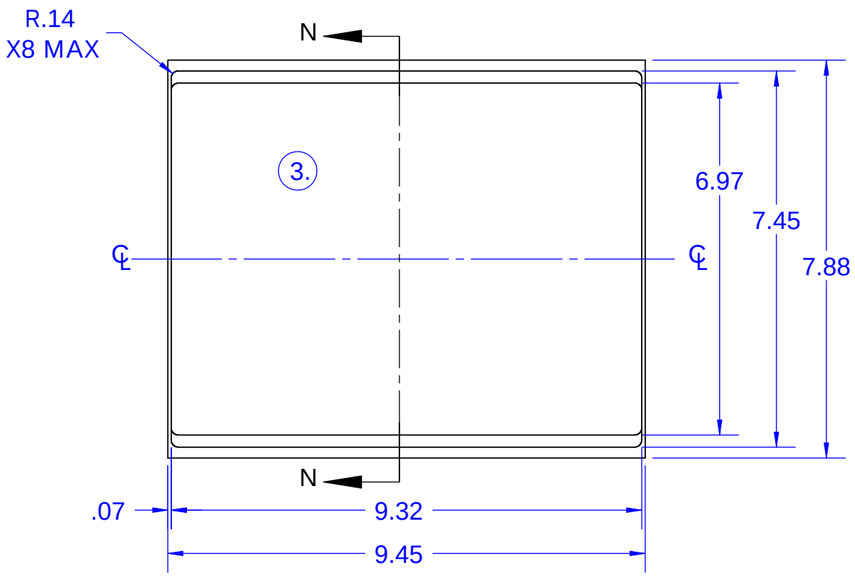

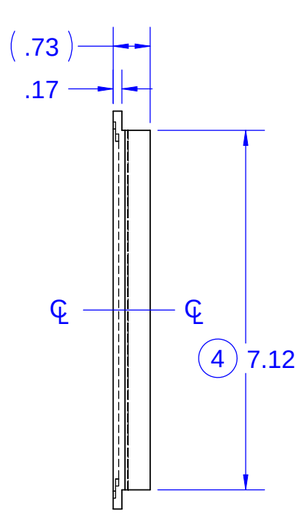

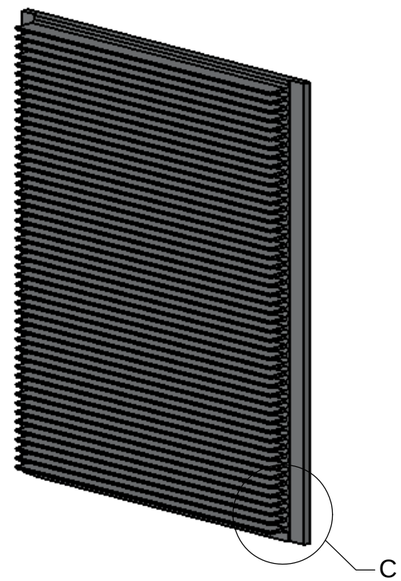

	NAME	DATE
DRAWN	BRUNO	12/1/09
CHECKED		
CHECKED		

MATERIAL: AL 6061
FINISH: NONE

TITLE: FINNED ALUM MODULE PLATE

T200

NEXT ASSY | USED ON

APPLICATION

UNLESS OTHERWISE SPECIFIED:
DIMENSIONS ARE IN INCHES
TOLERANCES:
FRACTIONAL: ±1/8
ANGULAR: ± 3°
.XX ±.01
.XXX ±.005

Senior Project
In Partnership with Boeing
Cal Poly
Mechanical Engineering Dept.
San Luis Obispo, CA
Bruno Caulk and Kevin Whipp

SIZE B | DRAWING NO. M01 | REV A

SCALE: 1:3 | SHEET 1 OF 1

REVISIONS			
REV.	DESCRIPTION	DATE	APPROVED

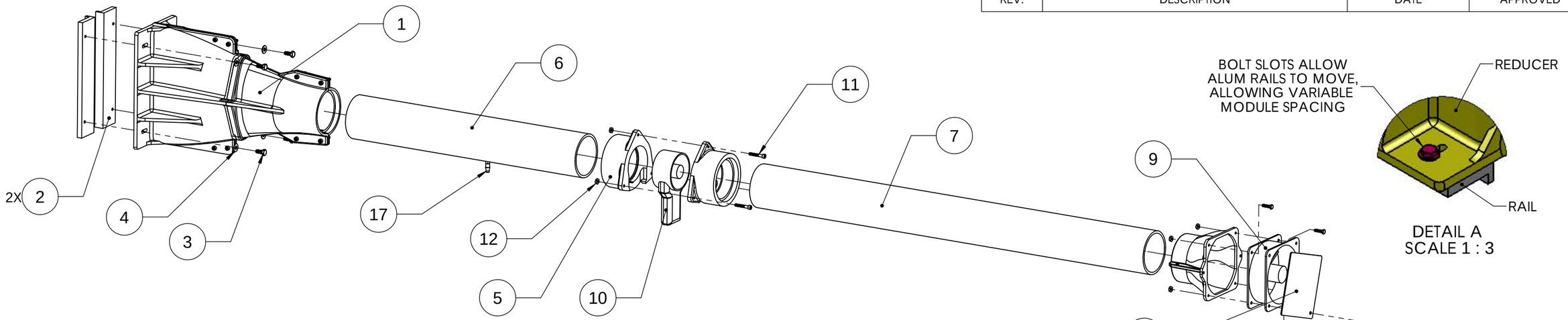

DETAIL A
SCALE 1 : 3

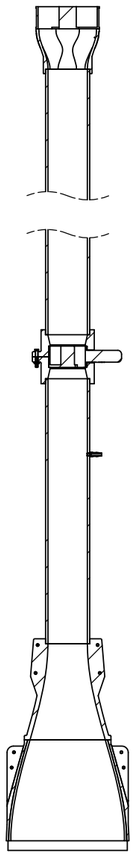

SECTION VIEW
SCALE 1:12

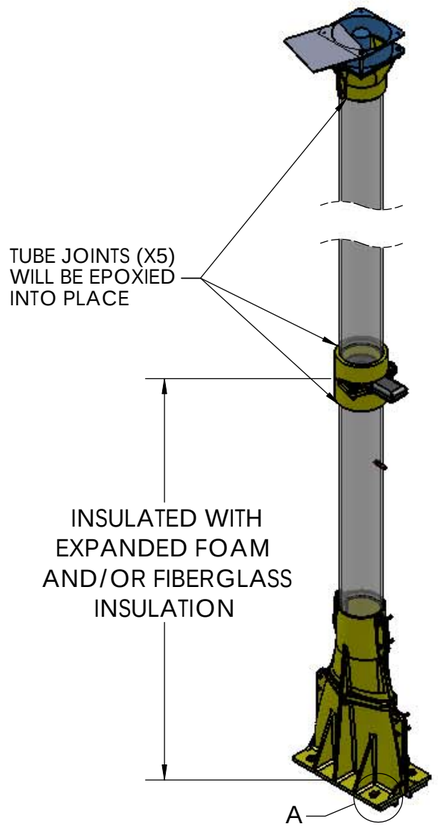

ITEM	PartNo	Description	VENDOR	Default/ QTY.
1	T301	AIR REDUCER ASSEMBLY	N/A	1
2	T302	UPPER RAIL		2
3	TBD	Hex Head Cap Screw 1/4-28, 5/8 length	TBD	4
4	TBD	WASHER, 1/4 DIA BOLT, .05 THICK	TBD	4
5	T304A/B	ANAMOMETER CONNECTOR	-	1
6	8486K474	21" LONG, ACRYLIC TUBE 3.125" ID	McMASTER	1
7	8486K474	36" LONG, ACRYLIC TUBE 3.125" ID	McMASTER	1
9	59124600N	119mm AXIAL FAN, PAPST 4600N	MOUSER	1
10	HHF91	ROTARY VANE ANEMOMETER	OMEGA	1
11	-	HEX CAP SCREW #10-24 7/8" LENGTH	-	3
12		#10-24 STEEL NUT		7
13	-	HEX CAP SCREW, #10-24 1 3/8 LENGTH	-	4
15	-	SIMPLE DAMPER, 1/16" STEEL SHEET		1
16	-	STEEL HEX CAP SCREW, #10-25, 0.75"	-	3
17	5121K341	BARBED TUBE ADAPTER, 1/4"-28 UNF MALE, PP	MCMASTER-CARR	1

	NAME	DATE
DRAWN	BRUNO	11/30/09
CHECKED		
CHECKED		

MATERIAL: NA
FINISH: NA

T100	
NEXT ASSY	USED ON
APPLICATION	

UNLESS OTHERWISE SPECIFIED:
DIMENSIONS ARE IN INCHES
TOLERANCES:
FRACTIONAL: ±1/8
ANGULAR: ± 3°
.XX ±.01
.XXX±.005

SECTOR h

Senior Project
In Partnership with Boeing
Cal Poly
Mechanical Engineering Dept.
San Luis Obispo, CA
Bruno Caulk and Kevin Whipp

TITLE:
BLOWER AND DUCT ASSEMBLY

SIZE	DRAWING NO.	REV
B	T300	B
SCALE: 1:8		SHEET 1 OF 1

NOTES:

1. THE ASSEMBLY CONSSITS OF 4 RAPID PROTOTYPED ABS PARTS CONSTTRUCTED AT CAL POLY.
2. PARTS T301A AND T301C WILL BE EPOXIED TOGETHER, LEFT TO DRY, AND THEN THE INTERIOR SURFACE WILL BE SANDED DOWN TO 400 GRIT SAND PAPER TO DECREASE DRAG. THE SAME WILL BE DONE WITH PARTS T301B AND T301D.
3. HALF #1 AND HALF #2 WILL THEN BE LIGHTLY GLUED ALONG CONNECTING SURFACES AND BOLTED TOGETHER AS SHOWN.
4. BECAUSE THE PART WILL BE RAPID PROTOTYPED, ONLY CRITICAL DIMENSIONS ARE SHOWN
5. THE ENTIRE REDUCER ASSEMBLY WILL BE COATED IN EXPANDED FOAM INSULLATION TO REDUCE ANY HEAT LOSSES BEFORE THE DOWNSTREAM TEMPERATURE MEASUREMENT AT THE ANEMOMETER.

REVISIONS				
ZONE	REV.	DESCRIPTION	DATE	APPROVED

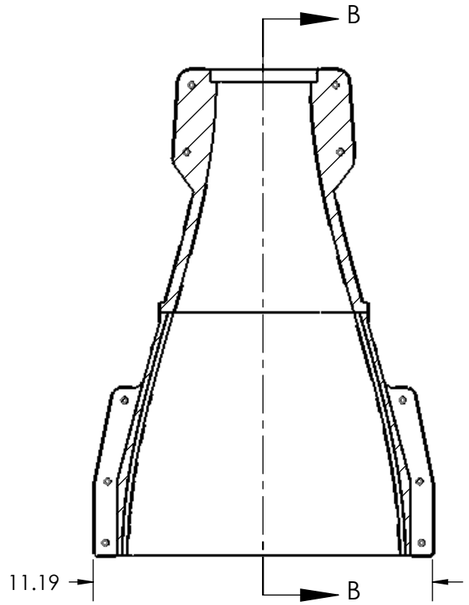

SECTION A-A

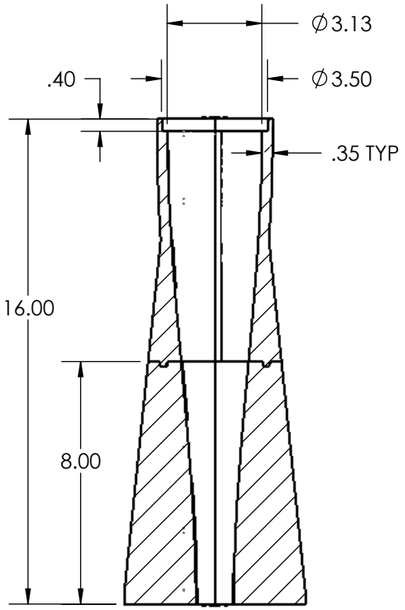

SECTION B-B

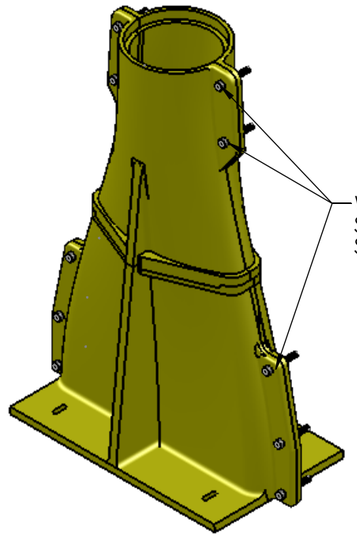

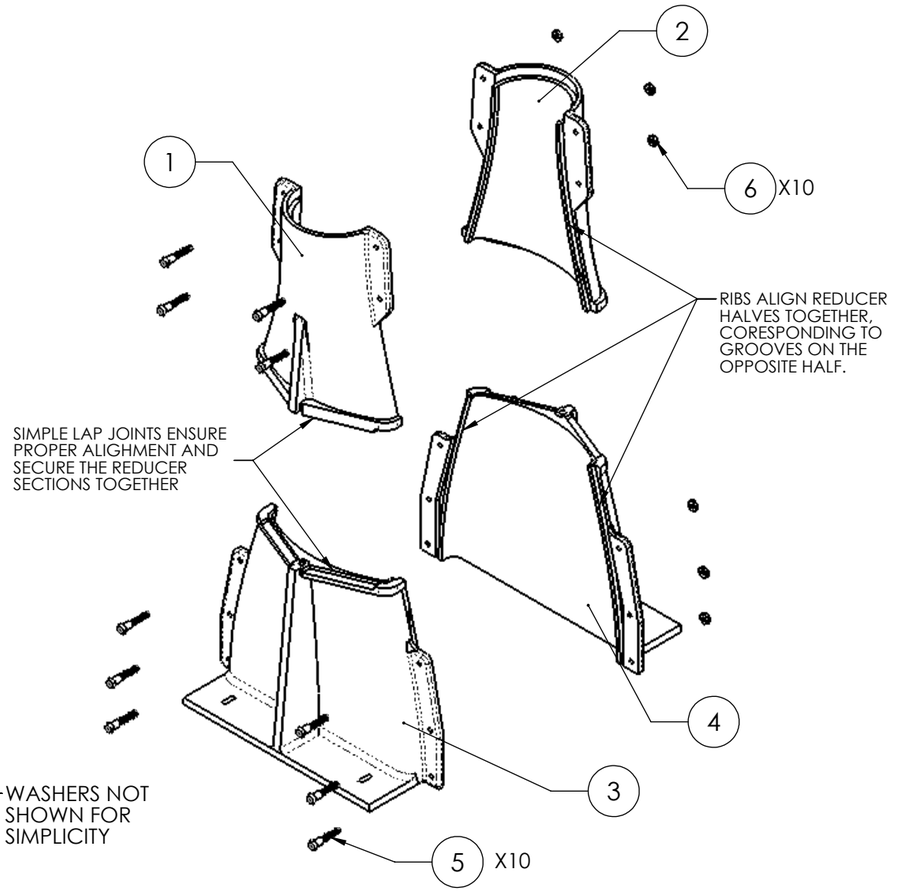

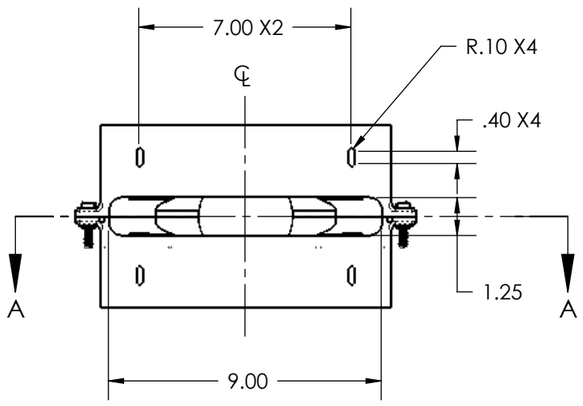

ITEM NO.	PART NO.	DESCRIPTION	QTY.
1	T301A	AIR REDUCER, TOP HALF #1	1
2	T301B	AIR REDUCER, TOP HALF #2	1
3	T301C	AIR REDUCER, BOTTOM HALF #1	1
4	T301D	AIR REDUCER, BOTTOM HALF #2	1
5		#10-24 HEX BOLT, L=7/8"	10
6		#10-24 STEEL NUT	10

	NAME	DATE
MATERIAL: ABS		
DRAWN	BRUNO	4/15/09
FINISH		
CHECKED		
CHECKED		

TITLE:

AIR REDUCER ASSEMBLY

T300

NEXT ASSY | USED ON

APPLICATION

UNLESS OTHERWISE SPECIFIED:
DIMENSIONS ARE IN INCHES
TOLERANCES:
FRACTIONAL: ±1/8
ANGULAR: ± 3°
.XX ±.01
.XXX±.005

SECTOR

Senior Project
In Partnership with Boeing
Cal Poly
Mechanical Engineering Dept.
San Luis Obispo, CA
Bruno Caulk and Kevin Whipp

SIZE	DRAWING NO.	REV
B	T301	A
SCALE: 1:5		SHEET 1 OF 1

NOTES:

1. PART WILL BE MACHINED IN HOUSE AT CAL POLY

REVISIONS				
ZONE	REV.	DESCRIPTION	DATE	APPROVED

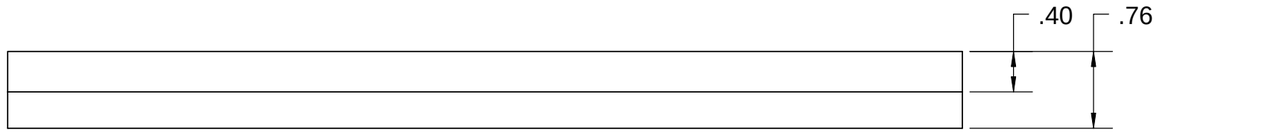

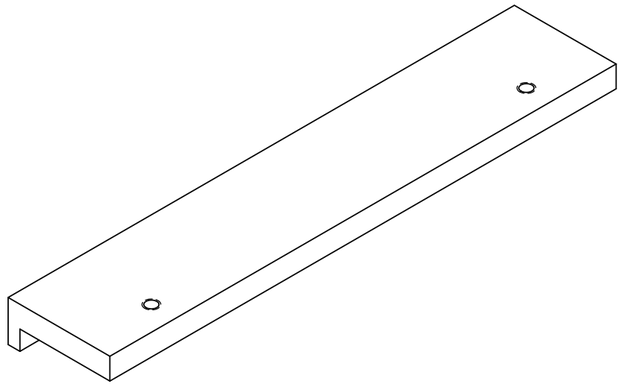

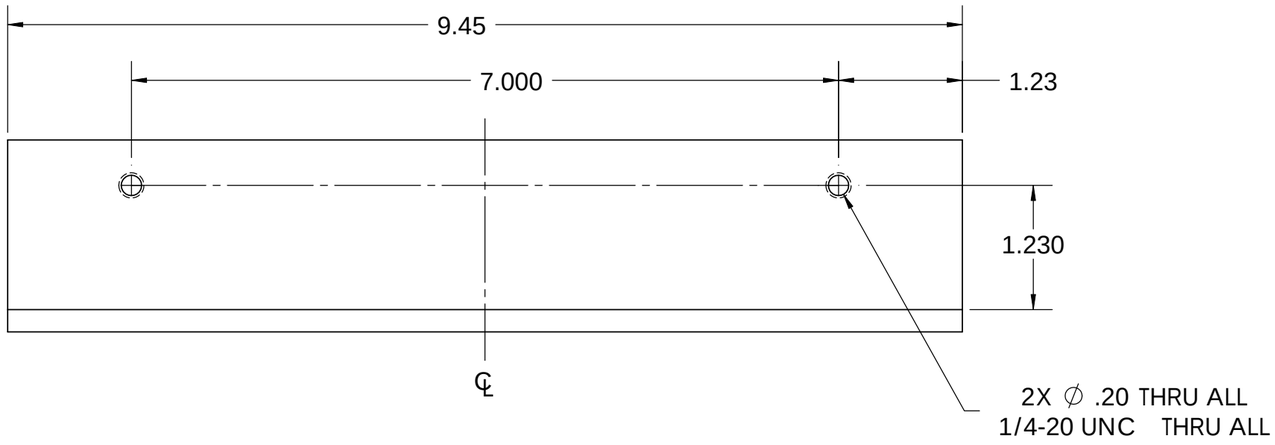

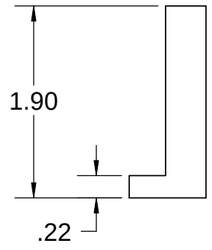

	NAME	DATE
DRAWN	BRUNO	4/15/09
CHECKED		
CHECKED		

MATERIAL: AL 6061
FINISH:

UNLESS OTHERWISE SPECIFIED:
DIMENSIONS ARE IN INCHES
TOLERANCES:
FRACTIONAL: ±1/8
ANGULAR: ± 3°
.XX ±.01
.XXX ±.005

T300

NEXT ASSY | USED ON

APPLICATION

Senior Project
In Partnership with Boeing
Cal Poly
Mechanical Engineering Dept.
San Luis Obispo, CA
Bruno Caulk and Kevin Whipp

TITLE: UPPER RAIL

SIZE: B | DRAWING NO.: T302 | REV: A

SCALE: 2:3 | SHEET 1 OF 1

NOTES:

1. PART WILL BE RAPID PROTOTYPED AT CAL POLY
2. ONLY CRITICAL DIMENSIONS ARE SHOWN
3. ASSEMBLY REQUIRES TWO INDEPENDANT RAPIDPROTOTYPED CONNECTORS: T304A & T304B. BOTH HAVE SIMILAR GEOMETRY WITH DIFFERENT DIMENTIONS DUE TO THE ANEMOMETER NOT BEING SYMETRICAL. (3.)

REVISIONS				
ZONE	REV.	DESCRIPTION	DATE	APPROVED

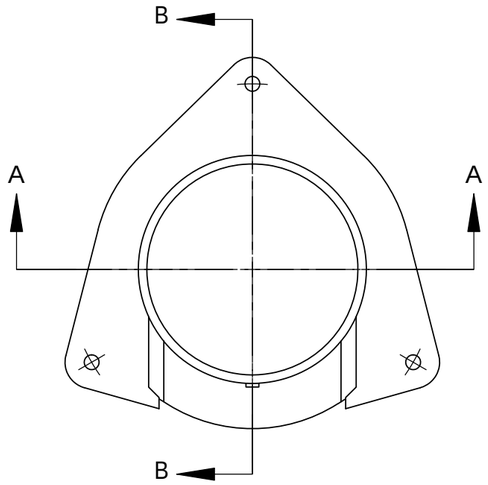

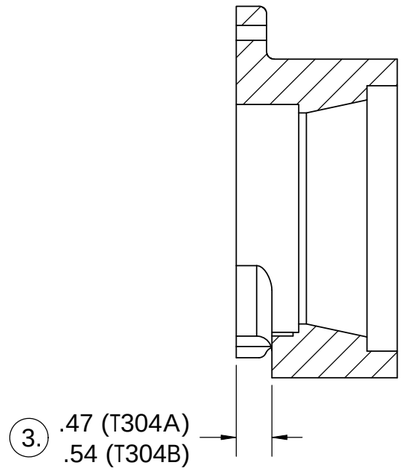

SECTION B-B
SCALE 1 : 2

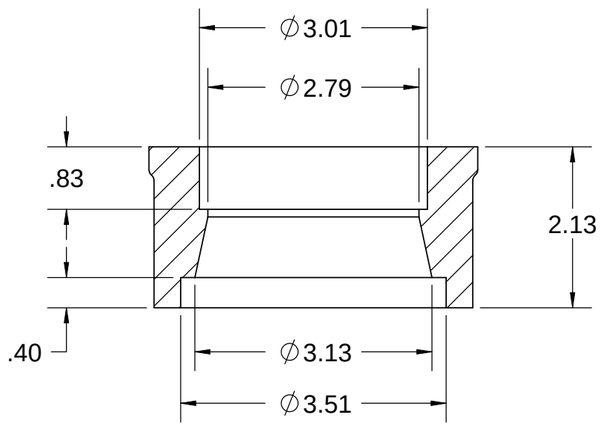

SECTION A-A
SCALE 1 : 2

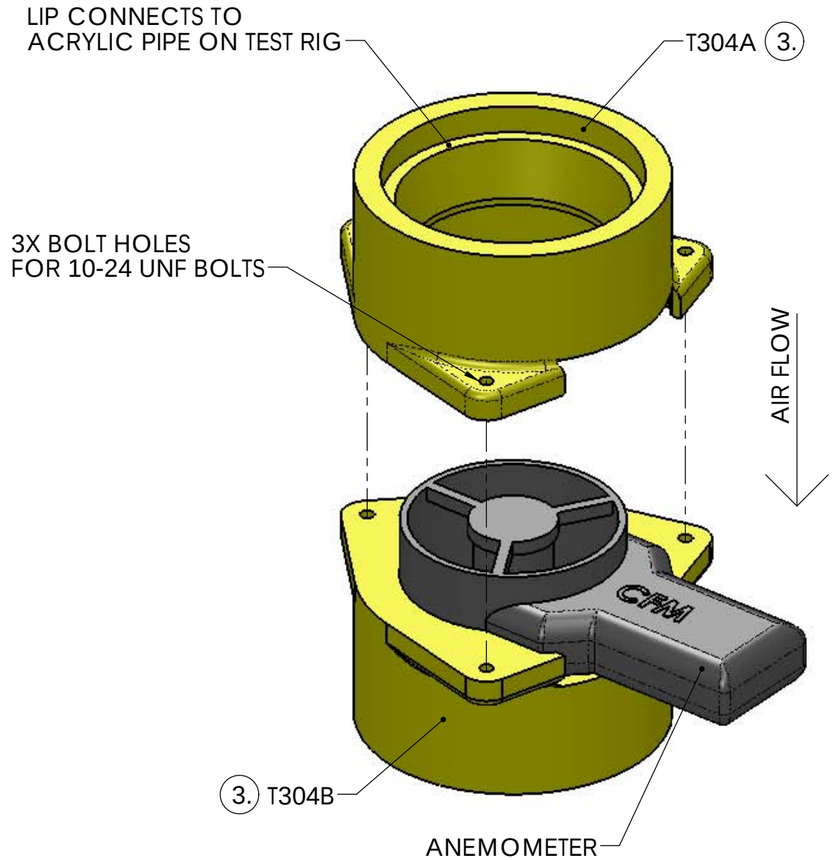

	NAME	DATE
DRAWN	BRUNO	4/30/09
CHECKED		
CHECKED		

MATERIAL: ABS
FINISH: N/A

T400
NEXT ASSY | USED ON
APPLICATION

UNLESS OTHERWISE SPECIFIED:
DIMENSIONS ARE IN INCHES
TOLERANCES:
FRACTIONAL: ±1/8
ANGULAR: ± 3°
.XX ±.01
.XXX±.005

SECTOR

Senior Project
In Partnership with Boeing
Cal Poly
Mechanical Engineering Dept.
San Luis Obispo, CA
Bruno Caulk and Kevin Whipp

TITLE:
ANAMOMETER CONNECTORS

SIZE	DRAWING NO.	REV
B	T304	A

SCALE: 1:4 | SHEET 1 OF 1

NOTES:

1. PART WILL BE RAPID PROTOTYPED AT CAL POLY.
2. ONLY CRITICAL DIMENISONS ARE SHOWN.
3. DESIGNED AS AN AIR REDUCER FOR EBM PAPST 4100 SERIES FAN

REVISIONS		
REV.	DESCRIPTION	DATE
A	INITIAL RELEASE	10/19/2009

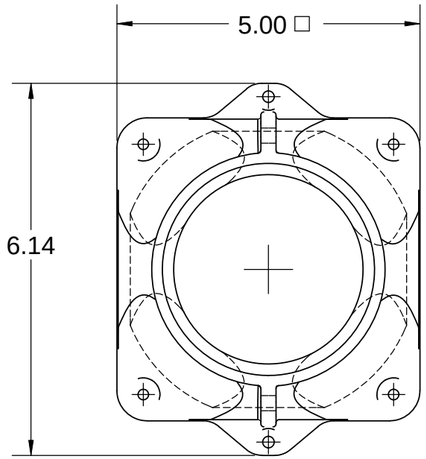

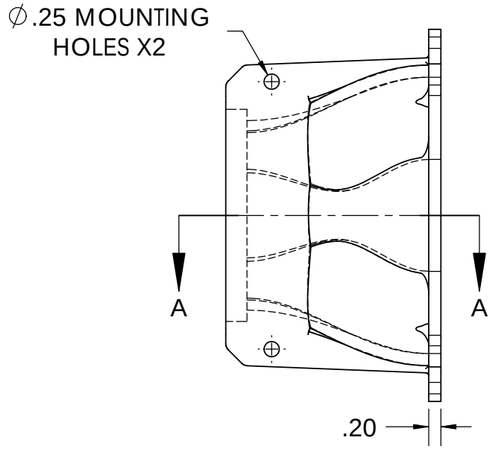

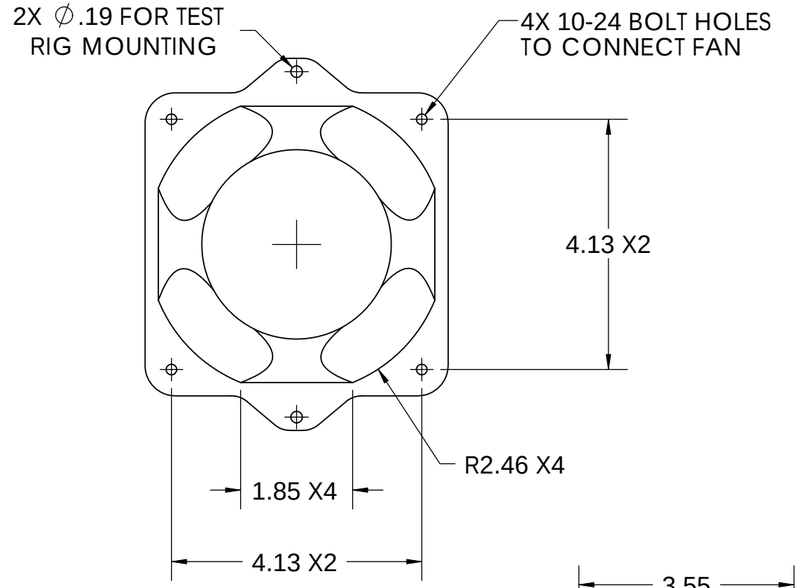

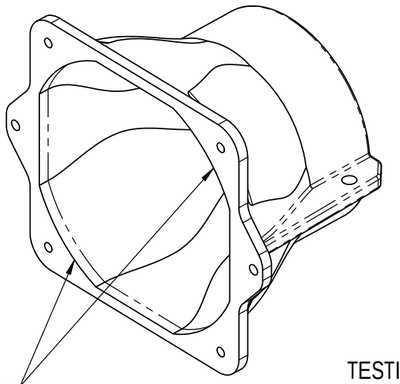

FAN OPENING PER EBM PAPST 4100 SERIES FAN

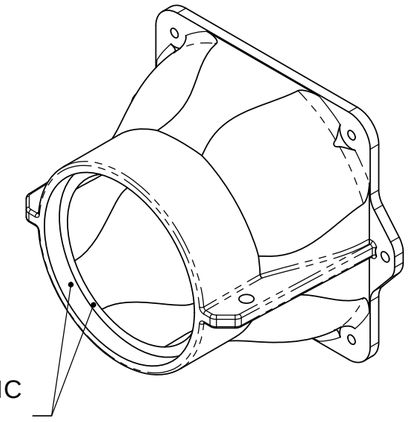

TESTING RIG ACRYLIC PIPE TO BE GLUED INSIDE OF LIP SHOWN

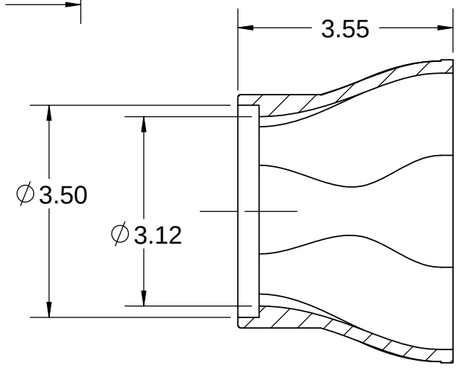

SECTION A-A

	NAME	DATE
DRAWN	BRUNO	9/29/09
CHECKED		
CHECKED		

MATERIAL: ABS
FINISH: N/A

T300

NEXT ASSY | USED ON

APPLICATION

UNLESS OTHERWISE SPECIFIED:
DIMENSIONS ARE IN INCHES
TOLERANCES:
FRACTIONAL: ±1/8
ANGULAR: ± 3°
.XX ±.01
.XXX±.005

Senior Project
In Partnership with Boeing
Cal Poly
Mechanical Engineering Dept.
San Luis Obispo, CA
Bruno Caulk and Kevin Whipp

TITLE: FAN CONNECTOR

SIZE: B | DRAWING NO.: T306 | REV: A

SCALE: 2:5 | SHEET 1 OF 1

REVISIONS			
REV.	DESCRIPTION	DATE	APPROVED

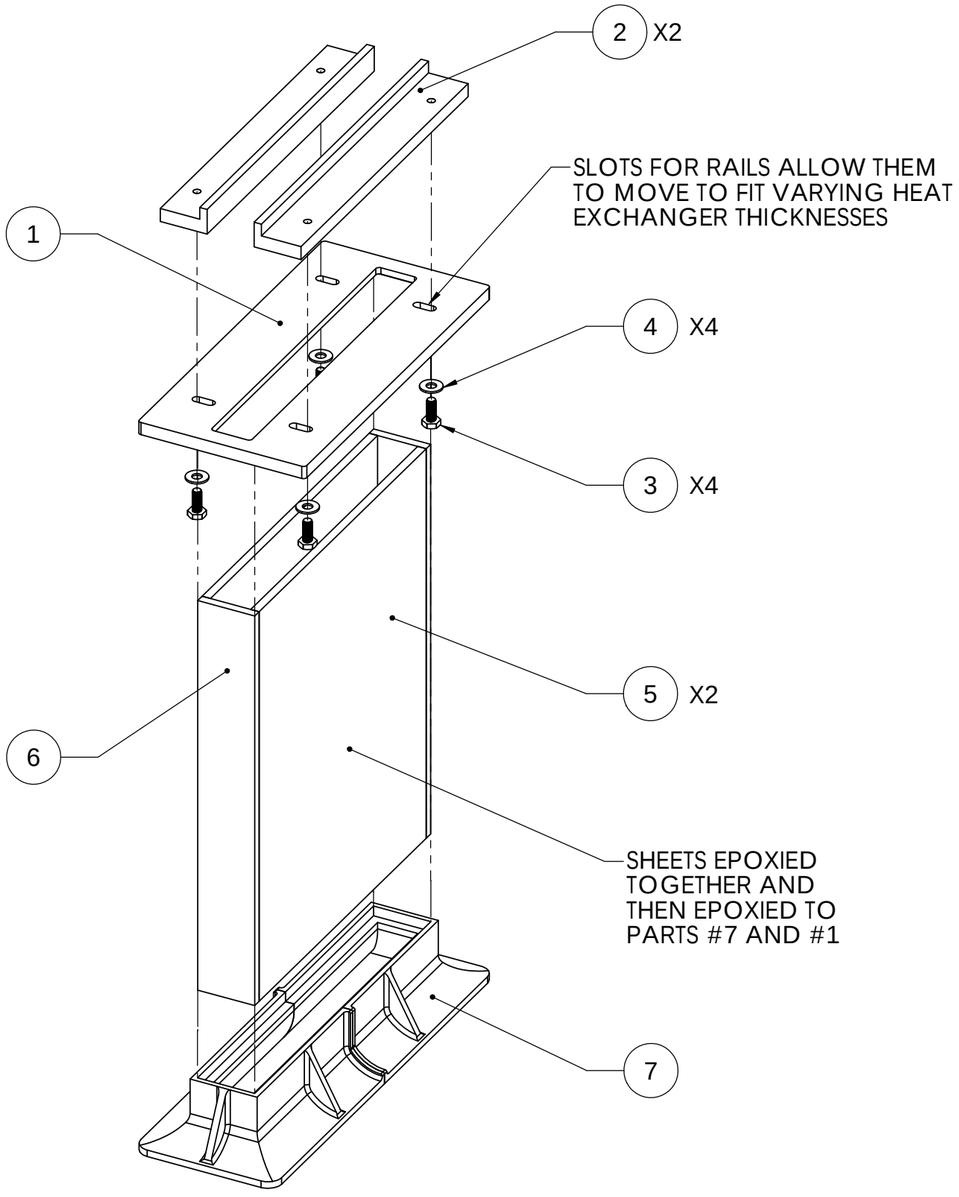

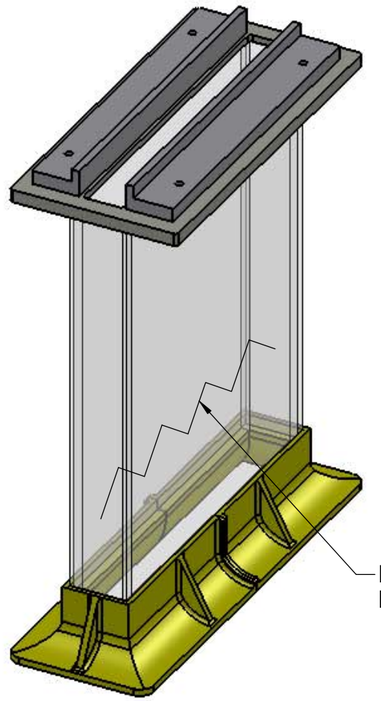

VIEW 1

RAPID PROTOTYPED GRADUAL INLET TO REDUCE ENTRANCE LOSSES

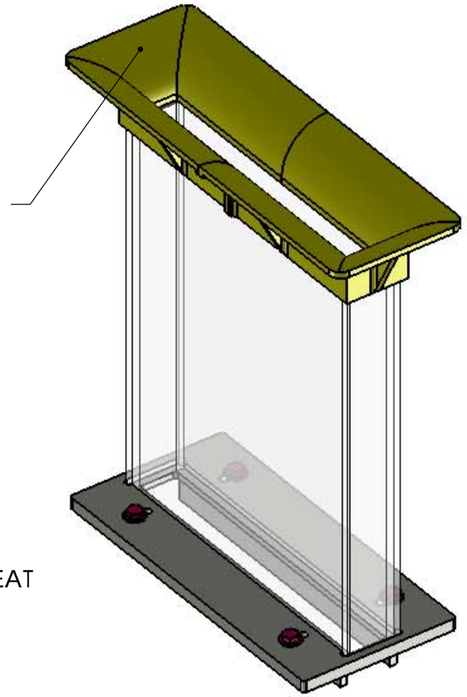

VIEW 2

ITEM NO.	PartNo	Description	VENDOR	QTY.
1	T402	LOWER PLATE CONNECTOR		1
2	T401	LOWER RAIL		2
3	TBD	Hex Head Cap Screw 1/4-28, 5/8 length	TBD	4
4	TBD	WASHER, 1/4 DIA BOLT, .05 THICK	TBD	4
5	-	12" BY 9.45", ACRYLIC SHEET 0.25" THICK	-	2
6	-	12" BY 1.7", ACRYLIC SHEET 0.25" THICK	-	2
7	T403	AIR INTAKE GUIDE		1

		NAME	DATE
MATERIAL NA	DRAWN	BRUNO	11/30/09
FINISH NA	CHECKED		
	CHECKED		

UNLESS OTHERWISE SPECIFIED:
DIMENSIONS ARE IN INCHES
TOLERANCES:
FRACTIONAL: ±1/8
ANGULAR: ± 3°
.XX ±.01
.XXX ±.005

T100	
NEXT ASSY	USED ON
APPLICATION	

Senior Project
In Partnership with Boeing
Cal Poly
Mechanical Engineering Dept.
San Luis Obispo, CA
Bruno Caulk and Kevin Whipp

TITLE:
BOTTOM COVER ASSEMBLY W/ SYNTHETIC JETS

SIZE	DRAWING NO.	REV
B	T400	B
SCALE: 1:4		SHEET 1 OF 1

NOTES:

1. ACRYLIC INTAKE PANNELS WILL BE INLAYED INTO THIS POCKET AND GLUED IN PLACE.
2. POCKETS ARE EXTENDED TO ALLOW FOR EASIER MECHINING OF THE CORNERS.
3. PART TO BE MECHINED IN HOUSE AT CAL POLY.

REVISIONS		
REV.	DESCRIPTION	DATE
A	INITIAL RELEASE	4/15/2009
B	INCREASED THICKNESS, ADDED POCKET FOR AIR INTAKE REDUCER ASSEMBLY	10/18/2009
C	REMOVED MIDDLE SUPPORT PIECE	10/26/2009

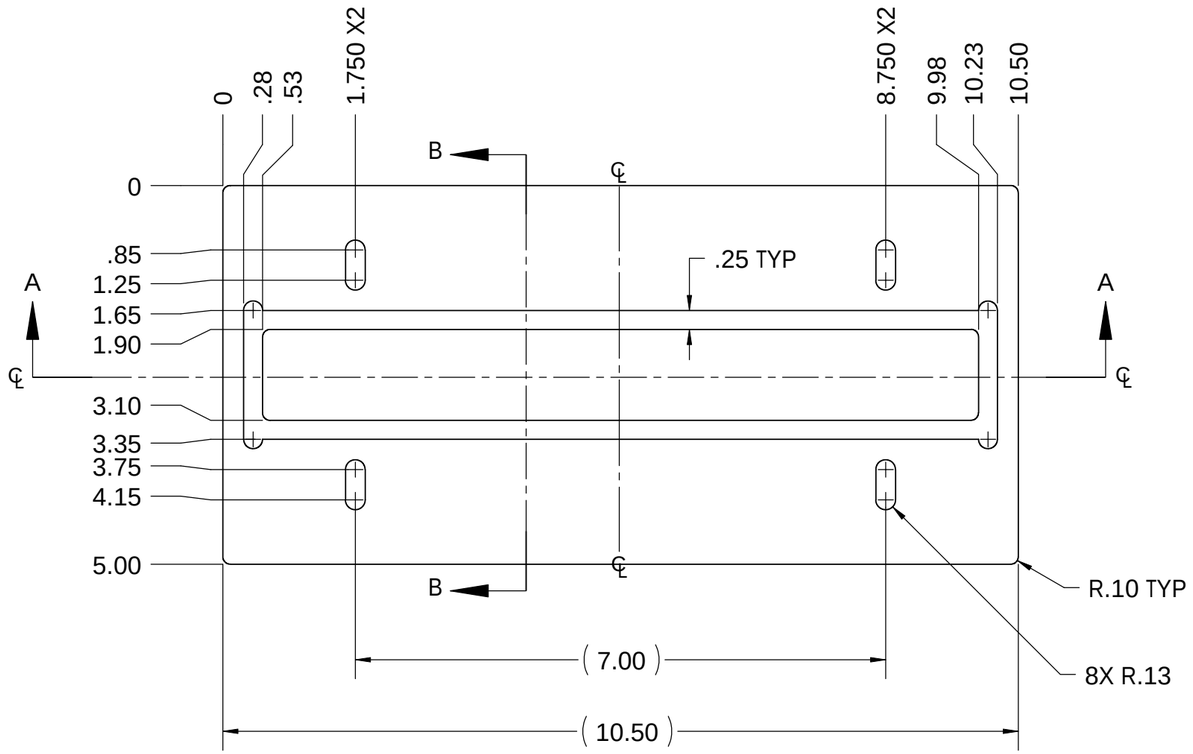

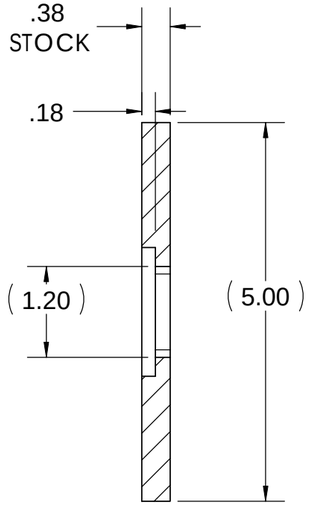

SECTION B-B

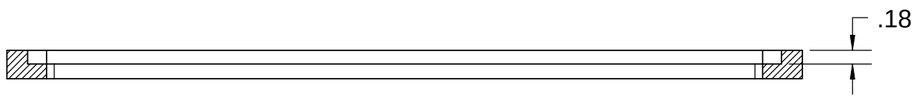

SECTION A-A

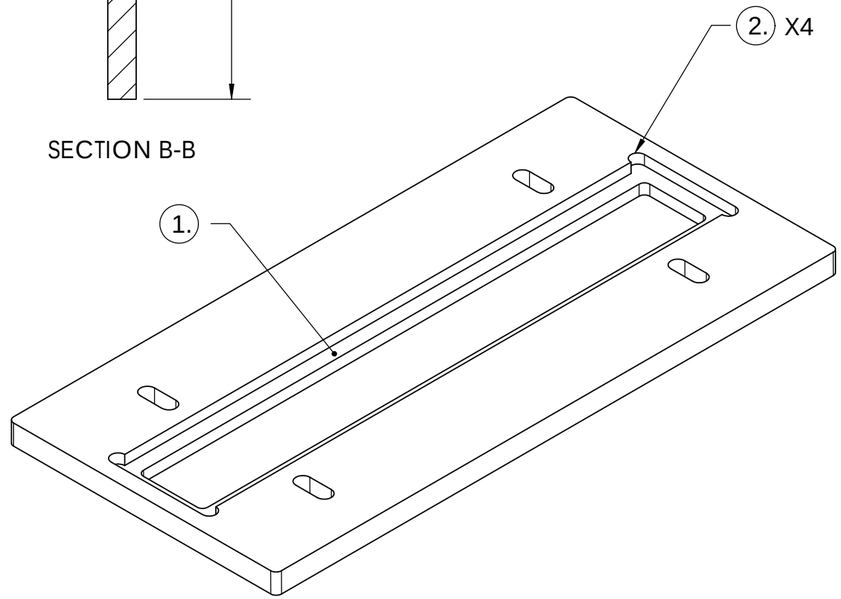

		NAME	DATE
MATERIAL: ALUM	DRAWN	BRUNO	10/18/09
FINISH: NONE	CHECKED		
	CHECKED		

UNLESS OTHERWISE SPECIFIED:
DIMENSIONS ARE IN INCHES
TOLERANCES:
FRACTIONAL: ±1/8
ANGULAR: ± 3°
.XX ±.01
.XXX±.005

T400

NEXT ASSY | USED ON

APPLICATION

Senior Project
In Partnership with Boeing
Cal Poly
Mechanical Engineering Dept.
San Luis Obispo, CA
Bruno Caulk and Kevin Whipp

TITLE:
LOWER PLATE CONNECTOR

SIZE	DRAWING NO.	REV
B	T402	C

SCALE: 1:2 | SHEET 1 OF 1

NOTES:

1. THE ASSEMBLY CONSSITS OF 2 RAPID PROTOTYPED ABS PARTS CONSTTRUCTED AT CAL POLY.
2. PARTS T403A AND T403B WILL BE LIGHTLY EPOXIED TOGETHER. RESIDUE WILL BE SANDED FLUSH.
3. THE INTERIOR SURFACE SHOWN WILL BE SANDED DOWN TO 400 GRIT SAND PAPER TO DECREASE DRAG.
4. BECAUSE THE PART WILL BE RAPID PROTOTYPED, ONLY CRITICAL DIMENSIONS ARE SHOWN

REVISIONS		
REV.	DESCRIPTION	DATE
A	INITIAL RELEASE	10/18/2009

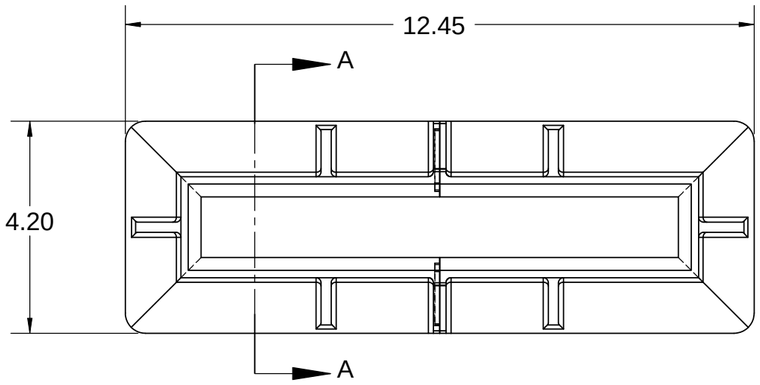

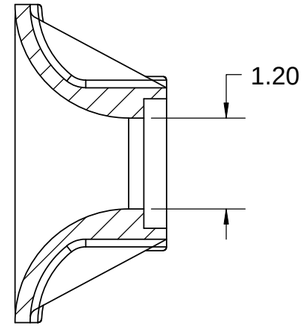

SECTION A-A
SCALE 1 : 2

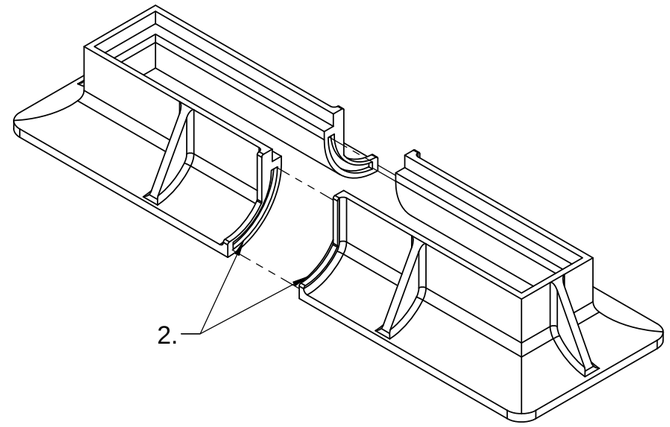

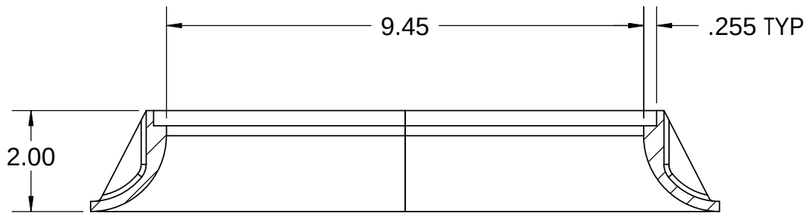

SECTION B-B

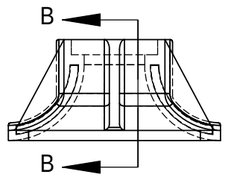

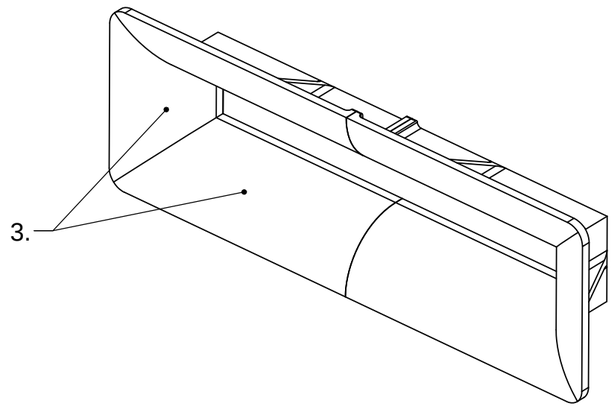

	NAME	DATE
MATERIAL: ABS	DRAWN: BRUNO	10/18/09
FINISH: N/A	CHECKED	
	CHECKED	

TITLE: AIR INTAKE GUIDE

T400

NEXT ASSY | USED ON

APPLICATION

UNLESS OTHERWISE SPECIFIED:
DIMENSIONS ARE IN INCHES
TOLERANCES:
FRACTIONAL: ±1/8
ANGULAR: ± 3°
.XX ±.01
.XXX±.005

Senior Project
In Partnership with Boeing
Cal Poly
Mechanical Engineering Dept.
San Luis Obispo, CA
Bruno Caulk and Kevin Whipp

SIZE	DRAWING NO.	REV
B	T403	A

SCALE: 1:3 | SHEET 1 OF 1

17 APPENDIX G: BILL OF MATERIALS

Testing Rig

No.	Part Description	Purpose	Price	QTY	Vendor	Vendor Part #	Cost	Status	Date
1	1"x8" Silicone Heater 10 W/Sq in. w/ adhesive	Provide simulated circuit board heat	$20.00	1	Omega	SRFG-108/10-P	$20.00	**ACQUIRED**	6/3/2009
2	1"x8" Silicone Heater 5 W/Sq in. w/ adhesive	Provide simulated circuit board heat	$0.00	12	Omega	SRFG-108/5-P	$0.00	**(Niles/Fort)**	10/26/2009
3	3/4" x 2" x 12" Aluminum 6061 Stock	Upper/Lower Rails	$11.01	6	McMaster-Carr	8975K781	$66.06	**ACQUIRED**	5/26/2009
4	Axial Fan, DC, S-Force Series from Papst (PN: 4114N/2H8P), 24V, 78 dBA, 120W, 119 x 119 x 38mm	Creates forced convection	$119.00	2	Allied Electronics	600-0448	$238.00	**ACQUIRED**	6/9/2009
5	12"x36"x2" Semi Rigid Cork Insulation	Heat resistive insulation around main body	$15.37	2	McMaster-Carr	9354K12	$30.74	**ACQUIRED**	5/26/2009
6	Polyethylene Foam Insulation 1" Thick, 36" X 48", Black	Insulation for air reducer and acrylic pipe	$26.86	1	McMaster-Carr	93265K48	$26.86	**ACQUIRED**	11/2/2009
7	12" Ratchet Bar Clamp/Spreader	Holds all sections together	$3.99	6	Harbor Freight	46807	$23.94	**ACQUIRED**	10/19/2009
8	9.25x7.35 FR4 .048" circuit board (2 layer)	Heating element / insulation interface	$10.00	2	Ebay Online Vendor	-	$20.00	**ACQUIRED**	10/6/2009
9	Rapid Prototyped Air Reducer	Plate to pipe air transition	$0.00	4	Provided on-campus	-	$0.00	**COMPLETE**	5/27/2009
10	Rapid Prototyped Anemometer Connector	Connects pipe to Anemometer	$0.00	2	Provided on-campus	-	$0.00	**COMPLETE**	10/5/2009
11	Rapid Prototyped Fan Connector	Connects pipe to Fan	$0.00	3	Provided on-campus	-	$0.00	**COMPLETE**	10/26/2009

12	Aluminum 6061 Stock, 3/8 "Thick, 5" Width, 1' Length	Slotted bottom half connector (mech. on campus)	$12.30	1	McMaster-Carr	8975K435	$12.30	**ACQUIRED**	10/26/2009
13	Acrylic Tubing 3 1/8 ID, 36" Length	Smooth circular piping for upper section	$65.85	2	McMaster-Carr	8486K474	$131.70	**ACQUIRED**	5/26/2009
14	1/16" Thick Aluminum Plate 4x4"	Flat surface for butterfly valve	$14.58	1	McMaster-Carr	89015K37	$14.58	**ACQUIRED**	5/26/2009
15	#10 -24 Hex Bolt L=7/8" (bag of 12)	Upper Assembly fasteners	$0.98	1	Home Depot	-	$0.98	**ACQUIRED**	5/24/2009
16	#10-24 Steel Nut (bag of 12)	Shroud fasteners	$0.98	1	Home Depot	-	$0.98	**ACQUIRED**	5/24/2009
17	#10 Steel Washer (Bag of 30	Shroud fasteners	$0.98	1	Home Depot	-	$0.98	**ACQUIRED**	5/24/2009
18	Quick Set Epoxy	Tube to RP part fastener	$4.99	1	Home Depot		$4.99	**ACQUIRED**	5/24/2009
19	Scaffolding Materials / Fasteners	Supporting Structure and rig fasteners	$58.58	1	Home Depot	-	$58.58	**ACQUIRED**	10/30/2009
20	Wire Connectors / Fasteners	Supporting Structure and rig fasteners	$10.54	1	Home Depot	-	$10.54	**ACQUIRED**	11/1/2009
21	tape and foam insulation	Necessary for electronic connections	$6.02	1	Home Depot	-	$6.02	**ACQUIRED**	11/1/2009
22	Five-Arm Knob, 1/4-20 Thru, Polyprop	Knob for Damper	$0.91	1	McMaster-Carr	59625K740	$0.91	**ACQUIRED**	6/2/2009
23	Scratch-Resistant Clear Cast Acrylic Sheet 1/4" Thick, 12" X 24"	Inlet channel and air heater holder	$36.83	1	McMaster-Carr	8536K162	$36.83	**ACQUIRED**	10/26/2009
24	Rapid Prototyped Air Intake Guide	Curved inlet to reduce entrance losses	$0.00	1	Provided on-campus		$0.00	**COMPLETE**	10/26/2009

Testing Rig Sub Total	704.99
Addl: 16% For tax and shipping:	$112.80
Testing Rig Sub Total	1323.92

Module Plates

No.	Part Description	Purpose	Price	QTY	Vendor	Vendor Part #	Cost	Status	Date
25	0.040 in thick Therm-a-gap 18x18 Type A	AECM thermal interface material	$0.00	1.5	Chomerics	69-12-20684-A580	$0.00	**(Niles/Fort)**	
26	8"x12"x.5" 6061 Aluminum	Used for the brazed aluminum foam heatsink	$13.18	2	McMaster-Carr	8975K445	$26.36	**ACQUIRED**	5/26/2009
27	10"x12"x3/8" 6061 Aluminum	Used for blank plates	$18.01	2	McMaster-Carr	8975K131	$36.02	**ACQUIRED**	10/21/2009
28	8"x12"x3/4" 6061 Aluminum	Used for the aluminum finned heatsink	$29.78	1	McMaster-Carr	8975K447	$29.78	**ACQUIRED**	10/20/2009
29	Machining Services for Blank Plates	Blank Plates to use with Foam Design	$150.00	2	Provided on-campus	-	$300.00	**COMPLETE**	10/26/2009
30	Machining Services for Finned Plate	Shaping the fins to dimension	$200.00	2	Provided on-campus	-	$400.00	**COMPLETE**	10/26/2009
31	Aluminum Foam Blank	Alum Foam Blank for heat exchangers	$160.33	6	ERG Mate. and Aero	-	$961.98	**ACQUIRED**	10/26/2009
32	1/8 Carbide End Mills (Lot Qty 5)	Tooling for finned plate	$20.00	1	Ebay Online Vendor	-	$20.00	**ACQUIRED**	10/28/2009
33	1 Deg Taper Ball End Mill	Tooling for finned plate	$15.00	1	Ebay Online Vendor	-	$15.00	**ACQUIRED**	10/28/2009

Module Plates Sub Total	1789.14
Addl: 16% For tax and shipping:	$286.26
Module Plates Total	2075.4024

Lab Equipment

No.	Part Description	Purpose	Price	QTY	Vendor	Vendor Part #	Cost	Status	Date
34	Thermocouple DAQ	For temperature measurements for all Boeing teams	$0.00	1	National Instruments	-	$0.00	**Provided on Campus**	10/22/2009
35	SCXI-1303 32 ch Terminal Block, for thermocouple inputs to connect to SCXI-1102	For other Boeing Teams to connect to DAQ	$296.10	1	National Instruments	SCXI-1303	$296.10	**Ordered**	10/23/2009
36	72" J-Type Thermocouples	Temperature Measurement	$7.40	20	TC Direct	201-307	$148.00	**ACQUIRED**	6/8/2009
37	MASTECH DC Power Supply 0-30V 0-30A	Power for heating elements	$259.00	1	Amazon	B000E129G8	$259.00	**ACQUIRED**	5/28/2009
38	Test Lead Adapter Stackable Banana Plug, Accepts Up to .22" Wire	To Connect Powered Equipment to Power	$1.89	10	McMaster-Carr	6933K532	$18.90	**ACQUIRED**	6/1/2009
39	Rotary Vane Anemometer	Measuring Flow Rate and outlet temp	$245.00	1	Omega	HHF91	$245.00	**ACQUIRED**	6/3/2009
40	Kill-A-Watt	Measures AC Fan Power Used	$39.66	1	Amazon	B000RGF29Q	$39.66	**ACQUIRED**	5/28/2009
41	Handheld digital manometer, Differential Input	Vacuum pressure measurement	$0.00	1	Omega	HHP-90	$0.00	**(Niles/Fort)**	10/26/2009
42	1/4" ID pvc clear tubing, 3/8" OD	for Manometer Connections (price per ft.)	$0.20	25	McMaster-Carr	5233K56	5	**ACQUIRED**	10/9/2009
43	BARBED TUBE FITTING, ADAPTER FOR 1/4" TUBE ID X 1/4"-28 UNF MALE THREAD	for Manometer Connections (pack of 10)	$3.49	1	McMaster-Carr	5121K341	3.49	**ACQUIRED**	10/9/2009
44	HEARING PROTECTION EARMUFF, NRR 21 DB OVERHEAD	Hearing Protection for fans	$11.99	3	McMaster-Carr	9205T1	35.97	**ACQUIRED**	10/9/2009

Lab Equipment Sub Total	1051.12
Addl: 16% For tax and shipping:	$168.18
Lab Equipment Total	1219.2992

.

Aluminum Finned Plates – *Experimental Results Spec Sheet*

Table H-1: Raw Test Data from **Aluminum Finned Plate** Configuration. Two points of data where measured for 4 different flow rates. Thermocouple channels 2 through 15 correspond to specific board locations displayed in Figure H-2

			Test 1			*Test 2*			*Test 3*			*Test 4*		
			Pt. 1	*Pt. 2*	*Avg.*	*Pt. 1*	*Pt. 2*	*Avg.*	*Pt. 1*	*Pt. 2*	*Avg.*	*Pt. 1*	*Pt. 2*	*Avg.*
Flow Rate (CFM)			72	71	**72**	50	50	**50**	31	31	**31**	16	16	**16**
Exit Temp (°C)	Thermocouple Channels	0	29.3	29.2	29.3	30.8	30.9	30.9	33.9	33.9	33.9	41.5	41.7	41.6
		1	28.9	28.9	28.9	30.7	30.7	30.7	34.2	34.1	34.2	40.4	40.5	40.5
Secondary Plate Center Temp (°C)		2	47.4	47.4	47.4	48.5	48.6	48.6	49.1	49.2	49.2	54.9	52.1	53.5
Primary Plate Temp (°C)		3	54.3	54.3	54.3	55.3	55.4	55.4	54.5	54.6	54.6	57.3	55.1	56.2
		4	57.0	56.9	57.0	57.3	57.5	57.4	56.6	56.7	56.7	57.3	57.6	57.5
		5	47.3	47.2	47.3	48.4	48.4	48.4	49.1	49.1	49.1	51.9	52.1	52.0
		6	52.6	52.5	52.6	53.2	53.4	53.3	53.0	53.1	53.1	54.6	54.8	54.7
		7	50.5	50.4	50.5	51.4	51.5	51.5	51.7	51.8	51.8	53.9	54.1	54.0
		8	46.3	46.2	46.3	47.3	47.4	47.4	47.9	47.9	47.9	50.5	50.8	50.7
		9	49.5	49.4	49.5	50.4	50.5	50.5	50.7	50.7	50.7	52.9	53.2	53.1
		10	47.9	47.8	47.8	49.0	49.1	49.1	49.7	49.7	49.7	52.4	52.7	52.6
		11	50.1	50.0	50.1	50.9	51.0	51.0	51.0	51.1	51.1	53.1	53.3	53.2
		12	48.8	48.7	48.8	49.8	49.9	49.9	50.3	50.3	50.3	52.8	53.1	53.0
		13	46.0	45.9	46.0	46.9	47.1	47.0	47.6	47.6	47.6	50.3	50.5	50.4
		14	56.4	56.3	56.4	56.7	56.9	56.8	56.1	56.1	56.1	57.0	57.3	57.2
		15	53.6	53.5	53.6	54.3	54.4	54.4	54.1	54.2	54.2	55.7	55.9	55.8
Entrance Temp (°C)		16	22.5	22.5	22.5	22.2	22.1	22.2	21.8	21.8	21.8	22.2	22.0	22.1
		17	22.4	22.3	22.4	22.0	22.0	22.0	21.7	21.8	21.8	22.0	21.9	22.0
		18	22.5	22.4	22.5	22.1	22.1	22.1	21.8	21.9	21.9	22.2	22.0	22.1
Pressure Change (in H20)			0.21	0.22	0.22	0.12	0.11	0.12	0.05	0.06	0.06	0.01	0.02	0.01
Average Air Velocity at Anemometer (ft/min)			1451	1451	1451	1028	1028	1028	621	620	621	317	317	317
Heater Voltage (V)			76.4	78.5	77.5	74.9	76.0	75.5	69.9	74.0	72.0	67.1	63.5	65.3
Power into Heaters (W)			174	177	176	161	162	162	140	140	140	110	111	111
Heat Dissipated (W) (assuming 95% Transformer Efficiency)					**167**			**153**			**133**			**105**

Table H-2: Calculated values of Heat Transfer directly from the Aluminum Finned Plate Configuration to air and for the Total Power input to the air for the from the experimentally determined values in the table above.

Flow Rate		72	50	31	16
Average Inlet Temp (°C)		22.4	22.1	21.8	22.1
Average Exit Temp (°C)		29.1	30.8	34.0	41.0
Exit Air Density (kg/m^3)		1.167	1.167	1.167	1.127
Mass Flow Rate (kg/s)		0.039	0.028	0.017	0.009
Specific Heat Capacity (kJ/kg-K)		1.005	1.005	1.005	1.005
Heat Transfer Rate into Air (Watts)		**263**	**241**	**210**	**162**
Pressure Difference (Pa)		54	29	14	3
Average Exit Air Velocity(m/s)		7.37	5.22	3.15	1.61
Power into Air Flow (W)	*Pressure Component*	1.81	0.68	0.20	0.02
	Velocity Component	1.07	0.38	0.08	0.01
	Total Power	**2.88**	**1.05**	**0.29**	**0.03**

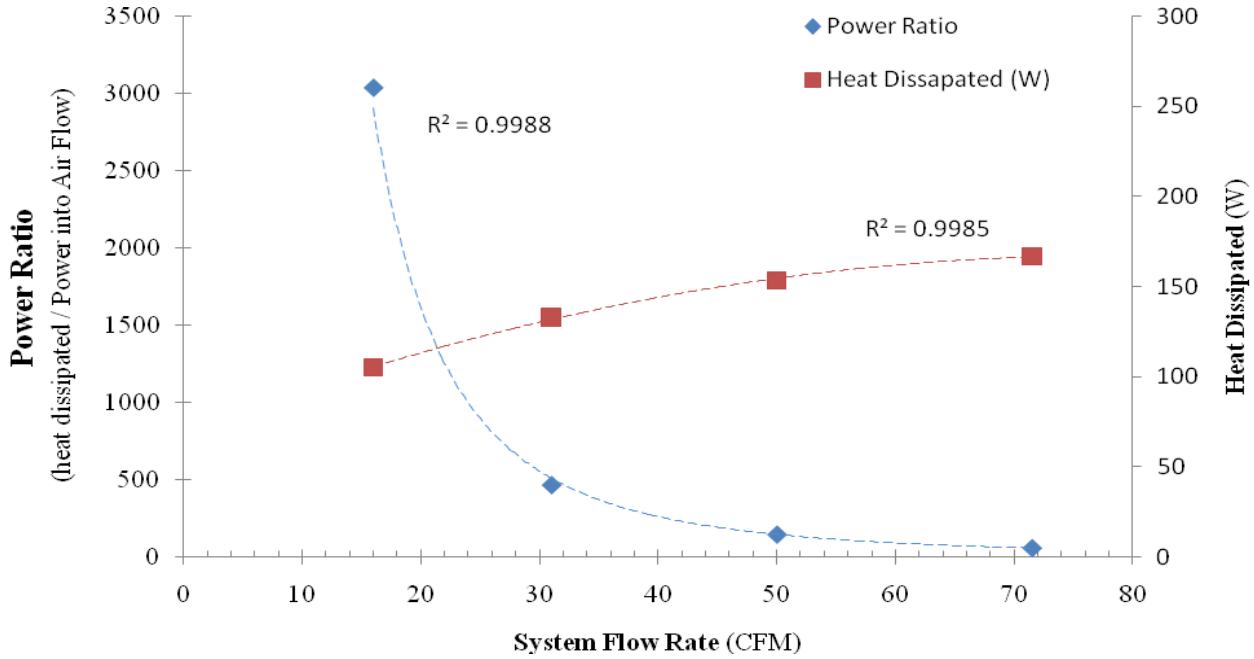

Figure H-1: Experimentally determined cooling characteristics for the **Aluminum Finned Plate** configuration. The right vertical axis, with data points shown as blue diamonds, represents a dimensionless ratio of heat removed to the physical power of the air flow. This ratio can be seen as an efficiency of the current plate configuration. The secondary vertical axis, with data points shown as red squares, displays the heat transfer from the circuit boards to the air exhaust in Watts. Both axes are greatly dependant on the air's flow rate through the heat exchanger.

Table H-3: Calculated data points shown in Figure H-1: Heat Dissipation and Power Ratio based on varying flow rates.

Flow Rate (CFM)	72	50	31	16
Heat Dissipated (W)	**167**	**153**	**133**	**105**
Power Ratio	**58**	**146**	**466**	**3039**

Figure H-2: Thermocouple layout on circuit board. Measured corresponding temperature values displayed in Table X-1.

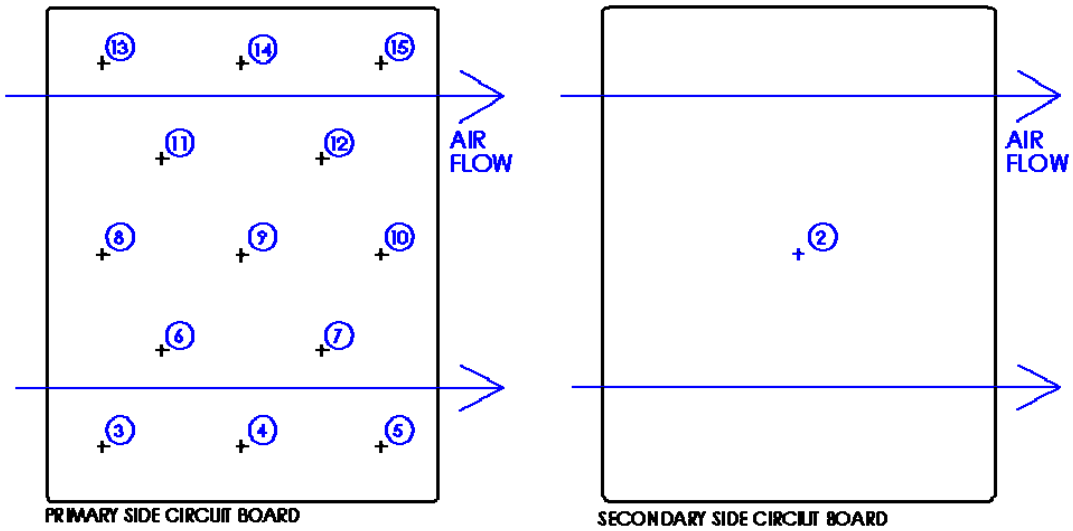

5ppi Aluminum Foam, 0.87" Thick – *Experimental Results Spec Sheet*

Table I-1: Raw Test Data from **0.87" Thick, 5ppi Alum Foam** Configuration. Two points of data where measured for 4 different flow rates. Thermocouple channels 2 through 15 correspond to specific board locations displayed in Figure I-2

		Test 1			Test 2			Test 3			Test 4		
		Pt. 1	**Pt. 2**	**Avg.**	**Pt. 1**	**Pt. 2**	**Avg.**	**Pt. 1**	**Pt. 2**	**Avg.**	**Pt. 1**	**Pt. 2**	**Avg.**
Flow Rate (CFM)		72	72	72	50	50	50	31	31	31	9	9	9
Exit Temp (°C)	0	33.1	34.2	33.7	37.9	37.9	37.9	41.9	40.3	41.1	48.9	48.0	48.5
	1	32.2	33.4	32.8	36.5	36.4	36.5	40.0	38.6	39.3	48.6	47.6	48.1
Secondary Plate Center Temp (°C)	2	46.1	47.5	46.8	48.6	48.6	48.6	49.2	47.4	48.3	54.3	52.7	53.5
Primary Plate Temp (°C)	3	54.6	55.8	55.2	53.7	53.8	53.8	52.0	50.4	51.2	52.1	50.9	51.5
	4	56.2	57.6	56.9	57.7	57.7	57.7	56.3	54.6	55.5	57.3	55.7	56.5
	5	48.0	49.4	48.7	50.6	50.6	50.6	51.1	49.4	50.3	55.7	54.1	54.9
	6	46.0	47.4	46.7	48.2	48.2	48.2	48.5	46.7	47.6	53.8	52.3	53.1
	7	48.6	49.9	49.3	51.1	51.1	51.1	51.5	49.7	50.6	55.9	54.2	55.1
	8	44.0	45.3	44.7	46.2	46.2	46.2	46.7	44.9	45.8	52.5	51.0	51.8
	9	46.9	48.3	47.6	49.3	49.3	49.3	49.8	48.0	48.9	54.9	53.3	54.1
	10	49.5	50.8	50.2	52.0	52.0	52.0	52.5	50.7	51.6	56.5	54.8	55.7
	11	46.1	47.4	46.8	48.3	48.3	48.3	48.6	46.8	47.7	53.9	52.4	53.2
	12	48.0	49.4	48.7	50.6	50.6	50.6	51.3	49.4	50.4	55.8	54.2	55.0
	13	43.1	44.7	43.9	45.6	45.6	45.6	46.2	44.3	45.3	52.2	50.7	51.5
	14	48.4	49.7	49.1	50.6	50.7	50.7	51.0	49.1	50.1	55.3	53.7	54.5
	15	48.2	49.6	48.9	50.9	50.9	50.9	51.5	49.1	50.3	55.9	54.3	55.1
Entrance Temp (°C)	16	21.0	22.2	21.6	22.4	22.4	22.4	21.9	20.3	21.1	22.3	22.4	22.4
	17	20.9	22.2	21.6	22.4	22.3	22.4	21.8	20.2	21.0	22.2	22.2	22.2
	18	21.0	22.3	21.7	22.5	22.5	22.5	21.9	20.2	21.1	22.3	22.4	22.4
Pressure Change (in H20)		2.78	2.76	2.77	1.38	1.36	1.37	0.50	0.49	0.50	0.04	0.06	0.05
Average Air Velocity at Anomometer (ft/min)		1471	1474	1473	1028	1027	1028	630	632	631	190	190	190
Heater Voltage (V)		101.2	107.9	104.6	96.0	96.0	96.0	86.5	86.5	86.5	51.2	51.7	51.5
Power into Heaters (W)		298	297	298	259	259	259	196	195	196	76	77	77
Heat Dissipated (W) (assuming 95% Transformer Efficiency)				**283**			**246**			**186**			**73**

Table I-2: Calculated values of Heat Transfer directly from the 0.87" Thick, 5ppi Alum Foam Configuration to air and for the Total Power input to the air for the from the experimentally determined values in the table above.

Flow Rate		72	50	31	9
Average Inlet Temp (°C)		21.6	22.4	21.1	22.3
Average Exit Temp (°C)		33.2	37.2	40.2	48.3
Exit Air Density (kg/m^3)		1.167	1.167	1.167	1.127
Mass Flow Rate (kg/s)		0.040	0.028	0.017	0.005
Specific Heat Capacity (kJ/kg-K)		1.005	1.005	1.005	1.005
Heat Transfer Rate in Air (Watts)		**463**	**408**	**329**	**125**
Pressure Difference (Pa)		690	341	123	12
Average Velocity at Exit (m/s)		7.48	5.22	3.21	0.97
Power into Air Flow	*Pressure Component*	23.45	8.05	1.80	0.05
	Velocity Component	1.11	0.38	0.09	0.00
	Total Power	**24.6**	**8.43**	**1.89**	**0.06**

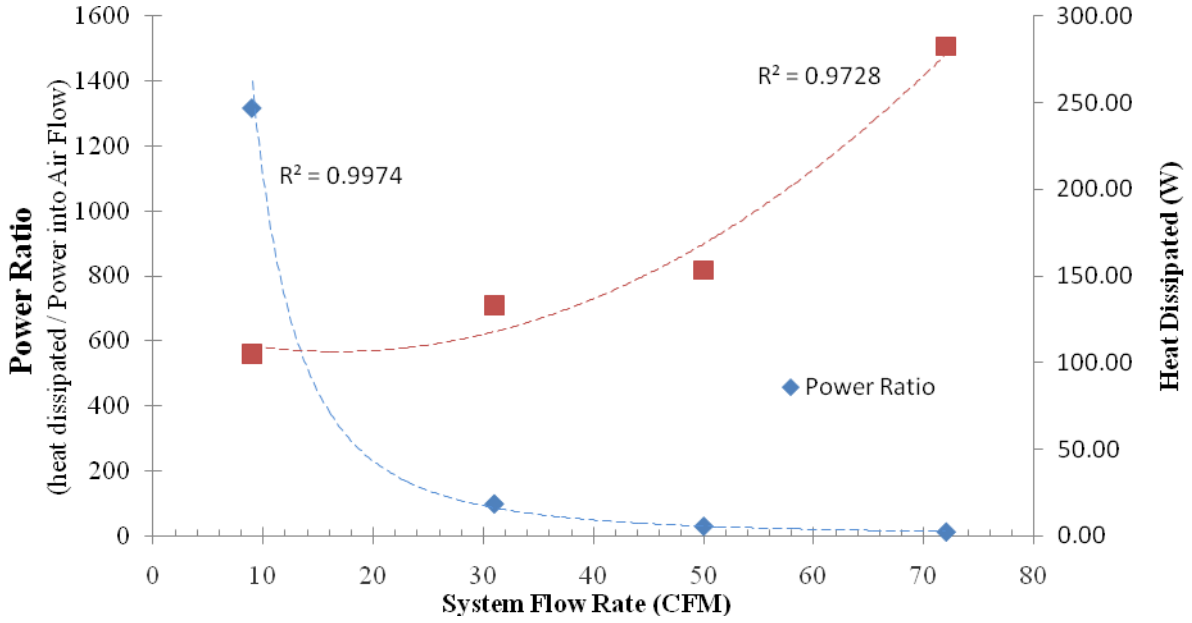

Figure I-1: Experimentally determined cooling characteristics for the **0.87" Thick, 5ppi Alum Foam** configuration. The right vertical axis, with data points shown as blue diamonds, represents a dimensionless ratio of heat removed to the physical power of the air flow. This ratio can be seen as an efficiency of the current plate configuration. The secondary vertical axis, with data points shown as red squares, displays the heat transfer from the circuit boards to the air exhaust in Watts. Both axes are greatly dependant on the air's flow rate through the heat exchanger.

Table H-3: Calculated data points shown in Figure I-1: Heat Dissipation and Power Ratio based on varying flow rates.

Flow Rate (CFM)	72	50	31	9
Heat Dissipated (W)	**283**	**246**	**186**	**73**
Power Ratio	**12**	**29**	**98**	**1318**

Figure I-2: Thermocouple layout on circuit board. Measured corresponding temperature values displayed in Table I-1.

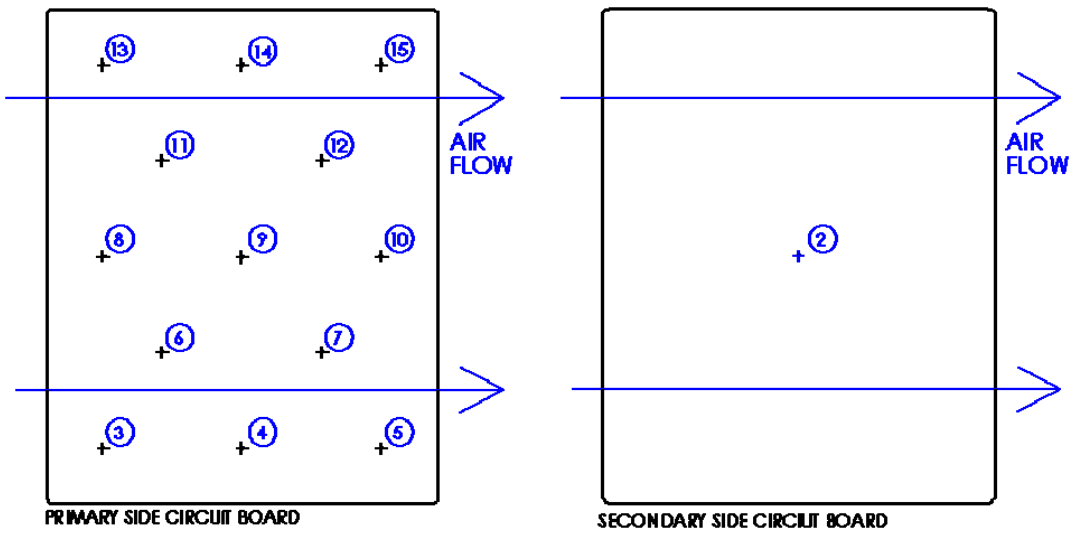

10ppi Aluminum Foam, 0.87" Thick – *Experimental Results Spec Sheet*

Table J-1: Raw Test Data from **0.87" Thick, 10ppi Alum Foam** Configuration. Two points of data where measured for 4 different flow rates. Thermocouple channels 2 through 15 correspond to specific board locations displayed in Figure J-2

		Test 1			Test 2			Test 3			Test 4		
		Pt. 1	**Pt. 2**	**Avg.**	**Pt. 1**	**Pt. 2**	**Avg.**	**Pt. 1**	**Pt. 2**	**Avg.**	**Pt. 1**	**Pt. 2**	**Avg.**
Flow Rate (CFM)		71	71	71	50	50	50	30	30	30	15	15	15
Exit Temp (°C)	0	36.1	36.3	36.2	39.8	38.6	39.2	44.9	45.0	45.0	52.4	52.6	52.5
	1	34.0	34.3	34.2	37.9	37.0	37.5	42.8	43.0	42.9	45.9	46.4	46.2
Secondary Plate Center Temp (°C)	2	47.6	47.9	47.8	48.9	47.6	48.3	50.0	50.2	50.1	52.8	52.9	52.9
Primary Plate Temp (°C)	3	55.0	56.3	55.7	55.4	54.4	54.9	53.1	53.3	53.2	51.5	51.7	51.6
	4	57.7	58.1	57.9	57.8	56.8	57.3	57.3	57.5	57.4	57.3	57.6	57.5
	5	47.6	47.9	47.8	49.2	48.5	48.9	50.8	51.0	50.9	53.9	54.2	54.1
	6	46.9	47.2	47.1	47.9	46.5	47.2	48.8	59.0	53.9	51.6	51.9	51.8
	7	49.5	49.8	49.7	50.8	49.6	50.2	52.0	52.2	52.1	54.6	54.9	54.8
	8	45.1	45.4	45.3	46.0	44.6	45.3	46.9	47.1	47.0	49.8	20.1	35.0
	9	48.0	48.3	48.2	49.1	47.7	48.4	50.2	50.4	50.3	53.0	53.3	53.2
	10	49.6	49.9	49.8	51.0	49.8	50.4	52.5	52.7	52.6	55.1	55.4	55.3
	11	47.1	47.3	47.2	48.0	46.6	47.3	48.8	49.0	48.9	51.6	51.9	51.8
	12	49.1	49.4	49.3	50.5	49.2	49.9	51.8	52.0	51.9	54.5	54.9	54.7
	13	44.4	44.7	44.6	45.3	43.9	44.6	46.2	46.4	46.3	49.2	49.5	49.4
	14	49.3	49.6	49.5	50.2	48.8	49.5	51.1	51.3	51.2	53.7	54.0	53.9
	15	48.8	49.1	49.0	50.3	49.1	49.7	51.8	52.0	51.9	54.6	54.9	54.8
Entrance Temp (°C)	16	22.5	22.6	22.6	22.5	20.5	21.5	21.9	21.9	21.9	22.0	22.0	22.0
	17	22.4	22.4	22.4	22.5	20.3	21.4	21.7	21.9	21.8	21.8	21.8	21.8
	18	22.4	22.5	22.5	22.5	20.3	21.4	21.8	21.9	21.9	21.9	21.9	21.9
Pressure Change (in H20)		2.67	2.69	2.68	1.36	1.36	1.36	0.50	0.50	0.50	0.16	0.15	0.16
Average Air Velocity at Anomometer (ft/min)		1456	1449	1453	1018	1019	1019	619	619	619	302	303	303
Heater Voltage (V)		105.2	113.7	109.5	103.3	101.8	102.6	88.9	94.3	91.6	73.5	72.9	73.2
Power into Heaters (W)		317	317	317	279	280	280	221	222	222	136	137	137
Heat Dissipated (W) (assuming 95% Transformer Efficiency)				**301**			**266**			**210**			**130**

Table J-2: Calculated values of Heat Transfer directly from the 0.87" Thick, 10ppi Alum Foam Configuration to air and for the Total Power input to the air for the from the experimentally determined values in the table above.

Flow Rate		71	50	30	15
Average Inlet Temp (°C)		22.5	21.4	21.9	21.9
Average Exit Temp (°C)		35.2	38.3	43.9	49.3
Exit Air Density (kg/m^3)		1.167	1.167	1.167	1.127
Mass Flow Rate (kg/s)		0.039	0.028	0.017	0.008
Specific Heat Capacity (kJ/kg-K)		1.005	1.005	1.005	1.005
Heat Transfer Rate in Air (Watts)		**499**	**467**	**367**	**220**
Pressure Difference (Pa)		668	339	125	39
Average Velocity at Exit (m/s)		7.38	5.17	3.14	1.54
Power into Air Flow	*Pressure Component*	22.37	7.99	1.76	0.27
	Velocity Component	1.06	0.37	0.08	0.01
	Total Power	**23.4**	**8.36**	**1.85**	**0.28**

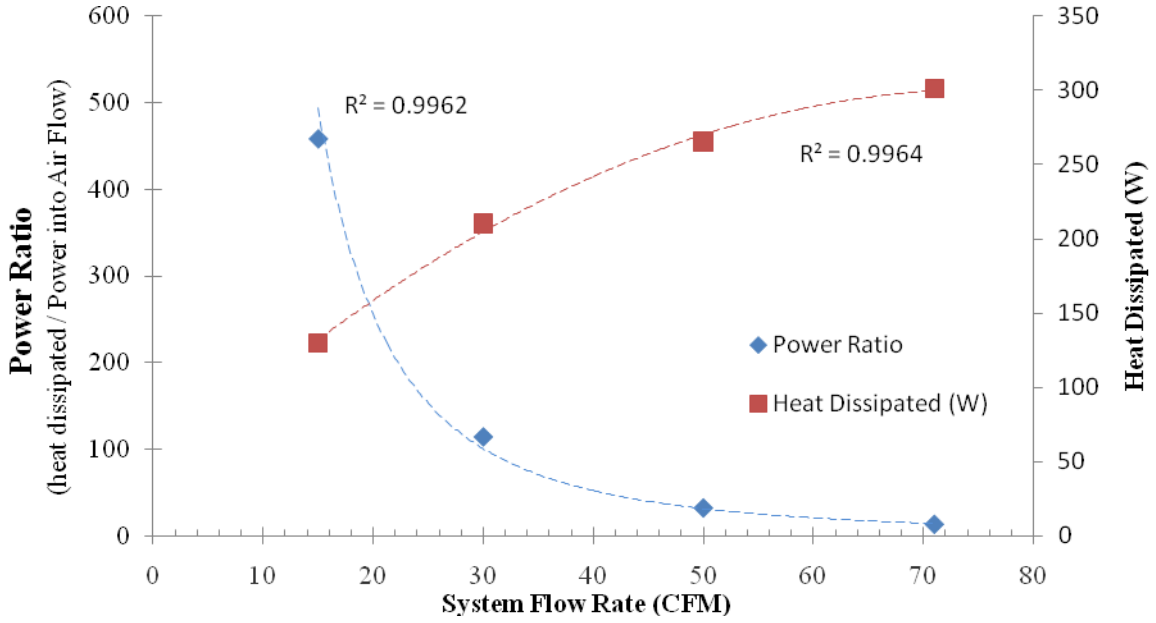

Figure J-1: Experimentally determined cooling characteristics for the **0.87" Thick, 10ppi Alum Foam** configuration. The right vertical axis, with data points shown as blue diamonds, represents a dimensionless ratio of heat removed to the physical power of the air flow. This ratio can be seen as an efficiency of the current plate configuration. The secondary vertical axis, with data points shown as red squares, displays the heat transfer from the circuit boards to the air exhaust in Watts. Both axes are greatly dependant on the air's flow rate through the heat exchanger.

Table J-3: Calculated data points shown in Figure J-1: Heat Dissipation and Power Ratio based on varying flow rates.

Flow Rate (CFM)	71	50	30	15
Heat Dissipated (W)	**301**	**266**	**210**	**130**
Power Ratio	**13**	**32**	**114**	**459**

Figure J-2: Thermocouple layout on circuit board. Measured corresponding temperature values displayed in Table J-1.

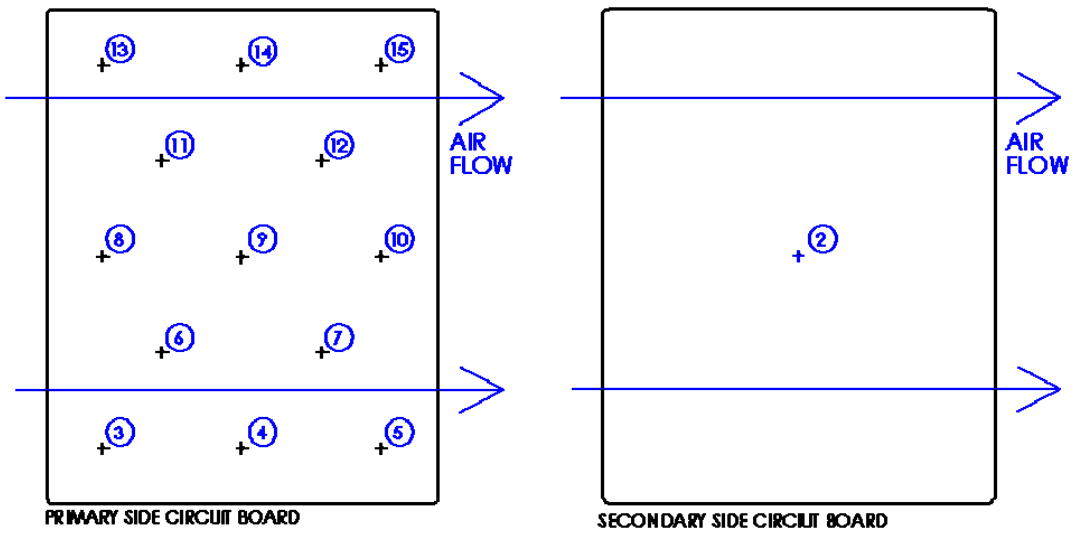

10ppi Channeled Alum Foam, 0.87" Thick – *Experimental Results*

Table K-1: Raw Test Data from **0.87" Thick, 10ppi Alum Foam** Configuration. Two points of data where measured for 4 different flow rates. Thermocouple channels 2 through 15 correspond to specific board locations displayed in Figure K-2

		Test 1			Test 2			Test 3			Test 4		
		Pt. 1	**Pt. 2**	**Avg.**	**Pt. 1**	**Pt. 2**	**Avg.**	**Pt. 1**	**Pt. 2**	**Avg.**	**Pt. 1**	**Pt. 2**	**Avg.**
Flow Rate (CFM)		73	73	73	51	51	51	31	31	31	16	16	16
Exit Temp (°C)	0	33.3	34.5	33.9	36.8	37.2	37.0	41.8	42.0	41.9	46.8	46.9	46.9
	1	33.4	34.7	34.1	36.9	37.3	37.1	41.9	42.3	42.1	47.1	47.0	47.1
Secondary Plate Center Temp (°C)	2	49.1	50.5	49.8	52.2	50.4	51.3	51.3	51.8	51.6	54.3	53.8	54.1
Primary Plate Temp (°C)	3	52.3	53.6	53.0	55.6	52.6	54.1	52.1	52.5	52.3	53.5	52.9	53.2
	4	55.5	56.8	56.2	49.2	55.9	52.6	55.6	55.9	55.8	56.9	56.3	56.6
	5	49.0	50.2	49.6	50.1	50.4	50.3	51.6	51.9	51.8	54.5	54.0	54.3
	6	48.6	50.0	49.3	49.2	49.7	49.5	50.2	50.7	50.5	53.3	52.7	53.0
	7	50.8	52.1	51.5	51.6	52.0	51.8	52.7	53.1	52.9	55.3	54.8	55.1
	8	46.2	47.6	46.9	47.0	47.5	47.3	48.2	48.8	48.5	51.7	51.1	51.4
	9	49.4	50.7	50.1	50.2	50.6	50.4	51.3	51.8	51.6	54.2	53.7	54.0
	10	50.3	51.6	51.0	51.4	51.7	51.6	52.7	53.1	52.9	55.4	54.9	55.2
	11	48.6	50.0	49.3	49.2	49.6	49.4	50.2	50.7	50.5	53.3	52.7	53.0
	12	50.2	51.5	50.9	51.2	51.5	51.4	52.4	52.8	52.6	55.1	54.6	54.9
	13	45.4	46.8	46.1	46.2	46.7	46.5	47.4	48.0	47.7	51.0	50.4	50.7
	14	51.5	52.8	52.2	52.0	52.3	52.2	52.7	53.1	52.9	55.0	54.5	54.8
	15	50.2	51.4	50.8	51.1	51.4	51.3	52.4	52.7	52.6	55.0	54.6	54.8
Entrance Temp (°C)	16	20.0	22.0	21.0	20.0	21.3	20.7	20.6	21.9	21.3	21.5	20.9	21.2
	17	19.9	21.9	20.9	19.9	21.2	20.6	20.5	21.7	21.1	21.3	20.7	21.0
	18	19.9	22.1	21.0	20.0	21.3	20.7	20.6	21.9	21.3	21.3	20.8	21.1
Pressure Change (in H20)		2.19	2.21	2.20	1.04	1.05	1.05	0.41	0.41	0.41	0.11	0.12	0.12
Average Air Velocity at Anomometer (ft/min)		1475	1,495	1485	1,026	1,029	1028	640	644	642	323	324	324
Heater Voltage (V)		105.2	104.7	105.0	97.9	105.0	101.5	98.8	98.9	98.9	79.3	72.4	75.9
Power into Heaters (W)		326	327	327	279	280	280	217	216	217	135	136	136
Heat Dissipated (W) (assuming 95% Transformer Efficiency)				**310**			**266**			**206**			**129**

Thermocouple Channels

Table K-2: Calculated values of Heat Transfer directly from the 0.87" Thick, 10ppi Alum Foam Configuration to air and for the Total Power input to the air for the from the experimentally determined values in the table above.

Flow Rate		73	51	31	16
Average Inlet Temp (°C)		21.0	20.6	21.2	21.1
Average Exit Temp (°C)		34.0	37.1	42.0	47.0
Exit Air Density (kg/m^3)		1.167	1.167	1.167	1.127
Mass Flow Rate (kg/s)		0.040	0.028	0.017	0.009
Specific Heat Capacity (kJ/kg-K)		1.005	1.005	1.005	1.005
Heat Transfer Rate in Air (Watts)		**526**	**464**	**357**	**221**
Pressure Difference (Pa)		548	260	102	29
Average Velocity at Exit (m/s)		7.54	5.22	3.26	1.64
Power into Air Flow	*Pressure Component*	18.88	6.27	1.49	0.22
	Velocity Component	1.14	0.38	0.09	0.01
	Total Power	**20.0**	**6.65**	**1.59**	**0.23**

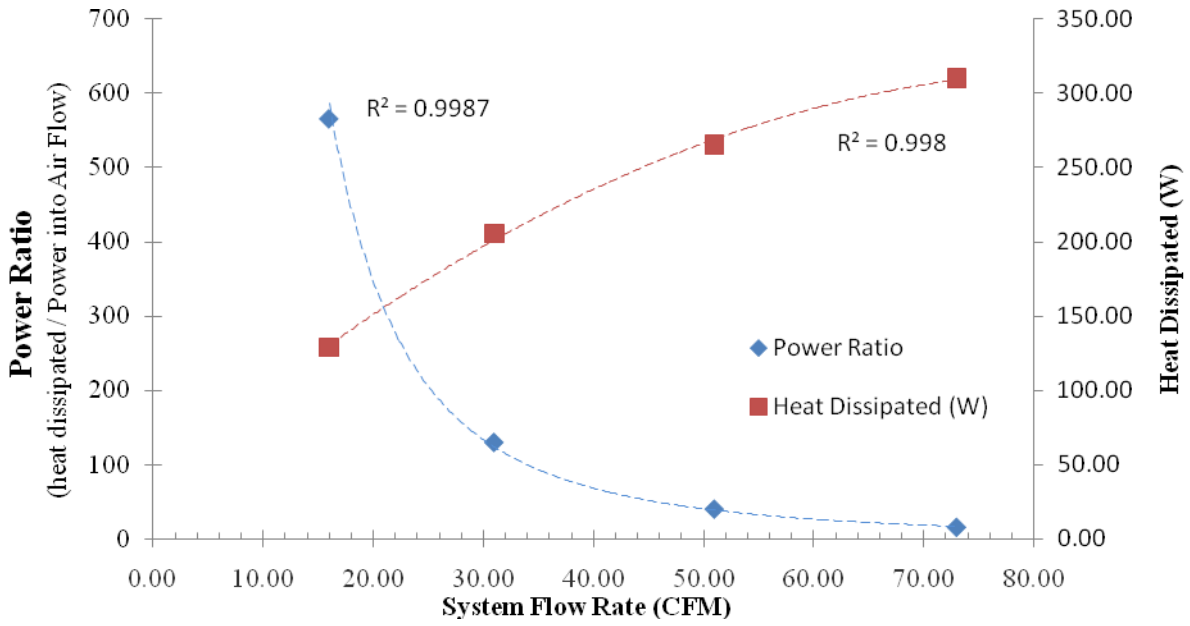

Figure K-1: Experimentally determined cooling characteristics for the **0.87" Thick, 10ppi Alum Foam** configuration. The right vertical axis, with data points shown as blue diamonds, represents a dimensionless ratio of heat removed to the physical power of the air flow. This ratio can be seen as an efficiency of the current plate configuration. The secondary vertical axis, with data points shown as red squares, displays the heat transfer from the circuit boards to the air exhaust in Watts. Both axes are greatly dependant on the air's flow rate through the heat exchanger.

Table K-3: Calculated data points shown in Figure K-1: Heat Dissipation and Power Ratio based on varying flow rates.

Flow Rate (CFM)	73	51	31	16
Heat Dissipated (W)	**310**	**266**	**206**	**129**
Power Ratio	**15**	**40**	**130**	**565**

Figure K-2: Thermocouple layout on circuit board. Measured corresponding temperature values displayed in Table K-1.

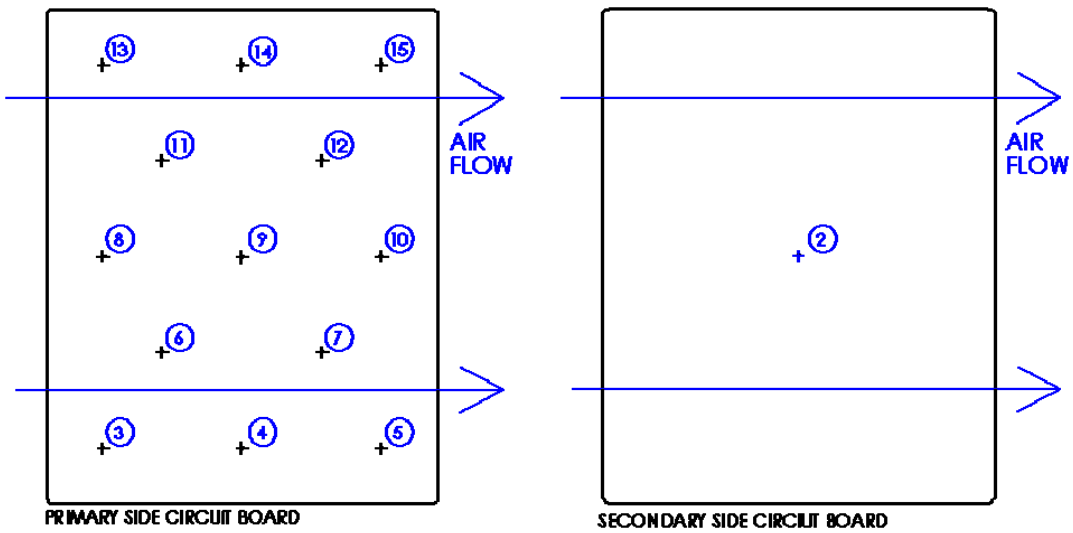

5ppi Aluminum Foam, 0.62” Thick – *Experimental Results Spec Sheet*

Table L-1: Raw Test Data from **0.87” Thick, 5ppi Alum Foam** Configuration. Two points of data where measured for 3 different flow rates. Thermocouple channels 2 through 15 correspond to specific board locations displayed in Figure L-2

		Test 1			Test 2			Test 3		
		Pt. 1	**Pt. 2**	**Avg.**	**Pt. 1**	**Pt. 2**	**Avg.**	**Pt. 1**	**Pt. 2**	**Avg.**
Flow Rate (CFM)		50	50	50	31	31	31	14	14	14
Exit Temp (°C)	0	38.5	37.3	37.9	42.1	42.6	42.4	51.2	52.3	51.8
	1	38.6	37.4	38.0	41.5	42.1	41.8	47.2	48.9	48.1
Secondary Plate Center Temp (°C)	2	47.9	46.6	47.3	48.0	49.0	48.5	54.6	54.9	54.8
Primary Plate Temp (°C)	3	49.4	48.8	49.1	47.4	48.6	48.0	51.8	52.0	51.9
	4	56.4	55.4	55.9	55.0	55.4	55.2	58.1	58.7	58.4
	5	48.6	47.2	47.9	48.9	49.7	49.3	55.0	55.6	55.3
	6	47.4	46.1	46.8	47.0	48.0	47.5	53.0	53.2	53.1
	7	50.0	48.7	49.4	50.0	50.8	50.4	55.8	56.3	56.1
	8	45.2	43.8	44.5	45.0	46.0	45.5	51.3	51.4	51.4
	9	48.4	47.1	47.8	48.3	49.2	48.8	54.5	54.8	54.7
	10	50.1	48.7	49.4	50.3	51.1	50.7	56.2	56.7	56.5
	11	47.1	45.8	46.5	46.9	47.9	47.4	53.1	53.4	53.3
	12	49.7	48.3	49.0	49.8	50.7	50.3	55.9	56.4	56.2
	13	45.8	44.5	45.2	45.3	46.3	45.8	51.5	51.7	51.6
	14	49.4	48.1	48.8	49.1	50.1	49.6	55.1	55.5	55.3
	15	47.8	46.4	47.1	48.7	49.5	49.1	56.1	56.1	56.1
Entrance Temp (°C)	16	21.6	20.9	21.3	20.6	22.0	21.3	22.4	20.8	21.6
	17	21.5	20.8	21.2	20.5	21.8	21.2	22.4	20.5	21.5
	18	21.6	20.9	21.3	20.5	22.0	21.3	22.5	20.5	21.5
Pressure Change (in H20)		3.18	3.18	3.18	1.16	1.16	1.16	0.25	0.25	0.25
Average Air Velocity at Anomometer (ft/min)		1,026	1,025	1026	629	628	629	288	290	289
Heater Voltage (V)		96.1	97.0	96.6	85.5	86.0	85.8	67.9	67.3	67.6
Power into Heaters (W)		276	276	276	214	213	214	142	141	142
Heat Dissipated (W) (assuming 95% Transformer Efficiency)				**262**			**203**			**134**

Table L-2: Calculated values of Heat Transfer directly from the 0.62” Thick, 5ppi Alum Foam Configuration to air and for the Total Power input to the air for the from the experimentally determined values in the table above.

Flow Rate		50	31	14
Average Inlet Temp (°C)		21.2	21.2	21.5
Average Exit Temp (°C)		38.0	42.1	49.9
Exit Air Density (kg/m^3)		1.167	1.167	1.167
Mass Flow Rate (kg/s)		0.028	0.017	0.008
Specific Heat Capacity (kJ/kg-K)		1.005	1.005	1.005
Heat Transfer Rate in Air (Watts)		**463**	**358**	**220**
Pressure Difference (Pa)		792	289	62
Average Velocity at Exit (m/s)		5.21	3.19	1.47
Power into Air Flow	*Pressure Component*	18.69	4.23	0.41
	Velocity Component	0.37	0.09	0.01
	Total Power	**19.1**	**4.31**	**0.42**

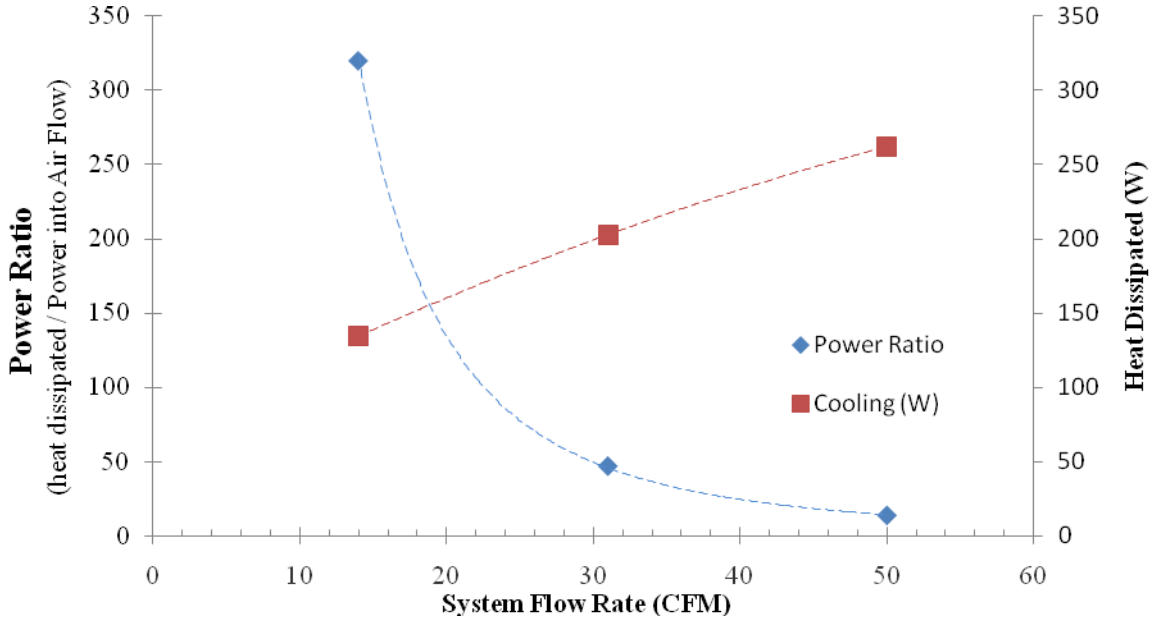

Figure L-1: Experimentally determined cooling characteristics for the **0.62" Thick, 5ppi Alum Foam** configuration. The right vertical axis, with data points shown as blue diamonds, represents a dimensionless ratio of heat removed to the physical power of the air flow. This ratio can be seen as an efficiency of the current plate configuration. The secondary vertical axis, with data points shown as red squares, displays the heat transfer from the circuit boards to the air exhaust in Watts. Both axes are greatly dependant on the air's flow rate through the heat exchanger. **Unlike the other heat exchanger design tests, a flow rate of 70 CFM could not be obtained due to excessive pressure drop.**

Table L-3: Calculated data points shown in Figure L-1: Heat Dissipation and Power Ratio based on varying flow rates.

Flow Rate (CFM)	72	50	31	9
Heat Dissipated (W)	**283**	**246**	**186**	**73**
Power Ratio	**12**	**29**	**98**	**1318**

Figure L-2: Thermocouple layout on circuit board. Measured corresponding temperature values displayed in Table L-1.

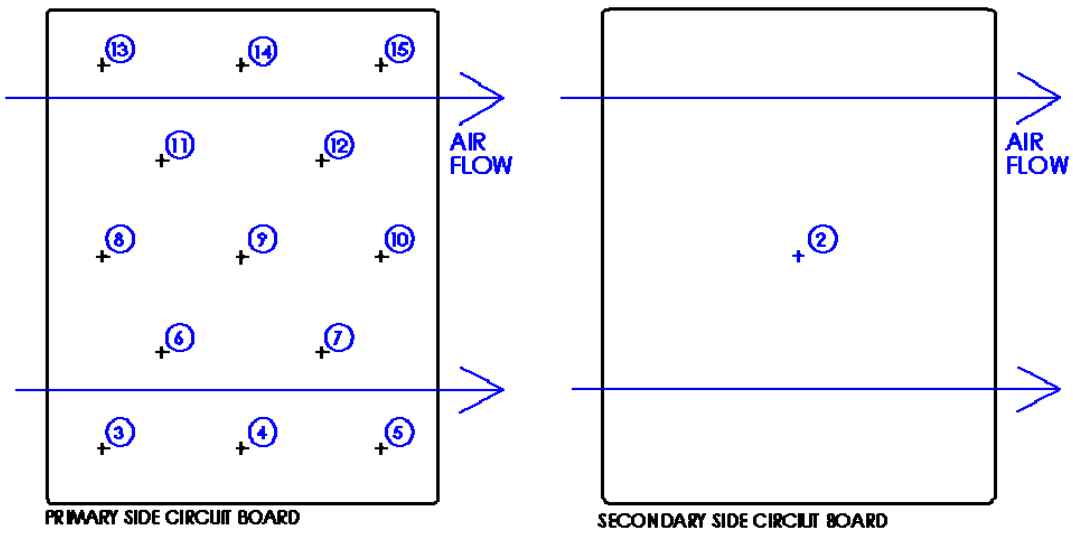

23 APPENDIX M: MATLAB SOURCE CODE

Optimization of finned plate geometry.

```
clc
clear

%This program determines a recommended optimum fin geometry.

%Variables

l = 0; %[in] Extruded Length of fin
t = 0; %[in] Thickness (or diameter) of fin

%Givens and Constants

w = 7.120*0.0254; %[m] Width of fins
k = 180; %[W/m*K] Aluminum 6061 Alloy
h = 40; %[W/m^2*K] Heat Transfer Coeff
T_b = 105 + 273; %K Temperature at base of fin
T_inf = 70 + 273; %K Tempeature of fluid

%Easily Calculated Constants

P = 2*w; %Perimeter around fin (neglect t because w>>t)

sp = .125*.0254;

%settings for loop resolution

lmindim = .01*0.0254;
lresolution = .01*0.0254;
lmaxdim = .5*0.0254;

tmindim = 1/16*0.0254;
tresolution = .01*0.0254;
tmaxdim = 0.25*.0254;

index1 = 1;

%create all possible scenarios

for l = lmindim:lresolution:lmaxdim

    lvector(index1) = l;

    for t = tmindim:tresolution:tmaxdim

        tvector(index1) = t;
        lvector(index1) = l;

        if lvector(index1)==lmaxdim && tvector(index1)==tmaxdim
            disp('hi')
        else
            index1 = index1 + 1;
        end

    end %end for t


end %end for l

%cycles through all the index points to allow calculations of each possible combination

for ncycle = 1:1:index1-1

    %Number of fins that will fit
    N(ncycle) = floor(9.450*.0254/(sp+tvector(ncycle)));

    %corrected length
    L_c(ncycle) = lvector(ncycle)+(tvector(ncycle)/2);
```

```
    %cross sectional fin area
    A_c(ncycle) = w*tvector(ncycle);

    %area of finned surfaces
    A_f(ncycle) = w*L_c(ncycle)*2;

    %area of exposed base between fins
    A_b(ncycle) = N(ncycle)*sp*w;

    %total exposed surface of fins and base
    A_t(ncycle) = N(ncycle)*A_f(ncycle)+ A_b(ncycle);

    %length fin must be to equal heat transfer of infinitely long fin
    infl(ncycle) = 2.646*(k*A_c(ncycle)/h/P)^(1/2);

    %calcuating various elements
    M(ncycle) = (h*P*k*A_c(ncycle))^(1/2)*(T_b-T_inf);
    m(ncycle) = (h*P/k/A_c(ncycle))^(1/2);

    %heat transfer from one fin
    q_f(ncycle) = M(ncycle)*tanh(m(ncycle)*L_c(ncycle));

    %fin performance factor (should be greater than 2)
    sigma_f(ncycle) = q_f(ncycle)/h/A_c(ncycle)/(T_b-T_inf);

    %fin efficiency
    eta_f(ncycle) = tanh(m(ncycle)*L_c(ncycle))/m(ncycle)/L_c(ncycle);

    %total rate of heat transfer from array of fins
    q_t(ncycle) = N(ncycle)*eta_f(ncycle)*h*A_f(ncycle)*(T_b-T_inf) +...
        h*A_b(ncycle)*(T_b-T_inf);

    %overall surface efficiency
    eta_o(ncycle) = q_t(ncycle)/h/A_t(ncycle)/(T_b-T_inf);

end %end for ncycle


% plot(efficiency)


disp1 = max(q_t);
disp2 = find(q_t==max(q_t(:)));


disp(['With a fixed h of ' num2str(h) ' [W/m^2*K]' ]);
disp(['Maximum heat transfer rate is ' num2str(disp1) 'Watts' ]);

disp(['Maximum rate occurs with length ' num2str(lvector(disp2)/.0254) 'inches']);
disp(['Maximum rate occurs with thickness ' num2str(tvector(disp2)/.0254) 'inches' ]);

disp(['Maximum rate has surface efficiency of ' num2str(eta_o(disp2))]);
disp(['Maximum rate has fin efficiency of ' num2str(eta_f(disp2))]);
disp(' ');

disp3 = max(eta_o);
disp4 = find(eta_o==max(eta_o(:)));

 subplot(5,2,1); plot(lvector/.0254)
 title('lvector, values of length [in]')
 subplot(5,2,2); plot(tvector/.0254)
title('tvector, values of thickness [in]')
 subplot(5,2,[3 4]); plot(infl/.0254)
title('infl, Length to assume infinte fin length [in]')
 subplot(5,2,[5 6]); plot(sigma_f)
title('sigma_f, Fin performance factor [-]')
subplot(5,2,[7 8]); plot(q_t)
title('q_t, Total Heat Transfer from surface [W]')
subplot(5,2,[9 10]); plot(eta_o*100)
title('eta_o, Overall Surface Efficiency [%]')
```

24 APPENDIX N: CFD ANALYSIS RESULTS

24.1 Solid Foam Block

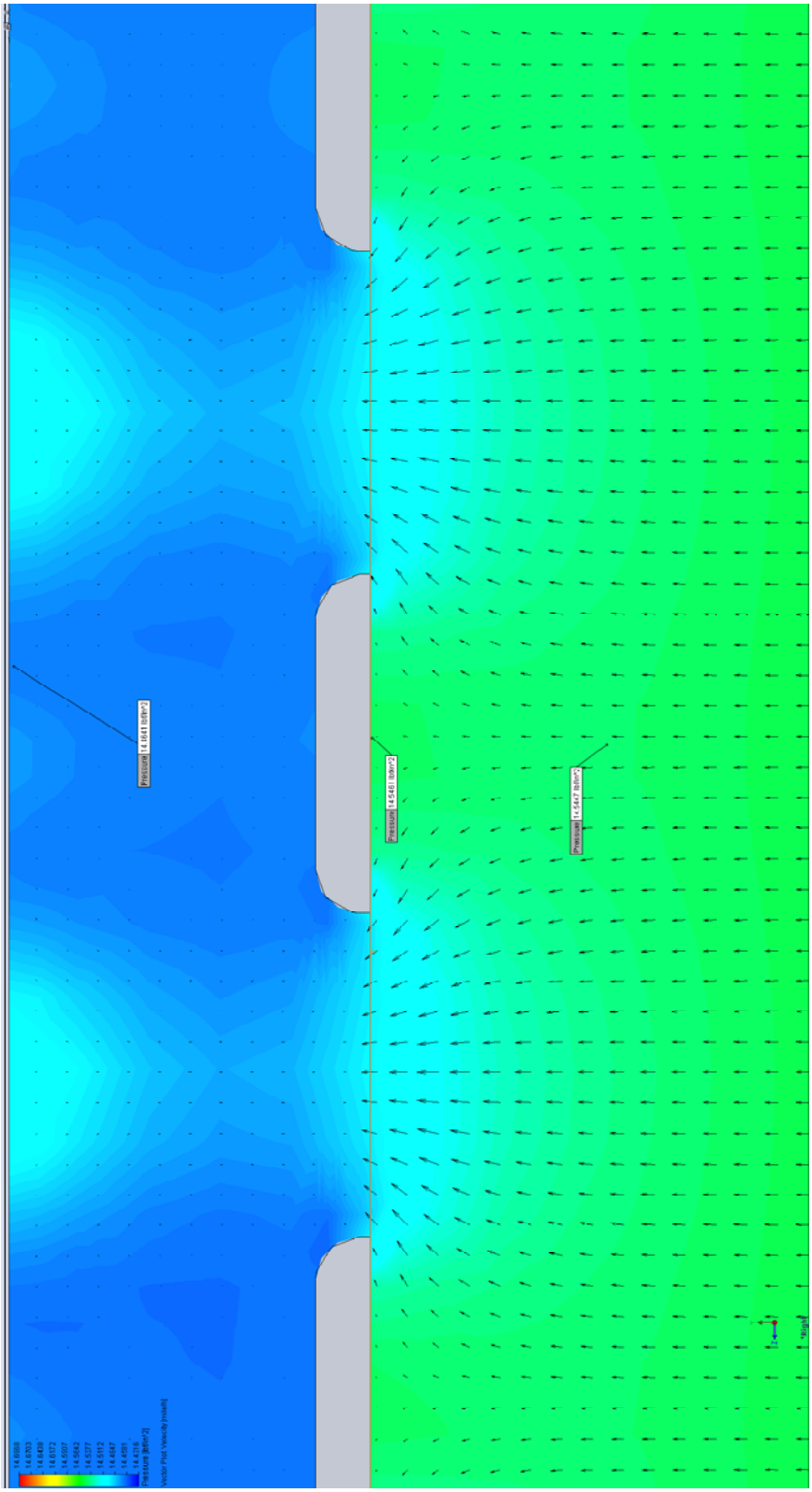

24.2 Full Length Channel Foam Block

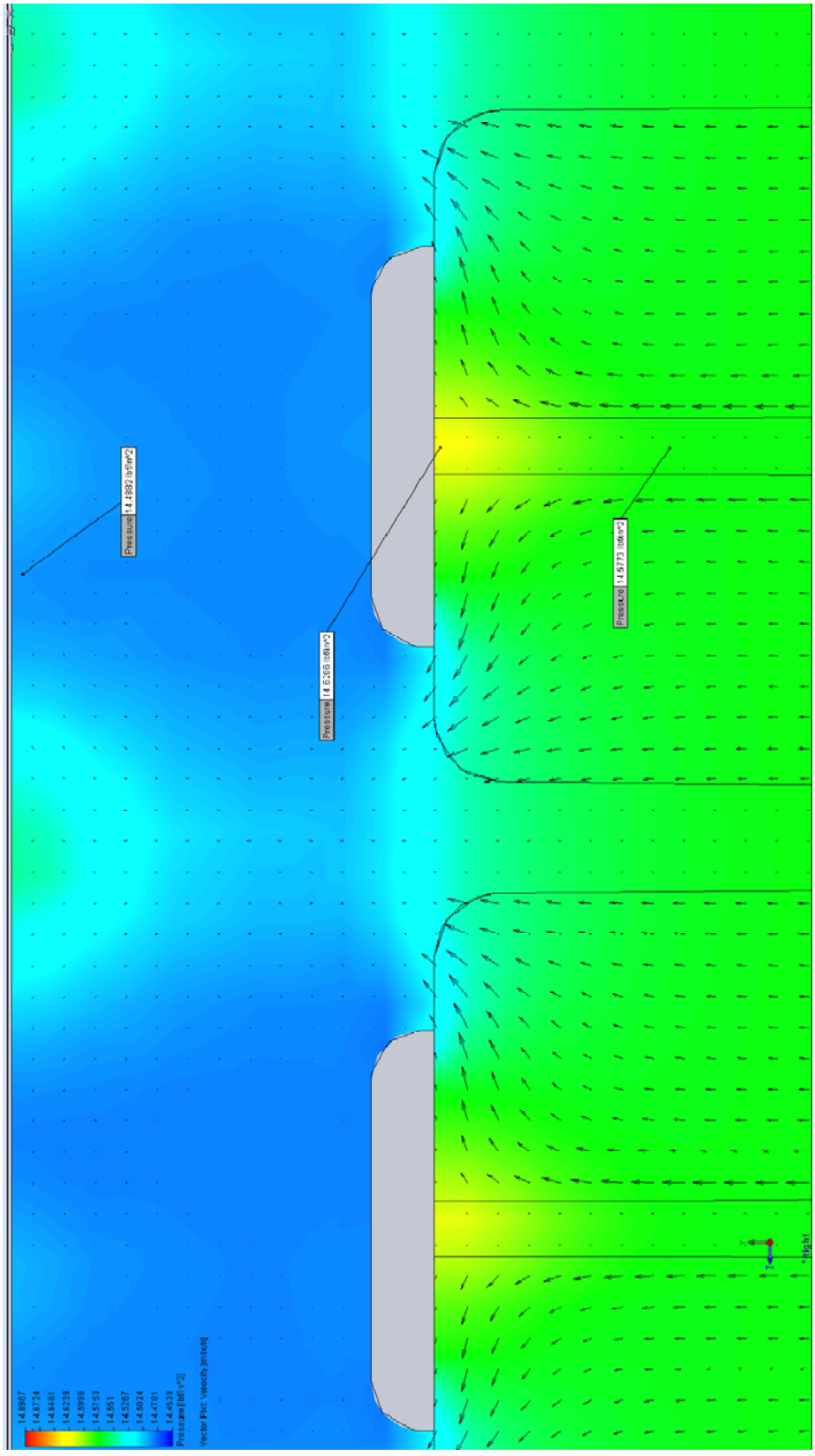

24.3 Partial Length Channel Foam Block

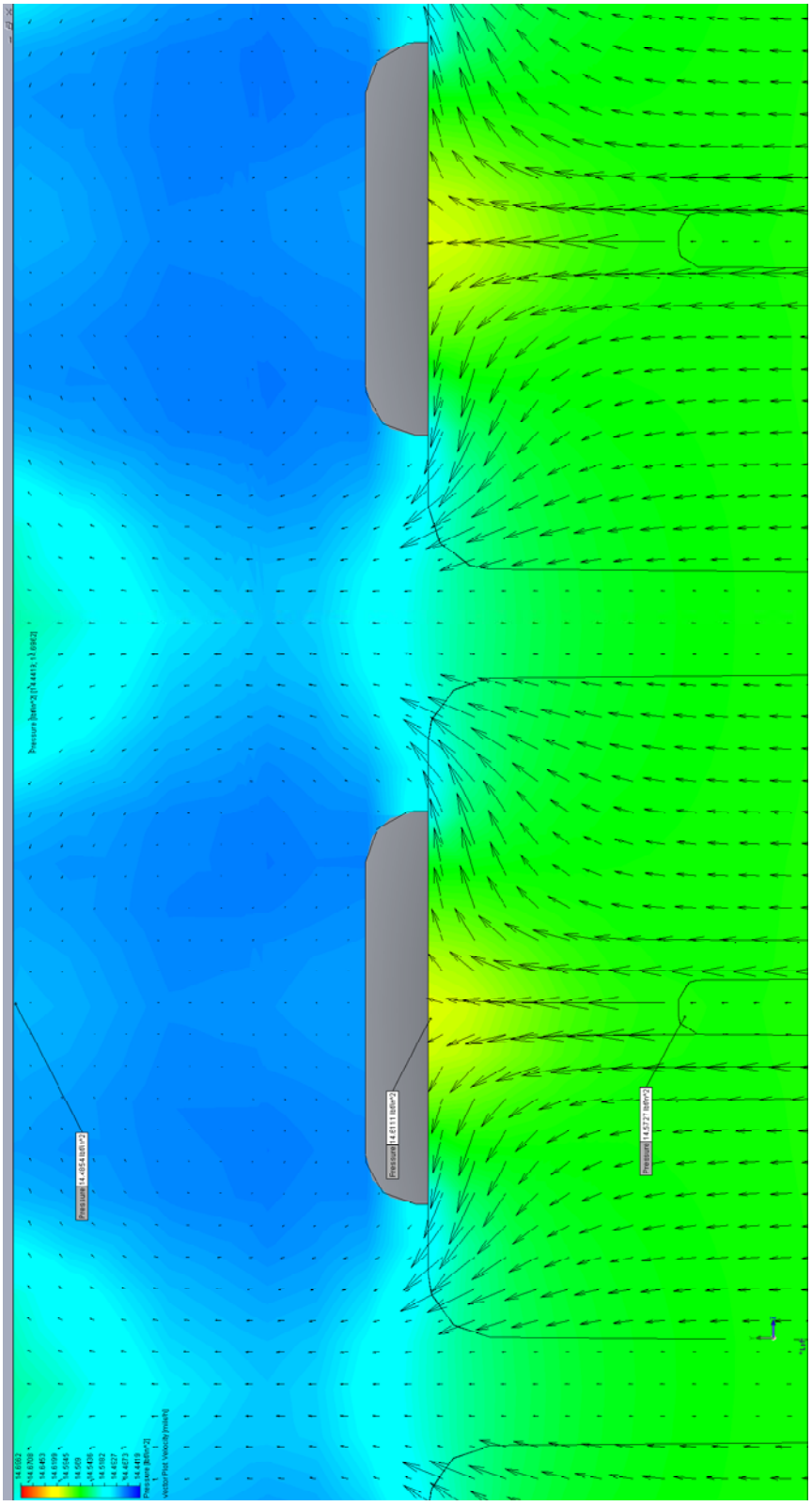

25 APPENDIX O: EBM PAPST FAN SPEC SHEET

- New Types
Preliminary -

4100N Series cont. Tubeaxial

119x119x38mm High Performance

- New axial fan series with highest air flow and pressure performance.
- 3-phase EC motor.
- Electronic protection against reverse polarity, locked rotor and overloading.
- Metal fan housing, Impeller of fiber-glass reinforced plastic PA. Fan housing with ground lug for M4 x 9 screw (Torx).
- Air intake over struts. Rotational direction CW looking at rotor.
- All models with integrated PWM Speed control an /2 Tacho Signal. Other options available.
- Electrical connection via 2 leads AWG 20, Sensor and Control leads AWG 22, UL 1007, TR 64.

Part Number	Curve	CFM @ 0	VDC	Volt. Range	Power (W)	Noise dBA	Noise Bel	Temp Range °C	Bearing Type	Speed (RPM)	Wgt. (lbs)
4114N/2H7P	1	294	24	16 to 30	90	76	8.5	-20 to +75	Ball	9500	0.94
4114N/2H8P	2	336	24	16 to 30	120	78	8.9	-20 to +75	Ball	11000	0.94
4118N/2H7P	1	294	48	36 to 60"	90	76	8.5	-20 to +75	Ball	9500	0.94
4118N/2H8P	2	336	48	36 to 60"	120	78	8.9	-20 to +75	Ball	11000	0.94

External Capacitor with 470 µF recommended.
*36 to 72 VDC available on request.
Preliminary Data - Subject to change without notice.

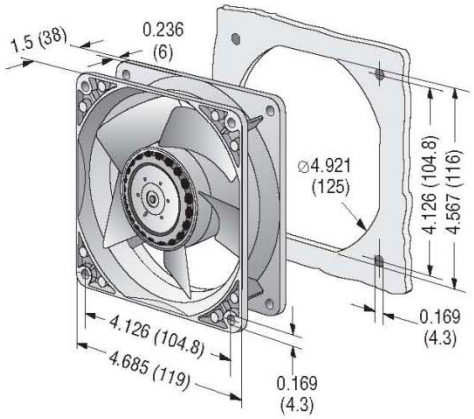

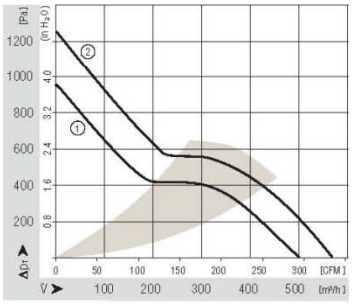

ebmpapst

e-mail: sales@us.ebmpapst.com · TEL: 860-674-1515 · FAX: 860-674-8536
ebm-papst Inc., 100 Hyde Road, Farmington, CT 06034 USA